# Exploring the link between star and planet formation with Ariel

Turrini, D.; Codella, C.; Danielski, C.; Fedele, D.; Fonte, S.; Garufi, A.; ... ; Wolkenberg, P.

Experimental Astronomy (2022) 53:225–278
https://doi.org/10.1007/s10686-021-09754-4

ORIGINAL ARTICLE

# Exploring the link between star and planet formation with Ariel

**Diego Turrini[1,2] · Claudio Codella[3] · Camilla Danielski[4] · Davide Fedele[2,3] · Sergio Fonte[1] · Antonio Garufi[3] · Mario Giuseppe Guarcello[5] · Ravit Helled[6] · Masahiro Ikoma[7] · Mihkel Kama[8,9] · Tadahiro Kimura[7] · J. M. Diederik Kruijssen[10] · Jesus Maldonado[5] · Yamila Miguel[11,12] · Sergio Molinari[1] · Athanasia Nikolaou[13,14] · Fabrizio Oliva[1] · Olja Panić[15] · Marco Pignatari[16,17,18] · Linda Podio[3] · Hans Rickman[19] · Eugenio Schisano[1] · Sho Shibata[7] · Allona Vazan[20] · Paulina Wolkenberg[1]**

Received: 30 June 2020 / Accepted: 13 April 2021 / Published online: 15 October 2021


## Abstract

The goal of the Ariel space mission is to observe a large and diversified population of transiting planets around a range of host star types to collect information on their atmospheric composition. The planetary bulk and atmospheric compositions bear the marks of the way the planets formed: Ariel's observations will therefore provide an unprecedented wealth of data to advance our understanding of planet formation in our Galaxy. A number of environmental and evolutionary factors, however, can affect the final atmospheric composition. Here we provide a concise overview of which factors and effects of the star and planet formation processes can shape the atmospheric compositions that will be observed by Ariel, and highlight how Ariel's characteristics make this mission optimally suited to address this very complex problem.

**Keywords** Ariel · Planet formation · Protoplanetary discs · Star formation · Galactic environment · Stellar characterization

## 1 Introduction

The study of the initial stages of the life of planetary systems, when planets are forming within the gaseous embrace of protoplanetary discs, has been undergoing a transformation in recent years. The improved resolution of observational facilities is

✉ Diego Turrini
diego.turrini@inaf.it

Extended author information available on the last page of the article.

allowing us to directly observe, for the first time, the gaps and rings in the gas and dust of protoplanetary discs that were the theoretically predicted signatures of the appearance of giant planets. These observations are being accompanied by improvements in the compositional characterisation of the discs themselves, allowing the first direct comparisons between the volatile budgets in protostellar objects and in the comets of our Solar System.

These advances have proceeded in parallel with the continuous growth of the known population of extrasolar planets, whose current size exceeds 4000 members and is allowing for population studies at the level of individual planets, of planetary systems as a whole, and of the link between stellar and planetary characteristics. The overall picture emerging from all these fields of study, while still incomplete, is nevertheless clearly indicating how the characteristics of each individual planet are uniquely sculpted by those of the environment in which it forms, in turn set by the star and its own formation process.

Ariel [1], the M4 mission of the European Space Agency deemed for launch in 2029, will characterise the composition of hundreds of exoplanetary atmospheres, proving us with an unprecedentedly large and diversified observational sample [1–4]. Ariel's observations will further revolutionize our view of the formation and evolution of both individual planets and planetary systems by systematically introducing a new dimension, their atmospheric composition, in the study of these subjects.

The insight on the link between the star formation process and the compositional build of planets will become an increasingly important piece of the puzzle of unveiling the nature of exoplanets over the coming years. The goal of this paper is therefore twofold. The first part (Sections 2-5) aims to explore the environmental factors linked to the star formation process and the evolution of protoplanetary discs that can impact the final build of the exoplanets that Ariel will observe. At the beginning of Ariel's observational campaign these factors might represent a source of uncertainty in the interpretation of the atmospheric data (e.g. an unknown composition of the host star). By the end of the nominal mission, however, Ariel's rich and diverse exoplanetary sample will allow to shed light on the interplay between these environmental factors and the planet formation process.

The second part (Sections 6-8), which builds upon the science cases devised in the previous phases of the mission [1, 3], aims to detail more closely the implications of the planet formation process for Ariel's observations. Specifically, Section 6 will discuss in detail the case of giant planets, which currently represent the bulk of Ariel's observational sample [4], while Section 7 will move to smaller planetary sizes and masses, discussing the interplay between the capture of the nebular gas and the outgassing from the planetary interior in shaping their atmospheres as primary, secondary or mixed. Finally, Section 8 will review the information that can be extracted by the architectures of the planetary systems hosting the planets that Ariel will observe to provide dynamical context to the interpretation of Ariel's atmospheric data. Because of the interdisciplinary nature of the discussion throughout this paper, each section and subsection will include one *coloured box* providing the associated *take-home message*, to help readers to identify and connect the key points for all specific subjects discussed.

## 2 Circumstellar discs as the birth environment of planets

The cores and atmospheres of planets are composed of protostellar dust, ices, and gas that have undergone physical and chemical interactions in planet-forming discs around newborn stars. To interpret the full range of planetary properties that Ariel will reveal, and to contribute to its list of science questions, it is therefore critical to have a firm foundation in this stage.

The formation of stars of mass up to several $M_\odot$ is accompanied by the emergence of a flattened expanse of material in Keplerian rotation around the star, called the protoplanetary disc. First signs of protoplanetary discs are present from the early infall stages when the star is accreting significantly (Class 0-I, [5]). Class 0 is the stage where the protostar is fully embedded in its parent envelope and rapidly gains its mass. In the Class I stage, the star has already accreted most of its mass. In both these stages, the disc is the channel for accretion onto the star from the surrounding envelope, but it only becomes observationally accessible in Class I stage. The most accessible phase, observationally, is the Class II phase where the star has accumulated its mass almost entirely, becomes directly visible and is no longer embedded in its parent envelope, leaving only the protoplanetary disc.

Across these stages, the disc is the channel for accretion onto the star from the surrounding envelope, and accretion may proceed up to several Myr on the pre-main sequence. Emerging evidence from the ALMA and VLA interferometers indicates that the *average* mass of discs arond Solar-like stars decreases from $10^{-1}\,M_\odot$ at Class 0 to $10^{-1.5}\,M_\odot$ and $10^{-2}\,M_\odot$ at Class I and II, respectively (e.g. [6]). In other words, the planet-forming mass reservoir drops from $100\,M_J$ to $\leq 10\,M_J$ (Jovian masses) when moving from embedded to easily observable discs. While the matter will be discussed in more detail later in the text, it is worth mentioning already here that these disc mass estimates suffer from a number of caveats mainly due to our poor knowledge of the dust opacity and the gas-to-dust mass ratio. The latter is often assumed to be similar to that of the interstellar medium (ISM), whose gas-to-dust mass ratio is estimated being 100:1 [7].

Discs extend up to a few hundred au, with several known cases extending over 500 au. The disc mass consists almost entirely of gas, so the hydrostatic pressure opposes the gravitational pull toward the plane of rotation and supports an extended vertical structure. The disc vertical struture is characterized in terms of the scale height, defined as $h_R = H/R$ with $H$ being the height above the disc midplane in au, and R the distance from the star in au. $H$ in turn is defined as the ratio between the local sound speed $c_s$ and orbital angular velocity $\Omega$. Typical values of $h_R$ range between a few $10^{-2}$ to 0.1 depending on the temperature profile, hence the sound speed, of the disc (e.g., [8, 9]), though recent evidence shows that gas and small dust grains can reach scale height of 0.15-0.25 at R$>$ 100 au (e.g. [10]). While the gas and small grains can reach such altitudes, large dust grains settle fast onto the disc midplane as shown e.g., by the ALMA survey of edge-on discs [11].

At the final stage, Class III, the star has typically already reached the main sequence, and can be surrounded by a debris disc (i.e. Vega-like stars, [12]). A debris disc is an extremely flat disc containing solids only, and rather than a disc it is geometrically better described as one or more rings or belts, analogous to our asteroid

and Kuiper belts [13]. With the high sensitivity of ALMA, we are finding that the boundary between protoplanetary and debris discs is blurred [14], with some debris discs containing gas, although much less than typical protoplanetary discs [15], and protoplanetary discs showing evidence of dust production by collisional mechanisms as debris discs [16].

Two main processes have been proposed as possible pathway for the formation of giant planets, the *core accretion* (also called nucleated instability) scenario and the *disc instability* scenario, with different implications for the disc environment associated with the birth of these planets. We briefly highlight the main characteristics of these two processes in the following, referring the readers to the recent reviews by [17] and [18] for more in-depth discussions.

In the disc instability scenario giant planets form as a result of a local gravitational instability in the circumstellar disc, which leads to the formation of a gravitationally bound object that collapses under its own self-gravity on timescales of the order of a few to a few tens of orbital periods.

Disc instability may happen through Classes 0-I, when the disc is massive and more likely to be unstable. The condition for disc instability is satisfied for low values of the Toomre parameter

$$G_T = \frac{c_s \Omega}{\pi G \Sigma} < 1 \tag{1}$$

with G being the gravitational constant and $\Sigma$ the gas surface density. Thus, for disc instability to occur the disc must be cold and massive, a condition that can be easily satisfied in the outer region of very young discs (roughly beyond a few tens of au). In Class II, and by the time the envelope is gone, it is likely that the disc has also had sufficient time to reach stability although, observationally, it is quite difficult to exclude the possibility that some of the massive discs with spiral structures seen in Class II may be undergoing disc instability.

In the core accretion scenario (further discussed in Section 6) the giant planets first form a planetary core by accumulation of solid material in the inner and denser regions of protoplanetary discs (within the first few tens of au), meanwhile acquiring a more or less extended gaseous envelope by capturing gas from the circumstellar disc. When the mass of this expanded atmosphere becomes comparable with that of the planetary core, the gas becomes gravitationally unstable and triggers a runaway gas infall phase that causes a very rapid mass growth of the planet. The time required for the planetary core to grow and trigger the instability of its extended atmosphere can vary between a few $10^5$-$10^6$ years, while the runaway gas accretion timescale is an order of magnitude faster, ranging between a few $10^4$ years and a few $10^5$ years.

Due to its longer timescales nucleated instability can operate well into Class II, as the time required for the growth of the planetary core can easily exceeds the age of typical Class I sources.

Because of the wealth of observationally constrained parameters of discs in Class II phase, the information we possess on discs is mainly related to this class, with only a few examples which could qualify as representative of disc instability conditions.

### 2.1 Gas and solids in protoplanetary discs

Almost the entire gas mass of the disc is in the form of molecular hydrogen ($H_2$) and helium (He), with the next most abundant molecule being CO, with abundance of $\leq 10^{-4}$ with respect to H. Direct total $H_2$ gas mass measurements are not feasible because $H_2$ lacks a permanent dipole moment, which makes its rotational emission unobservably weak. The first vibrational level requires $\sim$ 6000 K to excite, so ro-vibrational emission only probes a thin, hot surface layer of the inner disc, same as the fluorescent emission of $H_2$ [19]. Consequently the gas mass pursuit has focused on species such as CO and HD.

The *$H_2$ isotopologue, HD*, has a permanent dipole moment and rotational transitions in the far-infrared. Even accounting for isotope-selective chemistry, *HD can be assumed to have a fixed abundance relative to $H_2$ throughout almost the entire disc* [20]. The HD/$H_2$ ratio is determined by the local Galactic D/H ratio, which is $(2.0 \pm 0.1) \times 10^{-5}$ [21]. Detecting the $J = 1$–0 line with the *Herschel* Space Observatory allowed [22] to estimate a total mass of 0.05 $M_\odot$ in the disc around TW Hya (0.8 $M_\odot$ star). Later estimates, using more strongly constrained physical-chemical models and additional information from the HD $J = 2$–1 transition, found $(0.075 \pm 0.015)$ $M_\odot$ [20]. HD detections have also yielded mass estimates for two other T Tauri discs: DM Tau (0.65 $M_\odot$ star) with $(2.9 \pm 1.9) \times 10^{-2}$ $M_\odot$, and GM Aur (1.1 $M_\odot$ star) with $(2.5 \pm 20.4) \times 10^{-2}$ $M_\odot$ [23]. The three measurements, with gas masses of 20-80 $M_J$, are consistent with a dust-to-gas mass ratio of 1:100 [7].

It is important to note that particularly massive and bright discs were specifically targeted in these observations. [24] have recently analysed the upper limits on the HD $J = 1-0$ line flux of discs around intermediate mass stars putting a strong constraint on the gas mass of the disc around HD 163296, $M_{disc} \leq 0.067\,M_\odot$. Comparing this with the masses of five candidate protoplanets in this disc, they find a giant planet formation mass efficiency of $\gtrsim 10\,\%$ for present-day values. Because of the moderate energy of the low-level rotational lines (HD J=1, $E/k_B = 128.5$ K), the HD-based mass estimates rely on the knowledge of the disc thermal structure. This can be estimated comparing multiple transitions of optically thick lines with thermo-chemical models. An ideal disc "thermometer" is the CO rotational ladder (e.g. [25]). By fitting simultaneously the fluxes of the low-$J$ HD and multiple CO transitions with thermo-chemical models it is possible to obtain robust constraints to both the temperature structure and total gas mass [20].

*CO is the second most abundant molecule after $H_2$*, with an abundance of $\leq 10^{-4}$ with respect to $H_2$, and its rotational emission lines are readily detected in the millimetre. Historically, many of the gas mass measurements have relied on such CO observations in the past, for the lack of ability to detect more reliable tracers with pre-ALMA instruments. Such *measurements yield lower limits to the total gas mass reservoir*, as these bright *emission lines are* also *optically thick* and trace higher layers, and not the disc midplane where the bulk of the mass resides and planets form [26]. Another issue affecting CO is depletion due to freeze-out, as deep in the cold midplane CO readily freezes onto dust grains as soon as the temperature is below 20 K.

*Emission from CO isotopologues is less optically thick*, and in fact $C^{18}O$ and $C^{17}O$ are largely optically thin, making gas in the midplane accessible through millimetre observations. This method already yielded gas measurements with pre-ALMA instruments [27] and is currently widely used. An important limitation is still the CO freeze out, and other depletion mechanisms such as selective photodissociation, due to which the CO abundance may be decreased below the commonly assumed values, thereby rendering such mass estimates lower limits only (e.g. [28–30]). Depending on the disc surface density, even the commonly used $C^{18}O$ lines can be optically thick in inner $\sim 10-20$ au of the disc and the use of even rarer isotopologues is required. Recently, ALMA detected the rarest CO isotopologues $^{13}C^{18}O$ [31] and $^{13}C^{17}O$ [32, 33].

It was long unclear whether unexpectedly low CO-based total disc mass estimates were due to an overall lower gas mass or a lack of CO molecules ("CO depletion"). Detailed physical-chemical models constrained by the continuum spectral energy distribution, multiple CO transitions and spatially resolved line maps, HD fluxes or upper limits, and other data have confirmed that **elemental C and O can have a wide range of gas-phase abundances, from nominal to two orders of magnitude depleted**, depending on the disc [20, 34–37].

It should be noted that a measurement of the total optically thin CO isotopologue line flux by itself only yields a lower limit on the disc gas mass. Multi-line and continuum data can provide some insight into whether it is the CO abundance or the total gas mass which is low (e,g, [35, 37–39]). Recently, the rarest stable CO isotopologue $^{13}C^{17}O$ has been detected in the disc HD 163296, yielding a gas mass of $0.3 M_{\odot}$, a few times higher than obtained with more abundant isotopologues [32]. It is not yet clear whether the lower HD-based mass ($\leq 0.067\,M_{\odot}$, [24]) is due to an enhancement of volatile abundances or something else.

At the time of their formation, *discs inherit the dust-to-gas ratio from the molecular clouds*, and this fiducial value is often assumed to be 1:100 as measured in the ISM [7]. *Measuring the dust mass is reliable to roughly an order of magnitude*, which is much better than the uncertainties linked to the gas mass estimates, except in the rare cases when HD emission is available as a constraint. The mass locked in dust grains of order a millimetre to centimetre in size is calculated directly from the observed flux at a wavelength similar to the grain size, assuming optically thin emission and a cold temperature ($\approx 20\,K$). For example, disc dust masses extend from $10^{-5}$ to $< 10^{-3}\,M_{\odot}$ in Lupus [29]. The Lupus discs detected in CO lines typically have gas masses below $< 10^{-3}\,M_{\odot}$ (i.e., less than a Jovian mass of gas) which implies dust-to-gas ratios over 1:100.

As it has been recently shown, even at millimeter wavelength, the dust emission might not be optically thin throught the whole disc extent and self-scattering might bias the dust mass estimates that should be therefore considered as a lower limit (e.g. [40]). As discussed above, the few available HD-based disc gas masses are in the

10 to 100 $M_{Jup}$ range. The field is currently trying to establish whether the low CO-based masses are real or a consequence of depletion of gas-phase elemental C and O [41, 42]. Future observations at even longer wavelengths with e.g., the ngVLA, will help to better constrain the total dust mass (e.g., [43]). We expect substantial progress on understanding disc gas mass evolution and planet formation efficiency over the coming years, particularly by the time Ariel is due to fly.

Average dust masses derived from millimetre emission fail to reach 10 $M_{\oplus}$. This said, the dust mass just refers to the solid material presently in form of dust in the protoplanetary discs and *does not provide any indication of how much solid material is contained in form of rocks and larger bodies*. These contribute to a negligible fraction of the millimetre flux, dominated by the grains of comparable size to the wavelength. Dust mass measurements are improved by complementary measurements of the dust spectral index, which provides a better grasp of dust opacity - one of the key sources of uncertainty.

### 2.2 Chemical composition and molecular inventory of protoplanetary discs

Figure 1 summarises the inventory of molecules detected in discs (in the gas phase) at various wavelengths. Several carbon-, oxygen-, nitrogen- and sulphur-bearing species have been detected. Infrared observations of class II discs from the ground (with e.g., Keck/Nirspec and VLT/CRIRES) and from space (NASA/Spitzer and ESA/Herschel) revealed a molecule-rich inner disc. The most commonly detected species are OH and $H_2O$ (e.g., [44–51]). CO rovibrational emission has been a particularly powerful tracer of the structure of the inner disc and geometry of disc cavities and gaps (e.g., [47, 52–55]). A few simple organics molecules are also detected: HCN, $C_2H_2$ and $CO_2$ (e.g., [44, 46, 47, 49, 56]) as well as $CH_4$ (seen in absorption in the disc around GV Tau N, [57]). These hot transitions emit from the inner ($\lesssim$ 10 au) warm molecular layer where molecules form primarily through gas-phase reactions (see e.g., [58–60]). A further contribution can come from the thermal desorption of the ices within the $H_2O$ snowline. The large column density of OH and $H_2O$ requires an oxygen-rich inner disc. On the contrary, at longer wavelength, deep

| | |
|---|---|
| ***Ionization*** | $CH^+$, $^{13}CH^+$, $HCO^+$, $H^{13}CO^+$, $HC^{18}O^+$, $DCO^+$, $N_2H^+$, $N_2D^+$ |
| ***Hydrogen*** | $H_2$, HD |
| ***Carbon*** | CO, $^{13}CO$, $C^{18}O$, $^{13}C^{18}O$, $^{13}C^{17}O$, $CO_2$, $C_2H$, $C_2D$, $C_2H_2$, $C_3H_2$, $CH_4$ |
| ***Oxygen*** | OH, $H_2O$, $H_2CO$, HCOOH |
| ***Nitrogen*** | CN, $C^{15}N$, HCN, $HC^{15}N$, $H^{13}CN$, DCN, HNC, DNC, $NH_3$, $HC_3N$ |
| ***Sulphur*** | CS, $^{13}CS$, $C^{34}S$, SO, $SO_2$, $H_2S$, $H_2CS$ |
| ***Complex*** | $CH_3CN$, $CH_3OH$, $CH_3CHO$, $CH_3OCHO$, $CH_3COCH_3$ |

**Fig. 1** List of molecules detected in protoplanetary discs at any wavelength. An increasing number of molecular isotopologues is being discovered at millimeter wavelenghts by ALMA. The detection of acetaldehyde ($CH_3CHO$), methyl formate ($CH§_3OCHO$) and acetone ($CH_3COCH_3$) refers to the outbursting source V883 Ori [66, 67]. The detection of $C_3H_2$ actually refers to c-$C_3H_2$, the cyclic form of this isomer whose linear form is yet to be detected in discs

Herschel/HIFI observations of the ground state rotational transitions of $H_2O$ resulted in only 2 detections in the discs around TW Hya and HD 100546, while the lines remain largely undetected in other discs [39, 61] implying low abundance of cold $H_2O$ ($\lesssim 10^{-11}$). The ground state $H_2O$ emission is expected to come from the outer disc region ($> 50$ au) where $H_2O$ ice is photo-desorbed (e.g., [58]). The emerging scenario is that, in the outer disc, oxygen is depleted onto icy grains, which release oxygen back to the gas-phase in the inner disc as they cross the water snowline, yielding an oxygen-rich inner disc (see also [62])

Overall, the disc molecular inventory is made of a dozen of simple species. Complex molecules (i.e. composed of 6 or more atoms) are rare and the most complex species detected so far are: methanol ($CH_3OH$, [63]), methyl cyanide ($CH_3CN$, [64]) and formic acid (HCOOH, [65]). Recent observations of the FU Orionis-like object V883 Ori revealed the presence of more complex species such as $CH_3CHO$ and $CH_3COCH_3$ along with $CH_3OH$ [66, 67], opening the path to the investigation of complex species in discs. For most of the species, we do not have direct information of their radial and vertical distribution. Thanks to ALMA however, we are starting to spatially resolve the molecular emission, which informs us about the radial distribution of different volatiles.

**Outer disc** On 10 to 100 au scales, spatially unresolved gas-phase total elemental abundances or abundance ratios are, thus far, available for carbon (C), oxygen (O), nitrogen (N), and sulfur (S). These abundances are typically constrained by models including the disc physical structure, a chemical network, and ray-tracing of continuum and line emission. Sometimes, the vertically-integrated column density is the modelled quantity. In most cases, observational constraints include rotational lines of multiple species. The outer disc gas-phase elemental abundance and ratio measurements published to-date are summarized in Table 1.

**Table 1** Gas-phase elemental abundances in discs on 10 to 100 au scales

| Object | C/H ($\times 10^{-4}$) | C/O | N/O | S/H ($\times 10^{-5}$) | References |
|---|---|---|---|---|---|
| Sun | 2.69 | 0.55 | 0.16 | 1.32 | |
| DM Tau | 0.2 . . . 1.0 | $> 1$ | | $< 10^{-2}$ | 1,2,3 |
| GM Aur | $10^{-2}$ | | | | 1 |
| GO Tau | | $> 1$ | | $< 10^{-2}$ | 2 |
| HD 100546 | 1.35 | $< 0.9$ | | $*10^{-4}$ | 4 |
| | 0.135 | $< 0.9$ | | $*10^{-3}$ | 5 |
| IM Lup | | 0.8 | 10 | | 6 |
| LkCa 15 | | $> 1$ | | $< 10^{-2}$ | 2 |
| TW Hya | 0.01 | $> 1.1$ | | $*10^{-4}$ | 5,7,8 |

Notes. Reported abundances with respect to H nuclei may have systematic uncertainties of a factor of a few. The difference between C/O $< 1$ and $> 1$ is strongly constrained and largely unrelated to these absolute scalings. *References*: 1: [23]; 2: [79]; 3: [80]; 4: [81]; 5: [37]; 6: [82]; 7: [35]; 8: [20]; *: upcoming publications

**Inner disc** On 0.1 to 10 au scales, in what was traditionally expected to be the formation zone of most planets before ALMA surveys revealed the possible signatures of giant planets at tens or even hundreds of au from the host stars (e.g. [68]), elemental and chemical abundances are very hard to determine due to the small emitting area and the poorly known physical structure of these regions. New techniques are focusing on studying the composition of the material accreting onto the central star as a proxy of the inner disc:

1. Actively accretion-dominated photospheres of young stars above 1.4 $M_{\odot}$ [69]. Disc accretion rates are sufficient to cover the entire photosphere on weekly timescales in these stars, whose radiative envelopes are mixed with the deeper layers very slowly. Photospheric abundances provide a measurement of the absolute dust depletion level in gaps or cavities in the inner disc [70]. This technique will in the near future allow to study variations in the mutual ratios of many elements, including C, N, O, S, Si, Fe, Mg, Al, Ca, and Ti. A recent result of its application has been the determination that $(89 \pm 8)\,\%$ of all sulfur atoms in the inner few au of discs are locked in a refractory component, likely FeS [71], confirming the picture depicted by the data provided by the meteorites and minor bodies in the inner (e.g. [72, 73], and references therein) and outer (e.g. [74, 75], and references therein) Solar System.
2. Atomic emission lines from the inner accretion disc where all dust has evaporated [76]. While these lines are hard to relate to absolute abundances, C and Si line emission can constrain major disc features such as the re-appearance of volatile carbon (reduced in outer disc gas by $\approx 50\times$) within the dust-depleted inner cavity in TW Hya [37, 77] or dust-evolution driven time variability in the inner disc volatile composition [78].

## 3 The influence of the stellar and galactic environments

Planetary systems do not form and exist in isolation, but instead are subject to radiative and dynamical influences from their cosmic environment. The birth of stars and planets takes place at local density peaks in the hierarchically structured ISM (e.g. [83, 84]). The fractal nature of the ISM causes star formation to be spatially clustered (e.g. [85–87]). In other words, planetary systems are often born and sometimes evolve in the vicinity of other stars and planetary systems, which can have an important impact on their properties (see [88] and [89] for recent reviews).

The two dominant, external physical mechanisms that are generally considered to affect the properties of planetary systems are:

1. *external photoevaporation* by massive stars, which accelerates the dispersal of protoplanetary discs and potentially modifies their chemistry and thermal structure, including the location of the snowlines (e.g. [90, 91]);

2. *dynamical encounters* with other stars, which can perturb either the protoplanetary disc or, on longer timescales, disrupt the planetary system itself (e.g. [92–95]).

Observational indications of these mechanisms have been found. For instance, observations show a variation of the protoplanetary disc size with ambient stellar density [96], a variation of the protoplanetary disc mass with distance to the nearest massive star [97], a decline of the fraction of stars with discs in clusters at increasing values of local UV fluxes [98], and tidal features as evidence of past dynamical encounters between protoplanetary discs [99]. It requires little imagination to realise that these effects can transform the architecture of the resulting planetary systems, as well as affect the bulk composition of the planets and that of their atmospheres.

It depends on the observable quantity of interest and on the timescale considered whether external photoevaporation or dynamical encounters dominate. When only concerned with protoplanetary disc dispersal, external photoevaporation is almost always the dominant external mechanism, except in (rare) cases of high stellar densities and no massive stars [91, 100]. However, in the context of Ariel, we are not only interested in the truncation of the planet formation process, but also in the effect of external photoevaporation and irradiation on planet formation through changes in the chemistry and/or the thermal environment of discs. These processes require much less extreme circumstances (e.g. radiation fields of a few 100 $G_0$, [101]) than externally accelerated disc dispersal ($> 10^3$ $G_0$, [100]). For instance, the synthesis of complex organic molecules and amino acids on icy dust grains is expected to be accelerated under external UV or soft X-ray irradiation (e.g. [102–104]). Likewise, the formation of planetesimals may be accelerated by an external UV field (e.g. [105, 106]). For both of these examples, it is plausible that the effect of external UV irradiation is a runaway process, because small dust grains can get trapped in photoevaporative flows, causing a decrease of the extinction column and a corresponding loss of UV absorption (e.g. [107]).

When concerned with the architecture of planetary systems over long (∼Gyr) timescales, the expectation value for the number of disruption events by dynamical encounters increases linearly with the age of the system, under the assumption that the ambient environment does not evolve. Therefore, eventually the integrated impact of dynamical encounters is expected to outweigh that of external photoevaporation and to become the dominant form of external perturbation for older planetary systems. In this context, it is critical to consider the gravitational boundedness of the birth stellar population, because only gravitationally bound clusters can generate sustained dynamical perturbations – unbound stellar associations never live beyond a dynamical crossing time [108], implying that encounters are an extreme rarity. In the current solar neighbourhood, about 5–10% of stars are born in bound clusters (e.g. [109]), but this is expected to have been much larger in the past, with up to 50% of all stars and planetary systems with ages $> 8$ Gyr having been born in bound clusters and potentially having been exposed to extreme external disruption (e.g. [86, 110, 111]). Notwithstanding these arguments, a sufficiently dense field star population can rival that of stellar clusters (e.g. towards galactic centres), such that even the

field can generate a significant number of dynamical encounters over a sufficiently long timescale.

The above discussion has a number of crucial implications for the Ariel target selection and, more generally, for studying the link between planetary composition and formation environment. Above all, the fact that **the stellar and galactic environment beyond the confines of a planetary system can affect its architecture, composition, chemistry, and atmospheric properties**, implies that the target selection should aim for a diversity of possible formation environments.

Major efforts are currently being undertaken to link the properties of planetary systems to their large-scale stellar environment, with promising results (e.g. [112–115]). These studies show that planetary system architectures and planetary properties (e.g. multiplicity, semi-major axis distribution, Hot Jupiter incidence, planet radius distributions and uniformity) exhibit intriguing environmental dependences, which can be isolated most clearly for host stellar ages of 1-4.5 Gyr [112]. While it is not yet possible to unambiguously relate the current environmental conditions to those of the formation environment, there exist statistical trends that can already greatly inform the target selection of Ariel.

Specifically, the ambient stellar density of planetary systems at birth sets the strength of the external UV field, as well as the rates of external photoevaporation, dynamical encounters, and nearby supernovae, affecting isotopic abundance ratios (e.g. [116]). The birth density greatly increases with gas pressure and therefore age (due to cosmic evolution, up to about $\sim$ 8 Gyr ago, [86, 100, 111, 117]), which is likely to result in age trends of chemistry and atmospheric properties. Additionally, we may expect a trend with host stellar mass, because the impact of external radiative effects increases towards lower host stellar masses, due to lower binding energies and gas pressures of the protoplanetary discs (e.g. [100, 118]). These trends are accessible by Ariel within the solar vicinity, due to the wide range of ages (and thus cosmic formation environments, see e.g. [119]) and host stellar masses of the local population of planetary systems.

The above line of reasoning leads to the following recommendation. In addition to the well-documented internal, secular processes governing the formation and evolution of planetary systems, the cosmic formation environment is a major axis along which Ariel's planet sample should be expected to reveal new, surprising, and physically important trends. To realise this discovery potential, Ariel should aim to target a sufficiently large sample of planets around low-mass stars, with a wide range of ages from comparatively young ($\sim$ 1 Gyr) to older ($>$ 5 Gyr), because older planetary systems around low-mass stars are predicted to be most strongly influenced by environmental effects. In addition to this general guideline, it is to be expected that the ongoing efforts aimed at characterising the formation environments of at least some of the known exoplanetary systems will bear fruit before the Ariel target selection has been finalised.

## 4 The importance of stellar characterisation

Today we already know that planetary systems form around different types of stars, including low-mass stars like our Sun and more massive stars. Planets were found around both main sequence stars and evolved stars, and even around compact objects left from supernova explosions, like pulsars [120]. Thanks to Ariel we will gain new fundamental data on planets as they are today, but crucial properties related to their formation environments in the discs are long gone and cannot be observed anymore. On the other hand, part of this fundamental information is still available and preserved in the host stars.

### 4.1 Stellar host mass, type and metallicity: State of the Art from available observations

An important stellar property is its chemical composition. The iron abundance, expressed as [Fe/H] (the log number abundance of Fe/H relative to solar), is frequently used as a proxy for the metal content of the star. Already from the early studies of just four systems [121] noted that giant planets tend to orbit around metal-rich stars. It is well established that the frequency of gas-giant planets (whose planetary mass $M_p > 30\ M_\oplus$) correlates with the stellar metallicity [122–125]. While the Sun and other nearby solar-type stars have [Fe/H] $\sim 0$, typical exoplanet host stars have [Fe/H] $> 0.15$. Data shows that the percentage of stars with detected Jupiter-like planets with orbital periods less than 4 yr rises with the iron abundance from less than 3% for the FGK stars with subsolar metallicity, up to 25% for stars with [Fe/H] $\geq$ +0.3 dex [123]. On average, the metallicity distribution of stars with giant planets is shifted by 0.24 dex relative to that of stars without planets.

In contrast to the giant Jupiter-mass planets, less massive planets (either more similar to Neptune or super-Earths) do not form preferentially in higher metallicity environments [124, 126–128]. Indeed, the median metallicity for solar-type stars hosting low-mass planets is close to -0.10 dex, and a significant number of low-mass planets are orbiting around stars with metallicities as low as -0.40 dex [128]. This observational result is usually explained within the framework of core-accretions models (e.g. [129–131]) which assume that the timescale needed to form an icy/rocky core is largely dependent on the metal content of the protostellar cloud. In this way, in low-metal environments, the gas has already been depleted from the disc by the time the cores are massive enough to start a runaway accretion of gas. As a result, only low-mass planets can be formed. A possible correlation between planetary mass and stellar metallicity have been also suggested by [132].

The correlation between planetary occurrence and metallicity observed in main sequence stars may not extend to giant stars, as several studies have found contradictory results (e.g. [127, 133–137]). Several explanations have been put forward to explain the possible lack of a planet-metallicity correlation in evolved stars including the accretion of metal-rich material, higher-mass protoplanetary discs, and the formation of massive gas-giant planets by metal-independent mechanisms. Note that

red giants are the result of the evolution of MS dwarfs with spectral types G5V-B8V (stellar masses between 0.9 and 4 $M_{\odot}$). High-mass stars are likely to harbour more massive protoplanetary discs [138–142]. Simulations of planet population synthesis [138, 143] show that giant planet formation can occur in low-metallicity (low dust-to-gas ratio) but high-mass protoplanetary discs. This effect depends on the mass of the disc. The minimum metallicity required to form a massive planet is lower for massive stars than for low-mass stars. In this scenario, the fact that giant stars with planets do not show the metal-rich signature could be explained by the more massive protoplanetary discs of their progenitors. Planets around evolved stars show some peculiarities with respect to the planets orbiting around main-sequence stars, like a lack of close-in planets or higher masses and eccentricities (e.g. [134]). There is also a strong dependence of giant planet occurrence on stellar mass: stars of $\sim$1.9 $M_{\odot}$ have the highest probability of hosting a giant planet [137].

More observational evidence has been reported presenting correlations between planetary radius and host star metallicity [144, 145], as well as correlations between the eccentricity of planets versus metallicity [146, 147]. Although no clear correlations have been found between the stellar metallicity and the planetary semi-major axis, recent works discussed whether the stellar hosts of hot Jupiters ($a < 0.1$ au) show higher metallicities than stars with more distant planets. For example, [148] shows that the metallicity distribution of stars with hot gas-giant planets is shifted by 0.08 dex with respect to that of stars with cool distant giants. The authors also noted a paucity of hot Jupiters orbiting stars with metallicities below -0.10 dex, whilst cool Jupiters can be found around more metal-poor stars. Along these lines, [149] and [150] suggest that stars hosting massive gas-giant planets show on average lower metallicities than the stars hosting planets with masses below 4–5 $M_{Jup}$. Finally, unlike gas-giant planet hosts, stars with brown dwarfs do not show metal enrichment (e.g. [151]) although [152] found that stars with low-mass brown dwarfs tend to show higher metallicities than stars hosting more massive brown dwarfs.

The emerging picture is one in which **different planet formation mechanisms may operate altogether and their relative efficiency changes with the mass of the substellar object that is formed**. For substellar objects with masses in the range from 30 $M_{\oplus}$ up to several Jupiter masses, high host star metallicities are found, suggesting that these planets are mainly formed by the core-accretion mechanism. More massive substellar objects do not tend to orbit preferentially around metal-rich stars and are likely to be formed by gravitational instability or gravoturbulent fragmentation [153, 154].

Most of the planet-host stars with low iron content belong to the thick disc population [155, 156]. Thin-disc stars rotate faster than the local standard of rest and show solar $\alpha$-element abundances (Mg, Si, Ca, Ti). On the other hand, the thick disc

is enriched in alpha elements and lags behind the local standard of rest [157, 158]. It has been argued that to form a sufficiently massive core, the quantity that should be considered is the surface density of all condensible elements beyond the ice line [143], especially the elements O, Si, and Mg [159, 160]. In particular, Mg, and Si have condensation temperatures very similar to Fe [161]. It is therefore likely that stars with intermediate metallicity might compensate their lower metal content with other contributors to allow for planet formation to occur. Along these lines, [156] found that most of the planet-host stars with low Fe content are enhanced by $\alpha$ elements. This $\alpha$-enhancement is a common property of most of metal-poor stars and is an effect of galactic chemical evolution, as most of the present Fe is made in thermonuclear supernovae while most of the $\alpha$-elements like O or Si are made mostly in massive stars.

Regarding other chemical abundances besides Fe, planet-hosting stars are largely indistinguishable in their enrichment histories of refractory elements (e.g. [156, 162, 163]), or show rather modest overabundances, with respect to other stars without planets. Volatile elements (C, O, Na, S, and Zn) are important in the chemistry of protoplanetary discs and planets. Stellar abundances can be difficult to estimate and high resolution data with high signal-to-noise are necessary to quantifying them. Spectral lines can be weak and blended, depending by the specific element, and cooler stars ($T < 4500$ K) in particular present molecular bands that need a specific approach for treating elemental abundances. Interestingly, most volatiles show a decreasing trend of [X/Fe] with increasing [Fe/H], but the abundance trends for planet-hosting stars for volatile elements are similar to those for the comparison stars at the corresponding (high) values of [Fe/H] (e.g. [164–167]). More references can be found in [168].

The abundance of lithium is an important diagnostic of stellar evolution. Several works have suggested that stars with planets tend to have less lithium than stars without. In particular, [169] found an excess Li depletion in planet-hosting stars with effective temperatures in the range 5600-5850 K, but no significant differences at higher temperatures. While this result has been confirmed by the majority of studies (e.g. [170–173]), other works have reported an absence of depletion for planet-hosting stars (e.g. [127, 174]). High Li abundance has also been reported in several rapidly rotating red giants that might be attributed to recent planet engulfment (e.g. [175–177]).

Beryllium, like lithium, is another tracer of the internal structure and (pre) main-sequence evolution. A higher beryllium depletion has been found for stars with effective temperatures lower than 5500 K, but this process seems to be independent of the presence of planets [178]. Detailed chemical abundances of planet hosts has shown that the Sun and other solar analogues are depleted on refractory relative to volatile elements by $\sim$0.08 dex when compared with the majority of nearby solar twins (e.g. [171, 179–183]). After discussing several possible origins, [179] conclude that the most likely explanation is related to the formation of planetary systems like our own, in particular to the formation of rocky low-mass planets. Although appealing, this hypothesis has been questioned, and other works point towards chemical evolution effects [184–187], or an inner Galactic origin of the planet hosts (e.g. [188, 189]) as their possible causes.

One aspect that is currently challenging the detection of low-mass planets is stellar activity (e.g. [190]). Exoplanet host stars display a wide variety of chromospheric and magnetic activities dependent mostly on their spectral type (e.g. [168], and references therein). For example, [191] and [192] performed a detailed study of large samples of stars in planet search programs, using activity indexes to estimate the level of radial velocity jitter of the program stars. [193] compared the activity index $R'_{HK}$ measured in stars with and without planets finding similar distributions. In addition, no significant correlations between $R'_{HK}$ and the planetary properties were found. [183] found that stars with planets have significantly smaller values of vsin $i$ and $R'_{HK}$ compared to otherwise similar non-planet hosts. No differences in the X-ray emission between planet hosts and non-host were found by [194] although the authors reported higher X-ray luminosities for the stars hosting close-in giant planets. However, [195] found no correlation between the X-ray luminosity and the planet's mass or orbital distance.

Observations indicate that host stars of some close-in hot Jupiters undergo episodes of periodic or enhanced stellar activity, linked to the presence of the planet through magnetic or tidal interactions (see e.g. [168], and references therein). Periodic activity has been reported both in the Ca II H & K and/or Balmer line emission in several planet-hosting stars, such as $\nu$ And and HD 179949, and inferred from optical brightness variations in the case of $\tau$ Boo [196–198]. Another example is HD 17156, where enhanced chromospheric and coronal emissions were detected a few hours after the passage of the planet at the periastron [199].

### 4.2 Pristine chemical composition of the star and planet system

The original chemical composition of a stellar system, encompassing the star and its circumstellar disc, is part of the initial conditions for the planet formation process and sets some of the fundamental properties of the planets that the star will host. In particular, the initial chemical setup of the system will affect the envelope/mantle properties and the atmospheric composition of the planets. The relative ratios of elements such as O, C, Mg and Si will set the mineralogy of the planets and the impact of volcanic activity on their atmospheres (e.g., [200, 201]).

The information on the initial chemical composition of the system will be modified and partly erased throughout the planet formation process (e.g. due to the different behaviour of volatile and refractory elements and the effects of planetary migration, see Sections 6 and 7). The surface/photospheric composition of the host star, however, will preserve this information almost unchanged over time (e.g., [202]). The characterization of the stellar composition, therefore, provides fundamental information and the context to reconstruct the dynamical and formation histories of planets from their observed atmospheric composition (see also Section 6). While the definition of the Solar System abundances (both present and protosolar) is constantly updated thanks to photospheric and meteoritic data, and today we know them with good precision (though uncertainties still remain, see

e.g. the oxygen crisis, [72, 73], and references therein), the same is not true for all stars.

For most stars many elements are either not available or observed with much larger errors than Fe, and other elements like phosphorus and chlorine are not observable. Furthermore, the Milky Way disc is a complex system, where galactic chemical evolution (GCE) is changing chemical abundances over a timescale of billions of years, and the chemical enrichment history among stars with similar age and/or galactic location may show significant variations beyond observational errors. For this very reason, **the solar initial composition cannot be universally applied to different stellar systems**.

The characterization of the stellar host composition and of the initial planetary system composition needs to adopt a multi-disciplinary approach: available elemental spectroscopic data can be integrated with theoretical GCE simulations. In Fig. 2, left panel, the elemental ratios [C/O] and [Mg/Si] are shown for a stellar sample of the Milky Way disc by [157, 158], covering a metallicity range similar to that of the Ariel expected targets [4]. The Sun is also reported for comparison. Without considering 5% of disc stars with more exotic composition, the remaining 95% stars show a variation of [C/O] and [Mg/Si] between 0.3 and 0.4 dex in logarithmic notation, which corresponds to a variation between a factor of 2 and 2.5. GCE simulations for one possible chemical enrichment history are also shown in Fig. 2 for comparison.

The model was generated using the GCE code OMEGA from the NuPyCEE package [203, 204]. The yellow star symbol corresponds to the Sun formation time, 4.6 billions years ago. The model shown seems to provide an acceptable representation of the Sun, with a perfect match of the [C/O] ratio, and underestimating by about 0.1 dex (this corresponds to 25%) the [Mg/Si] ratio. The chemical enrichment history from the same model is shown in Fig. 2, right panel, for C, O, Mg and Si, in the relevant metallicity range [Fe/H] currently foreseen for the Ariel sample [4]. Within the metallicity range considered, it is interesting to observe the different trend of Si and C compared to O and Mg. This is due to the different chemical enrichment history of these elements (e.g., [205–207]).

For a benchmark of the correct initial composition of all Ariel targets, an extended set of consistent GCE models will need to be generated covering the observations for element ratios like [C/O] and [Mg/Si], at the correct age of the stellar hosts. These models will have all the elements available, at any time, to compare with stellar observations and inform theoretical planet simulations. The relative abundance scatter obtained from these simulations need to be simulated, and their impact on planet simulations is still unknown.

### 4.3 Pristine radioactivity, local enrichment and galactic chemical evolution

Together with stable isotopes and elements, stars also make radioactive isotopes. Some of them have an half-life long enough to affect the formation and evolution

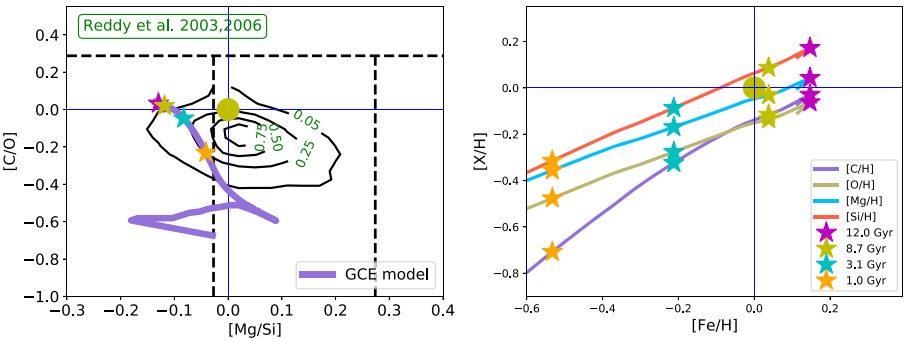


**Fig. 2** *Left Panel:* stellar statistics distribution with respect to [C/O] and [Mg/Si] from observations [157, 158] and GCE models. The elemental ratios are reported in logarithmic notation, scaled to solar value. The Sun is reported as reference, with blue lines indicating the solar ratios. Dashed black lines indicate the element classification relevant for planet behavior according to [200]. GCE simulations are reported (magenta line), with reference time symbols at 1 Gyr, 3.1 Gyr, 8.2 Gyr (which corresponds to the age of the Sun) and 12 Gyr after the formation of the Milky Way (orange, cyan, yellow and magenta star, respectively). *Right Panel:* [C/H], [O/H], [Mg/H] and [Si/H] are reported with respect to [Fe/H] for the same GCE model reported in the left panel

of new-forming planetary systems. The $^{26}$Al and $^{60}$Fe isotopes have a half-life of $7.17\times10^5$ years and $2.62\times10^6$ years, respectively. Traces of extinct $^{26}$Al and $^{60}$Fe were found in the early Solar System condensates, and we know that their heat contribution is crucial during planetesimal formation ([208], and references therein). The short half-life of $^{26}$Al and its abundance derived from early Solar System material exclude a relevant GCE contribution. Therefore, its abundance in the protosolar nebula is due to the contribution of local stellar sources, like the explosion of nearby supernovae, baking these species relatively nearby and shortly before the formation of the Sun. The argument is more controversial for $^{60}$Fe, where its low abundance relative to $^{26}$Al in the early Solar System is making unclear if its composition was a GCE product or if it was dominated from local stellar sources, as for $^{26}$Al ([209], and references therein).

Today we have evidence that pollution of radioactive material from other stars continued over time, not only during the formation of the Solar System. For instance, traces of the radioactive isotope $^{60}$Fe have been discovered in fresh Antarctic snow, signifying further pollution from recent supernovae [210]. Extinct $^{60}$Fe has been detected in the ocean crust, falling through Earth's atmosphere and oceans about 2.2 million years ago (e.g., [211]). This has been connected with a mass extinction event affecting many species in our oceans about 2.6 million years ago, due to the radiation from the same nearby supernova (e.g., [212]). This makes really hard to define what is the correct amount of $^{26}$Al and $^{60}$Fe to use in simulations of planet formation.

Values obtained from meteorites for the early Solar System are the outcome of local stellar pollution or, perhaps, the combined outcome of stellar pollution and GCE for $^{60}$Fe. Even an ideal stellar system, composed by a solar twin with the exact same elemental composition, may have a complete different concentration of initial $^{26}$Al

and $^{60}$Fe. And, as we mentioned before, GCE simulations alone are not providing a correct answer, since the half-life of these isotopes is too short. In preparation to Ariel's observations, a new generation of theoretical simulations will be needed. The initial $^{26}$Al and $^{60}$Fe abundances need to to be varied within a realistic range, from background GCE concentrations (e.g., [209]), up to realistic abundances guided from stellar simulations of different types of stars that can produce $^{26}$Al and $^{60}$Fe (e.g., [213–216]).

The radioactive isotopes $^{40}$K, $^{232}$Th, $^{235}$U and $^{238}$U all have half-lifes of the order of 1 billion years or larger. Therefore, their galactic enrichment history behaves more like that of stable isotopes, and GCE simulations are needed to calculate their evolution in the interstellar medium. Once the planets are formed, the abundance of these species determines their internal heating history, sustaining tectonic activity and the magnetic field. The potassium observed today on the surface of the stellar host does not tell much about the initial $^{40}$K, and thorium and uranium are extremely hard to observe in stellar spectra. A possible strategy would be to get the realistic range of these abundances from GCE simulations, where the stellar sources of these isotopes are properly considered.

This analysis is more difficult for thorium and uranium, since they are product of the rapid neutron capture process (r-process). The dominant astrophysical source of the r-process is still matter of debate, and several sites like neutron-star mergers have been proposed (e.g., [217, 218], and references therein). An approach complementary to the one mentioned above is to perform a study of the production of $^{40}$K and actinide elements, to define observations from the abundance pattern measured in the stellar host that can be used as a diagnostic of their concentration. For instance, the r-process element europium measured from the surface of the stellar hosts could be used as a diagnostic for the initial abundance of the radioactive isotopes $^{232}$Th, $^{235}$U and $^{238}$U. At present, there is no available estimation of how much the abundances of these isotopes may change in the galactic disc in the metallicity range of interest for Ariel targets.

## 5 Organics as C-O-N carriers

In the last 10 years there has been a number of surveys dedicated to assess the molecular content of protoplanetary discs, targeting mostly the simpler bi- and tri-atomic molecules such as CO, CN, $H_2O$, $HCO^+$, $DCO^+$, $N_2H^+$, HCN, DCN (e.g. [51, 219–223]), as well as a few S-bearing species, e.g. CS, $H_2CS$, $H_2S$ (e.g., [224–231]). The content of complex organic molecules (COMs), on the contrary, is still only poorly known because of their lower gas-phase abundances ($< 10^{-8}$ with respect to the abundance of atomic hydrogen). According to disc models this is due to the fact that COMs are frozen on the icy mantles of dust grains in the cold disc interior and only a tiny fraction of them is released in gas-phase through thermal or photo-/CR-desorption (e.g. [232–235]). Hence, (complex) organic molecules in protoplanetary discs remain hidden in their ices and can be unveiled only through interferometric observations at high sensitivity and resolution, e.g. with ALMA.

The study of COMs in protoplanetary discs is key to estimate the fraction of C, O, and N atoms that are trapped in organic molecules. While it is generally thought that most of these atoms are incorporated in ices (in the form of, e.g. $H_2O$, $CO_2$, CO, etc), there is the possibility that organic molecules trap a significant amount of them, as also suggested by recent observations of comets in the Solar System (e.g. [236]). **As organic molecules are carriers of C, O, and N, it is crucial to estimate their abundance and the location of their snowlines, to infer accurate C/O/N ratios in the gas and solids of discs, with direct implications for the final C/O/N ratios of planets**.

Thanks to ALMA a few simple organics have been imaged in discs. Among those, formaldehyde ($H_2CO$) and methanol ($CH_3OH$) are key to investigate organics formation. While $H_2CO$ can form both in gas-phase and on grains, $CH_3OH$ forms exclusively on grains. An illustrative example are the resolved ALMA images of $H_2CO$ in nearby protoplanetary discs [228, 229, 235, 237–244]. These allowed us to infer the $H_2CO$ abundance and distribution in protoplanetary discs and to constrain the mechanism(s) for its formation in this environment. This is key, given that $H_2CO$ is one of the bricks for the formation of complex organic and prebiotic molecules.

The distribution of $H_2CO$ suggests that the bulk of the observed $H_2CO$ in the disc is formed via gas-phase reactions. This is indicated both by the o/p ratios measured in TW Hya [245] and by the vertical distribution of molecular emission in the edge-on disc of IRAS 04302 where $H_2CO$ mostly arises from an intermediate disc layer, the so called molecular layer [231, 244]. However, for IRAS 04302 $H_2CO$ emission is detected also in the outer disc midplane, where molecules are expected to be frozen onto the dust grain icy mantles. Also for a few discs the observations show a secondary emission peak of $H_2CO$ located outside the CO snowline which may argue in favour of $H_2CO$ formation on grains in these outer disc regions, following freeze-out of CO and its subsequent hydrogenation on the icy grains [238, 239, 241, 242] (see e.g. Fig. 3 Right). This may indicate that ice chemistry is efficient in the outer regions of discs and could produce methanol as well as other complex organics, which are then partly released in gas-phase via non-thermal processes. However, only a few of them has been so far detected, i.e. cyanoacetylene and methyl cyanide ($HC_3N$, $CH_3CN$, [64, 246]), methanol ($CH_3OH$, [63, 243]), and formic acid (HCOOH, [65]). Typical abundances are: $10^{-12}$-$10^{-10}$ ($H_2CO$), $10^{-12}$-$10^{-11}$ ($CH_3OH$, HCOOH, $HC_3N$), $10^{-13}$-$10^{-12}$ ($CH_3CN$).

At the protostellar stage observations are hindered by the presence of many kinematical components that may hide the chemical content of the disc, e.g. the surrounding envelope and the outflow. To date only one protostellar disc has been chemically characterised on Solar System scale, the disc of HH 212 (see Fig. 3 Left). This pioneering work shows enriched chemistry associated with the disc surface layers, with the detection of a number of complex organic molecules, e.g. $CH_3OH$ ($10^{-7}$), HCOOH ($10^{-9}$), $CH_3CHO$ ($10^{-9}$), $HCOOCH_3$ ($10^{-9}$), $NH_2CHO$

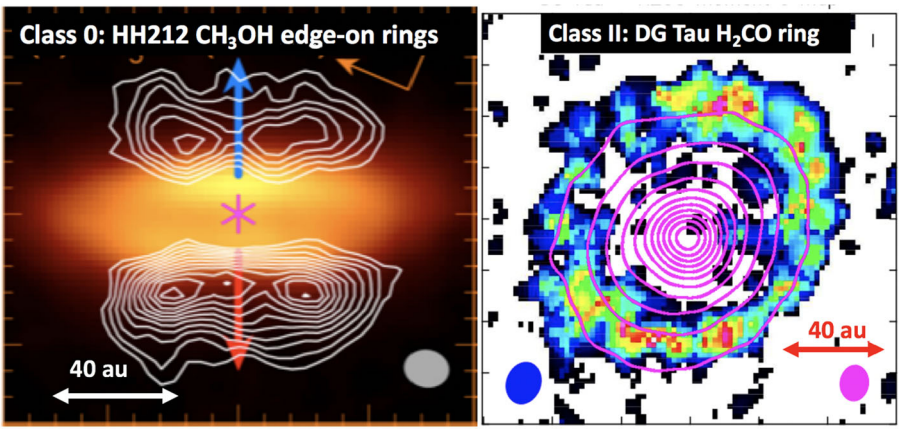


**Fig. 3** The protostellar discs around the Class 0 star HH 212 and the protoplanetary disc of the Class II star DG Tau as observed with ALMA. *Left*: continuum (colour) and $CH_3CO$ (contours) of the protostellar discs around HH 212. *Right*: continuum (contours) and $H_2CO$ (colour) of the protoplanetary disc of DG Tau. Figures adapted from [247] and [241]

($10^{-10}$) (e.g. [247–250]). These abundances are larger than what observed at the protoplanetary stage.

This chemical enrichment may be due to slow shocks occurring at the interface between the infalling envelope and the forming disc (e.g. [251]). The chemically enriched gas should then settle in the rotationally-supported disc, where the chemical composition is likely stratified and affected by the dynamics and the dust coagulation. The scenario obtained for HH 212 needs to be confirmed by collecting observations on a statistical sample. Answers are expected soon from the FAUST ALMA Large Program (Fifty AU STudy of the chemistry in the disc/envelope system of Solar-like protostars, http://faust-alma.riken.jp) and from the ALMA-DOT program (ALMA chemical survey of disc-outflow sources in Taurus, [228]). The goal of these projects is to reveal the chemical composition of the envelope/disc system on Solar System scale in a sample of discs from the protostellar to the protoplanetary stages.

In order to test the inheritance scenario, i.e. whether the molecular setup of protoplanetary discs is largely inherited from the molecular clouds from which the stars formed, it is also crucial to compare the chemical composition of protostellar objects with that of Solar System objects (the final stage of Sun-like stars formation process). Comets are ideal for this purpose, as they sample the pristine composition of the outer Solar System. A comparative study of the comet 67P Churyumov-Gerasimenko, visited and characterized in detail by the ESA mission Rosetta, with two Solar-like protostellar systems, IRAS16293-2422B and SVS13-A, shows similar abundances of $NH_2CHO$ and $HCOOCH_3$, and in general of CHO-, N- and S-bearing species, which suggests inheritance from the presolar phase [252, 253]. Also in this case these promising results need to be confirmed by further comparative studies.

## 6 Giant planets and their composition

Giant planets, from Neptune-like to super-Jovian planets, currently represent the bulk of Ariel's observational sample [4]: as a result, efforts are being devoted to improve our understanding of what factors can shape their atmospheric composition as will be observed by Ariel [3]. In the following we focus on three of these factors: the link between orbital migration and metallicity (Section 6.1), the distribution of accreted material between the core and the growing envelope (Section 6.2), and the compositional features arising from different migration histories (Section 6.3).

### 6.1 Planetary migration and bulk metallicity

Many hot Jupiters are found to be highly enriched in heavy elements compared to their stellar-host metallicity. Theory suggests that some of these planets are expected to consist of several tens and even hundreds of Earth-masses of heavy elements (although still with large uncertainties, see [255–258]). This introduces great challenges to the giant planet formation theories since the expected enrichment from the standard formation process is very moderate and typically cannot exceed about 20 $M_{\oplus}$ (e.g. [259]). As a result, the enrichment of the planets must be explained.

One could imagine that the planetary enrichment occurs after the planet has formed and gas accretion terminated, a natural pathway being planetesimal capture. This process, however, is quite inefficient once the giant planets approach their final mass values (being able to supply a few Earth-masses of heavy elements at most, [260], and references therein) and becomes even less efficient in presence of post-formation migration. [254] and [261] recently investigated the enrichment of warm gas giants via planetesimal capture during inward migration. [254] performed orbital simulations of migrating giant planets of different masses and planetesimals in a protoplanetary gaseous disc and inferred the heavy-element mass that is accreted by the planet. [261] focused on Jovian planets but traced also their mass and radius evolution during their migration.

> Shibata et al. [254] found that **migrating giant planets capture planetesimals with total masses of several tens of Earth masses**, if the planets start their formation at tens of au in relatively compact discs (less than 100 au, as generally assumed for the solar nebula). A similar result is obtained in the study by [261] focusing on large (gas extending to a few 100 au) but not exceedingly massive discs (disc masses of the order of a few $10^{-2}$ $M_{\odot}$) if the giant planets have formation regions comparable to those recently observed by ALMA, i.e. extending from a few tens to about a hundred au from the host star (e.g. [68]).

Depending on the characteristics of the considered protoplanetary disc, planetesimal capture seems to be efficient in a rather limited range of semi-major

axis [254] or for migration tracks spanning several tens of au [261]. Nevertheless, both studies showed that the total captured planetesimal mass increases with increasing migration distances. It was also shown that mean motion resonances trapping and aerodynamic gas drag inhibit planetesimal capture of a migrating planet, and therefore large scale migration and/or massive/enriched discs are required to explain the enrichment of planets with several tens Earth masses of heavy elements.

Figure 4 summarizes the results of the study performed by [254], which suggests that enriched giant exoplanets at small orbits have not formed *in situ* since they must have migrated inward in order to accrete large amounts of heavy elements. As will be discussed in more detail in Section 8, however, recent population studies investigating the architectures of known multi-planets extrasolar systems [262–265] suggest that a significant fraction of these planetary systems underwent or are crossing phases of chaotic evolution possibly associated to migration by planet-planet scattering [266, 267].

A widespread presence of chaos-driven migration in the life of planetary systems, in alternative or in conjuction with disc-driven migration, would introduce a layer of uncertainty in unequivocally linking the formation and dynamical history to its heavy element enrichment. As an example, a giant planet forming and migrating between 30 and 20 au while embedded in the disc, as in the accretion tracks by [254], and later being scattered to a fraction of au by planet-planet scattering could be characterized

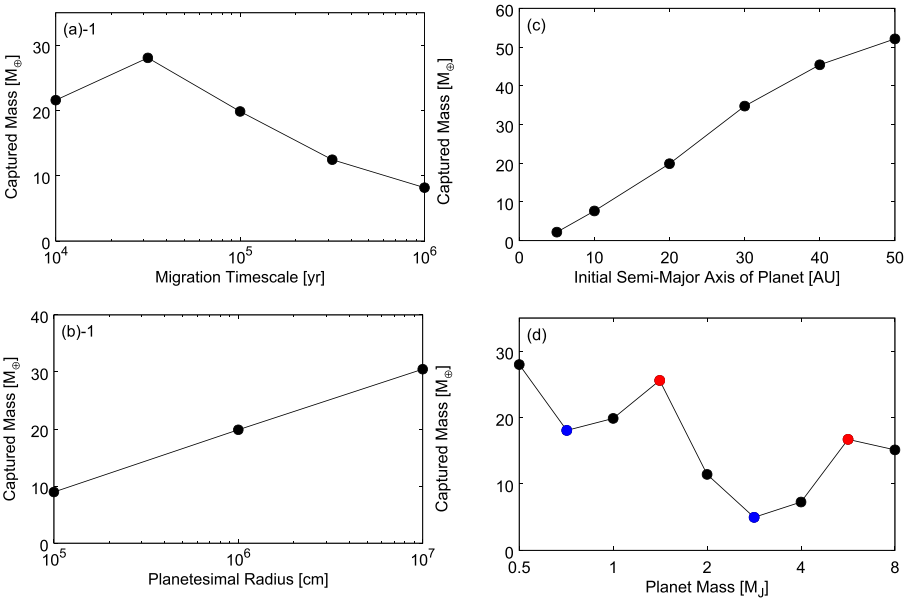


**Fig. 4** Results of the parameter study of planetesimal capture by a migrating protoplanet performed by [254]. Shown is the total mass of captured planetesimals in Earth masses as a function of: the migration timescale of the planet **a**-1, the radius of planetesimals **b**-1, the initial semi-major axis of the planet **c**-1, and the mass of the planet **d**-1

by the same heavy element enrichment than a giant planet that started forming at about 10 au and experienced only disc-driven migration (see e.g. the top right panel of Fig. 4). As we will illustrate in Section 6.3, however, the different compositional signatures of the accreted heavy elements allow for breaking this degeneracy.

### 6.2 Envelope enrichment through core formation

Several recent works follow the ablation of accreted solids in the gaseous envelope in the planet formation phase and find a significant pollution of the growing gas envelope by the accreted solids (e.g. [268–270]). It is found that when the planetary core mass is less than a few Earth masses most of the accreted solids, both rocks and ices, are deposited in the gaseous envelope and don't reach the core. As the formation processes continues, the internal temperatures increase, the gravity becomes stronger and the gas is denser, and thus a larger fraction of the solids stays in the envelope.

The resulting structure right after the planet formation is then of a **gradual composition distribution instead of a core-envelope structure**. This primordial gradual metal distribution may evolve to a metal enrichment of the envelope in the long term. Under certain conditions, that are common in gas giant interiors, convection and therefore **convective-mixing can spread the composition gradient to the outer envelope in time**, and increase the outer envelope metallicity [271].

The measured metal enrichment by the Ariel mission, and the derived statistics for different planetary types, can be used to constraint the formation outcomes and the convective behaviour. For example, in absence of fragmentation the envelope enrichment is greater in the case of pebble accretion than in planetesimal accretion. As is shown in the left panel of Fig. 5, pebbles dissolve better and earlier in the envelope than planetesimals, and therefore results in a more enriched envelope for the same planetary mass. The break-up of planetesimals during accretion can enhance the envelope pollution that is shown in Fig. 5 [269, 272]. Overall, ablation of pebbles is more efficient for small core/envelope masses while planetesimal break-up and ablation play a significant role for envelope masses greater than a few Earth masses [272, 273].

After the formation phase the local metal enrichment can be redistributed in the planet's envelope by convective-mixing. Long-term evolution of the structure by convective-mixing successfully explains the properties of our Solar System giant planets [274–276], and is expected to take place in giant exoplanet interiors. The efficiency of the mixing depends on the metals distribution: an outer moderate enrichment tend to mix efficiently, while a deeper steeper distribution remains stable, as is shown in the right panel of Fig. 5 for Jupiter. Thus, the initial metal enrichment by the formation building blocks affects the long-term atmospheric abundances of the planet.

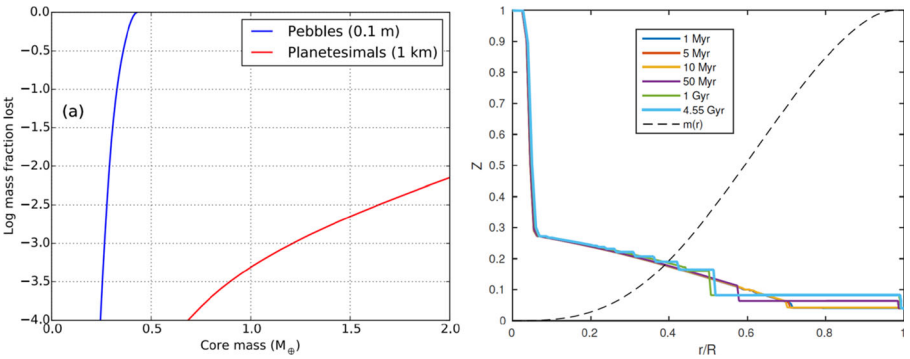


**Fig. 5** *Left:* Mass deposition in the envelope (lost) as a function of the growing core mass, for rocky planetesimals (red) and pebbles (blue). Fragmentation is ignored. Rocky planetesimals lose approximately 1% of their mass when the forming planet has a core mass of 2 Earth masses, whereas the pebbles are fully evaporated before the planet's core mass reaches 0.5 Earth mass [268]. *Right:* the change in time in the metal distribution (Z) in the interior of Jupiter. At early ages convective-mixing is efficient in the outer shallow composition gradient, while the inner steeper gradient remains stable [275]

### 6.3 Compositional signatures of different formation regions

A number of studies have been devoted in recent years to link the information supplied by the composition of giant exoplanets to their formation and migration histories. Before discussing the insight they provide, however, it is important to point out that their task is made particularly challenging by our still incomplete understanding of the chemical environment of protoplanetary discs, the birthplace of giant planets. As highlighted by the discussions in Sections 2 and 5, even if modern observational facilites are providing an unprecedented view of protoplanetary discs, their physical and compositional characterization is still hindered by a number of uncertain parameters and observational limitations. A particularly critical source of uncertainty is associated with the initial molecular setup of protoplanetary discs, as it is unclear whether protoplanetary discs inherit their composition from the prestellar phase or undergo a complete reset due to the radiation environment of their young stars.

As discussed in Section 5, the results of the recent comparisons between the volatile inventory of the comets in the Solar System and Solar-like protostellar systems appear to support a strong role of inheritance from the prestellar phase [74, 252, 253]. However, even in this scenario, discs are expected to chemically evolve [277, 278] and cool down over time. Their temperature decrease will cause the snowlines of the more volatile elements to drift inward with respect to their original positions [278, 279]. Finally, the differential radial drift of the dust grains with respect to the gas will cause volatile elements initially frozen on the grains to cross the snowlines in the disc and sublimate, locally enriching the gas [280–282]. A recent, detailed review of these processes and how they are expected to shape the compositional environment of protoplanetary discs is provided by [283].

It is important to note, however, that the magnitude of the previously listed effects is linked to the abundance of dust grains and pebbles in discs and that the conversion

of dust and pebbles into planetesimals act to reduce the rate of compositional evolution of protoplanetary discs. The smaller surface-to-volume ratio of planetesimals with respect to dust and pebbles will slow down the rate of gas-grain chemistry and, due to the thermal inertia of the planetesimals that effectively isolate the ices trapped in their interior, will limit the effects of ice sublimation at the crossing of snowlines (e.g. [261]). Observational evidences from both protoplanetary discs [284] and meteorites in the Solar System [285] points toward an efficient conversion of the bulk of dust into planetesimals on a timescale of less than 1 Myr, and possibly of the order of $10^5$ years [286]. Such conversion would thus appear to proceed at a pace comparable or faster than the global evolution timescale (of the order of 1 Myr) estimated by astrochemical models of evolving discs [278], suggesting the possibility of an early "freezing" of the composition of protoplanetary disks.

While we are still limited by our incomplete understanding of the compositional nature of protoplanetary discs, a growing literature has been focusing over the past decade on exploring the link between the abundances of the two most abundant high-Z elements, carbon (C) and oxygen (O), and the planet formation process (see e.g. [287, 288], and references therein for recent overviews). The general expectation since the early results from [222] is for low metallicity giant planets, where the bulk of C and O are accreted from the gas, to be characterized by super-solar C/O ratios, while for high-metallicity giant planets, where C and O are dominated by the capture of solids, to be characterized by sub-solar C/O ratios. As a consequence, studies have been investigating the possibility to use the C/O ratio as a proxy into the formation region of giant planets (see e.g. [287] and references therein for an overview and [289, 290] for recent results).

Critical factors to this end, however, are the distribution of C and O across the different phases (rocks, organics, and ices) and volatile molecules (e.g. $H_2O$, $CO_2$, CO, $CH_4$), our understanding of which has been significantly evolving over the past decade thanks to the data provided by meteorites, comets, polluted white dwarfs, and protoplanetary discs (e.g. [72, 74, 75, 222, 236, 261, 289–300]), and the extension of the planet-forming region in discs, recently put into question by observational surveys of protoplanetary discs with ALMA (e.g. [68, 301–305]).

A study performed in the framework of the Ariel Consortium ([261], see Fig. 6, left plot) confirms the general picture described above for the planetary C/O ratio also in the case of giant planets forming at tens and beyond one hundred of au from the host star, as suggested by the results of ALMA surveys. The same results, however, show how for giant planets forming so far from their host stars the information provided by the C/O ratio may be less detailed than expected. In the framework of the inheritance scenario coupled with the early conversion of dust into planetesimals considered in the study, the reason for this is easily understood if one considers that, due to their higher volatility, CO and $CH_4$ condense about a order of magnitude farther aways from the star than $CO_2$ (see Fig. 6, right plot). This in turn means that over a large fraction of the planet-hosting region suggested by ALMA's observations, the gas in the disc will be populated mainly by CO and $CH_4$. Giant planets forming beyond the $CO_2$ snowline will therefore accrete material from a region where the C/O of the gas will be dominated by the contributions of these two molecules ($C/O \gtrsim 1$, see the right plot of Fig. 6). While gaseous CO and $CH_4$ will increase the C abundance of the gas

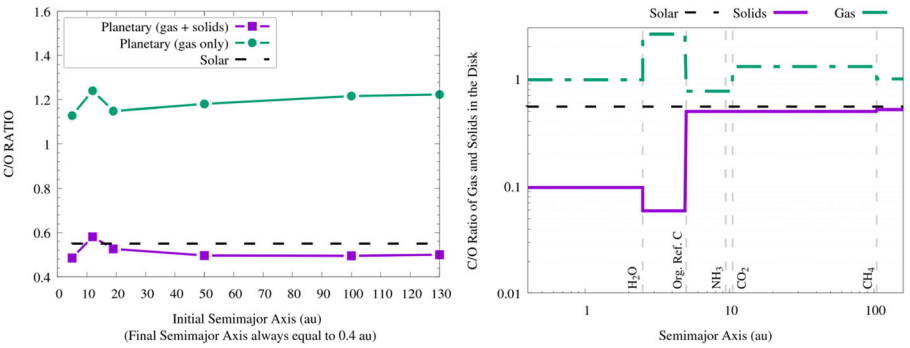


**Fig. 6** *Left* : C/O ratio of giant planets undergoing extensive migration from formation regions consistent with those observed with ALMA. *Right* : C/O ratio of the gas and solids in the protoplanetary disk taking into account the roles of refractories and refractory organics as carriers of O and C (see main text and [261] for details). The $CO_2$ snowline is located at about 10 au and the disc gas is dominated, from that point outward, by CO and $CH_4$ (C/O$\gtrsim$1). As a result, giant planets forming beyond the $CO_2$ snow line and accreting limited solids will have C/O$\gtrsim$1, while giant planets accreting large quantities of solids will have C/O slightly smaller than the stellar value. Figure adapted from [261]

and reduce that available for condensates, the abundances of these molecules will cause the C/O ratio of solids in this region to be only slightly smaller than the stellar value (see Fig. 6, right plot).

As a result, giant planets starting their formation at orbital distances spanning the range revealed by ALMA surveys will accrete significant fractions of their mass, if not most of it, beyond the $CO_2$ snowline. Those giant planets whose mass growth is dominated by gas (low metallicity giant planets), e.g. forming across orbital regions previously depleted of planetesimals by the formation and migration of another giant planet, will have C/O$\gtrsim$1 [261]. Those capturing significant amounts of solids in the form of planetesimals (high metallicity giant planets) will have C/O slightly below than the stellar value almost independently on their exact formation region (see Fig. 6, left plot, and [261]). The limited changes in the C/O values shown in the left plot of Fig. 6 are smaller than the accuracy of current retrieval tools (e.g. [306]), meaning that those C/O values would be observationally indistinguishable from each other. This translates in the fact that the C/O ratio might only allow to distinguish low metallicity, gas-dominated giant planets from high metallicity, solid-enriched giant planets and provide the information that they formed and captured most of their heavy elements farther out than the $CO_2$ snowline [261].

The picture discussed above has been derived assuming the compositional inheritance of the volatile materials in the protoplanetary disc from the pre-stellar phase. As discussed at the beginning of this section and in Section 5 (see also [74] and [283] for more detailed discussion), while there are lines of evidence supporting such a scenario, it does not represent the only possible compositional setting for the planet formation process. The partitioning of the volatile molecules between gas and planetesimals can be markedly different in a compositional reset scenario, in principle making the picture described above for the planetary C/O ratio invalid. As discussed

in [261], future studies will need to quantify the effects of the different compositional scenarios on the planetary C/O ratio for giant planets forming over a wide range of orbital distances, to clarify the limits of its diagnostic power. Similarly, the effects of different couplings between the planet formation and the disc evolution timescales will need to be explored. Nevertheless, the available observational data on the roles of refractories and refractory organics as carriers of O [72, 291, 292, 300] and C [297–299] support the possibility that the quantitative changes in the planetary C/O ratio between one compositional scenario and another could be less marked than previously thought and, consequently, that the C/O ratio may provide only limited information.

The vast coverage of Ariel in terms of molecules offers a straightforward way out of this limitation by allowing for the use of multiple elemental ratios [1, 3]. An illustrative example is provided by Fig. 7, which shows the results obtained in the study by [261] using an extended set of four elemental ratios including, in addition to C and O, other cosmically abundant elements as nitrogen (N) and sulphur (S).

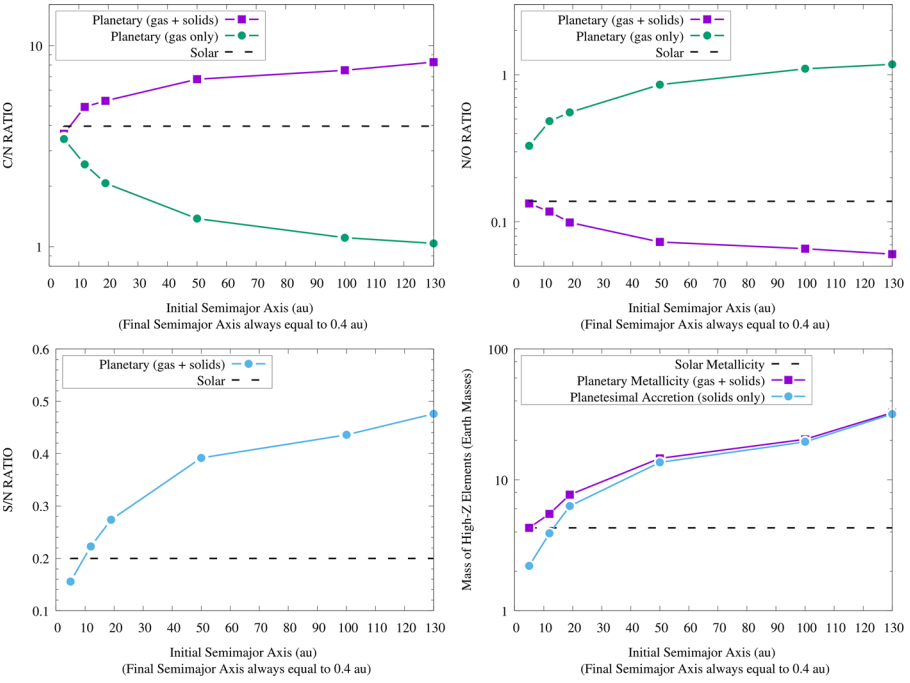


**Fig. 7** C/N (top left), N/O (top right) and S/N (bottom left) elemental ratios of a Jupiter-sized giant planet as a function of different formation regions and migration tracks [261]. The Jovian planet starts its formation at the specified orbital distances and undergoes disc-driven migration until it becomes an hot Jupiter. The horizontal dashed lines indicate the stellar elemental ratios, assuming a solar composition for the host star and the protoplanetary disc [72]. The different curves in the top half of the figure refer to different mass growth scenarios involving the accretion of both gas and planetesimals ("gas + solids") or the sole gas ("gas only"). Also shown is the comparison between the total mass of heavy elements accreted by the giant planet and the one due only to planetesimal capture (bottom right), which highlights how the S/N ratio can be used as a proxy into the planetesimal contribution to metallicity. Figure from [261]

The inclusion of N alongside C and O allows for computing two additional ratios: N/O and C/N. Due to the higher volatility of N with respect to C and O, the N/O ratio grows with migration for low metallicity giant planets and decreases for high metallicity ones, while C/N behaves the opposite way. The farther the giant planet starts its migration from the host star, the more its C/N and N/O ratios will diverge from the stellar ones [261].

The inclusion of S alongside N allows for computing the S/N ratio: given that the bulk of S is efficiently trapped into refractory solids (e.g. [71, 72, 291, 292]) while the bulk of N remains in gas phase as highly volatile $N_2$ for most of the extension of discs (e.g. [277, 278, 282, 307, 308]), this ratio offers a direct probe into the planetary metallicity and, specifically, the fraction of the planetary metallicity due to the accretion of planetesimals (see Fig. 7). The S/N ratio, therefore, can be used to constrain, independently on the knowledge of the planetary mass and radius, the disc-driven migration experienced by the giant planet as discussed in Section 6.1 (see [261] for a discussion). Recent works focusing on the study of Jupiter's formation in the Solar System [282, 308] further highlighted how the combination between a super-stellar metallicity (e.g. obtained through the mass-radius relationship) with a stellar S/N ratio in a giant planet can indicate its formation beyond the $N_2$ snow-line ($N_2$ being the main N carrier in protoplanetary discs). Note that, due to its high volatility, $N_2$ condenses as ice at a few tens of au even in cold discs [277, 278, 308], while for warmer discs (e.g. 280 K at 1 au, as generally assumed for the solar nebula and adopted by [261]) $N_2$ may remain in gas form until a few hundreds of au from the star, farther out than even the planet-hosting region suggested by ALMA's surveys.

> The use of **multiple elemental ratios involving elements of different volatility** permitted by Ariel's spectral coverage allows to greatly **reduce the degeneracy intrinsic in any single measure** and to more robustly constrain the formation and dynamical history of giant planets [261].

It is important to point out that the discussion above focuses on specific absolute values that have been derived assuming a composition of the protoplanetary disc matching the protosolar composition (see e.g. [73, 309], and references therein). As discussed in Section 4, different stars will be characterized by different metallicities and, more importantly, different elemental ratios. As a result, the elemental ratios of planets orbiting different stars cannot be directly compared and the specific values reported above (e.g. C/O $>$ 1) should not be considered as absolute references.
This obstacle can be overcome with the use of planetary elemental ratios normalised to their relevant stellar values, analogously to the case of the normalized metallicities values adopted by [256]. The use of normalized elemental ratios (not necessarily limited to the cases of C/N, N/O, C/O and S/N discussed above) removes the intrinsic compositional variability between different planetary systems and opens up the possibility of more reliable comparisons between the respective formation and migration histories of giant planets orbiting different stars.
Furthermore, as discussed by [261] the use of normalized elemental ratios associated with elements characterized by different volatility provides additional constraint on

the nature of giant planets. The C/O, C/N, N/O and S/N ratios normalised to their stellar values (indicated with the superscript *) reveal that high metallicity giant planets will be characterized by C/N* > C/O* > N/O* (see Fig. 8). Gas-dominated, low metallicity giant planets, instead, will be characterized by N/O* > C/O* > C/N* (see Fig. 8). Giant planets for which planetesimal accretion is the main source of metallicity will have S/N* > C/N*, while those for which both gas and solids contribute to the metallicity will have instead C/N* > S/N* (see Fig. 8).

Finally, since the normalization to the stellar values brings the planetary elemental ratios of elements with different cosmic abundances on a common scale, any element whose main carrier is characterized by a lower or similar volatility than S (see e.g. [3, 72]) can be used to compute normalized elemental ratios with respect to N and gain insight on the source of the planetary metallicity [261]. The use of normalized elemental ratios therefore allows to compare the constraint on the metallicity derived for different giant planets using different low-volatility elements (e.g. S/N*,Al/N*,Na/N*,Cr/N*).

## 7 High-density planets: formation and atmospheres

The *Kepler* exoplanet survey revealed that a vast majority of close-in exoplanets are smaller in size than Neptune [310]. Such planets are called *high-density planets* in this manuscript, as the bulk of their mass is represented by condensates with higher densities that the gas providing most of the mass of gas giants like Jupiter and Saturn. Given their high occurrence, understanding their formation is a central issue in exoplanetary science.

High-density planets, in general, are formed in a complicated way through various processes including solid and gas accretion, orbital migration, giant collisions, late veneers, mass loss, etc. Thus, the sole knowledge of basic physical properties such as mass, radius, and orbital elements is not enough to unveil their nature (e.g. [1, 3], and

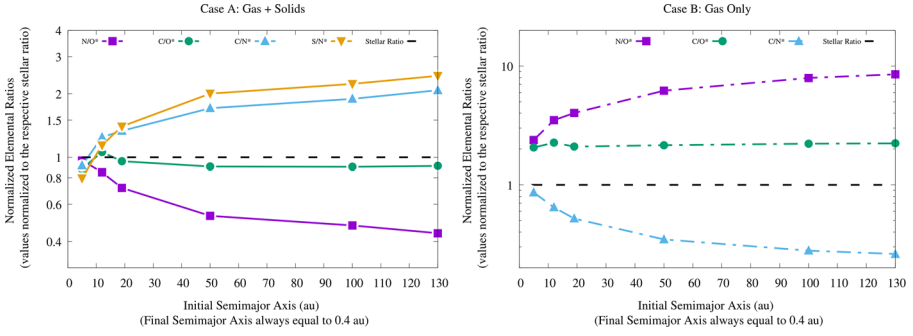


**Fig. 8** *Left:* comparison of the normalized C/O, N/O, C/N, and S/N elemental ratios of the gaseous envelope when the metallicity of the giant planet is dominated by the accretion of planetesimals (high metallicity case). *Right:* comparison of the normalized elemental ratios in the gaseous envelope when the metallicity of the giant planet is dominated instead by the accretion of gas (low metallicity case). Each elemental ratio is normalized to the relevant stellar elemental ratio. Figure from [261]

references therein). The characterisation of their bulk and atmospheric compositions is therefore the key to understand the formation and diversity of high-density planets [1, 3].

One of the biggest uncertainties in the planet formation process is the orbital migration that occurs via angular momentum exchange between the planet and the circumstellar disc (the so-called type-I migration). Planetary migration leads to the delivery of cold materials from beyond the snowline to the inner regions of discs and, thus, brings about a variety in composition of close-in planets. Since planetary migration occurs in a circumstellar disc composed predominantly of hydrogen and helium, migrating planets generally capture the surrounding disc gas by gravity to form an atmosphere. Such atmospheres of high-density planets are often termed primordial atmospheres or captured atmospheres.

Figure 9 shows the predicted masses, radii, and volatile contents of synthesised planets around M dwarfs of 0.3 $M_\odot$ with slow (*left panel*) and fast (*right panel*) migration. Here we have carried out those calculations by adding the effects of atmospheric accumulation and loss [313] in the population synthesis models [311].

The symbols for radii of 1–4 $R_\oplus$ are shown with different colours and sizes, indicating that the high-density planets are diverse in bulk composition; namely, they have different ice-to-rock ratios and different atmospheric masses. As seen in the

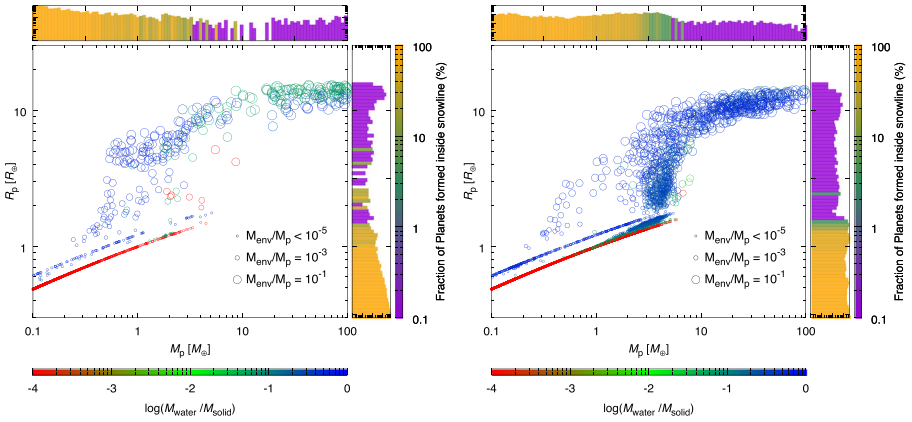


**Fig. 9** Theoretical prediction of masses, radii, and volatile contents of planets around a 0.3 $M_\odot$ star. The population synthesis models include planetesimal accretion, gas accretion, orbital migration, collision of planetary embryos, viscous dissipation of the protoplanetary disc, and photo-evaporation of planetary atmospheres ([311], Kimura et al. in prep.). The rate of the type-I migration differs between the two panels: In the left and right panels, 1% (slow) and 10% (fast), respectively, of the migration rate from [312] are assumed. The synthesised planets are composed of a solid body (ice plus rock) and a H-He atmosphere. In the mass-radius relationship diagram, symbols are colour-coded according to the total mass of water, which comes from icy planetesimals, and are sized according to the atmospheric mass relative to the solid planet mass. Also, in the mass and radius histograms, where the number is given in log, the colour coding indicates the percentage of planets formed inside the snowline. The synthesised planets have been sampled according to their transit probabilities

histograms, the bulk composition of high-density planets also differs depending on the migration rate. Thus, knowledge of bulk composition places a crucial constraint to migration rates. It is noticed, however, that some of the planets in Figure 9 have the same mass-radius relationships but different composition. Such degeneracy in composition prevents us from constraining the bulk composition (see also [3], for a discussion). Observation of their atmospheres with Ariel is of obvious significance.

While the disc gas consists predominantly of hydrogen, the atmospheres are not always hydrogen-dominated. Instead, they would contain heavier molecules than $H_2$ and He. Such contamination (or enrichment) occurs because of degassing from volatile-rich planetesimals and magma oceans (e.g. [314]) and chemical interaction between the atmospheric gas and minerals from magma oceans (e.g. [313]). In some extreme cases, the planets might lose all their primary atmosphere due to evaporation processes and interaction with the host star, and might have an outgassed, secondary atmosphere [314, 315].

A mixture of both acquired and core-degassed volatiles is likely to form the atmospheric inventory. Moreover, the specifics of how volatile species chemically bond with rocky interiors found in solid (silicate mantle) or molten (magma ocean) state suggest that the sources of less soluble versus soluble species may differ. That is, CO and $CO_2$ that are less soluble in silicate melts could be provided directly from the captured disc gas, while $H_2O$ could be provided from thermal evolution of the interior [314] as well as upper atmosphere chemistry [316]. Thus, detailed investigation of atmospheric constituents helps us understand such processes, including contamination by and partitioning processes of heavy volatiles.

Contamination of heavy elements, however, tends to reduce the atmospheric scale height due to increase in mean molecular weight ($\mu$), and thereby hinders atmospheric characterisation via transmission spectroscopy. Figure 10 shows the relationship between the total mass of $H_2O$ contained in the atmosphere and the mean molecular weight of the atmospheric gas for several choices of the solid planet mass by the same method as [313]. Here we have calculated the structure and mass of the atmosphere enriched with water that is connected to the circumstellar gas disc. For reference, the orange symbols indicate the maximum amounts of volatiles that can be degassed from a magma ocean with $H_2O$ content of 1 %.

As shown in this figure, the mean molecular weight of the atmosphere is at most five, which is about twice as high as that of the atmospheric gas with solar abundances. Note that we have ignored any carbon-based molecules such as $CO_2$ here for simplicity; for the gas of $\mu = 5$, for example, if $H_2O$ is replaced completely with $CO_2$, $\mu$ increases (and, thus, the pressure scale height decreases) by 10 %.

Ariel has the capability to **constrain the atmospheric mean molecular weight of high-density planets** [4]. This can be achieved already with Tier 1 resolution for the most favourable cases. In the less favourable cases, additional observational time will be required to constrain the mean molecular weight, though this additional time is estimated to be less than what would be needed to achieve full Tier 2 resolution [4].

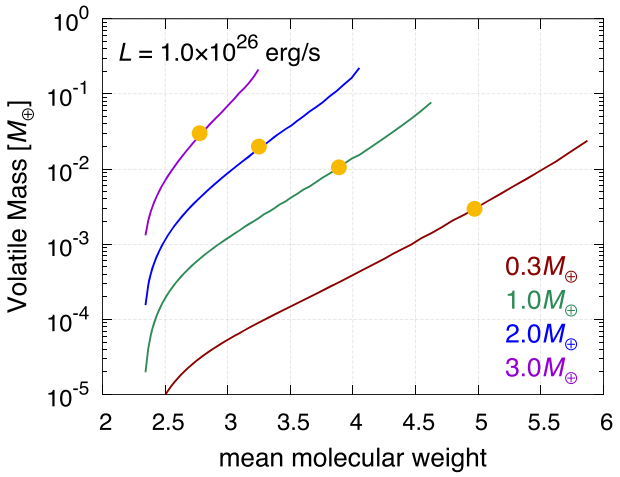


**Fig. 10** Possible range of mean molecular weight of the atmospheric gas for sub- and super-Earths. We have calculated the mass of the enriched atmosphere in dynamical equilibrium with the protoplanetary disc as a function of the mean molecular weight by the same method as [317] and [313]. The orange symbols indicate the maximum amounts of volatile that would be degassed from a magma ocean with water content of 1 %. In these calculations we have assumed that the planet is located at 0.2 AU from an M dwarf of 0.3 $M_\odot$ and the energy flux in the atmosphere is $1 \times 10^{26}$ erg/s

More refined assessments are ongoing (Mugnai et al., in preparation), with a particular focus on verifying the possibility of coupling the estimation of the atmospheric mean molecular weight with the detection of the main molecular constituents (especially water, [3]). Nevertheless, the current picture indicates that Ariel should be able to provide indications on the *primary/secondary atmospheres ratio among low gravity planets* [3, 4].

## 8 Planetary architectures: dynamical context to composition

Before moving to the conclusions it is worth emphasizing once again that, as discussed in Section 6.1, disc-driven migration is not the only dynamical process capable of delivering giant planets from their formation regions to the orbital distances where Ariel will observe them today. Other migration mechanims (planet-planet scattering, ejection from resonances, orbital chaos) can achieve the same outcome while having markedly different implications for the composition of the planets they affect (see e.g. [3, 260], and references therein). Furthermore, as discussed in Section 3 there is emerging evidence suggesting a role played by the galactic environment in shaping the characteristics of planetary systems.

Recent population studies of multi-planet systems highlight how their architectures record a strong role of violent processes, such as chaos and planet-planet

scattering, in shaping the dynamical histories of known exoplanets [262–265, 318, 319]. As such mechanisms act when most solid mass in planetary systems has been incorporated into a limited number of massive bodies, the migrating planets they produce will encounter and accrete less material than their counterparts migrating in protoplanetary discs. At the same time, however, stochastic encounters between planets may result in catastrophic collisions with major implications for the composition and interior structure of the emerging planet.

Consequently, this strong **role played by migration mechanisms other than disc-driven migration introduces a layer of uncertainty** in linking Ariel's compositional data to the formation histories of the observed exoplanets. The same population studies, however, suggest that the combined use of **metrics linked to the angular momentum of planetary systems** [262–264] allows for extracting information from their architectures and **constrain their dynamical past**.

In particular, [264] and [320] have shown how the information provided by the normalized angular momentum deficit (NAMD), an architecture-agnostic measure of the dynamical excitation of planetary systems, allows to build a relative scale of violence of their past histories. Intuitively, the NAMD can be interpreted as the "dynamical temperature" of planetary systems: the higher the value, the more excited is the dynamical state of the system. As in the case of temperature, if one can identity meaningful reference values (as with the freezing and boiling points of water), it is possible to build a scale of dynamical excitation on which to measure the violence of the past of planetary systems.

As discussed by [264] and [320], Trappist-1 and the Solar System provide two such reference values, the first as a system characterized by an orderly and stable evolution [321, 322] while the second as the boundary between orderly and chaotic evolution [323]. As shown in Fig. 11 the higher the NAMD of a planetary system with respect to that of the Solar System, the higher the likeliness that chaos and violent dynamical events sculpted its past. Conversely, NAMD values increasingly closer to that of Trappist-1 are associated to increasing likeliness of stable and orderly histories.

As a consequence, the measure of the "dynamical temperature" of planetary systems permitted by the NAMD can provide a dynamical context for the interpretation of Ariel's compositional observations. In other words, the *combination of Ariel's observations* with the information provided by *planetary system architecture* (specifically masses and orbital elements of its planets) will allow to extract additional and more detailed information on the history of the planets and their host system. It should be noted that the planetary physical and dynamical parameters don't need to be known at the time of Ariel's observations but can be included in the interpretation of Ariel's data at a later time, meaning that *Ariel's scientific impact will grow over time*

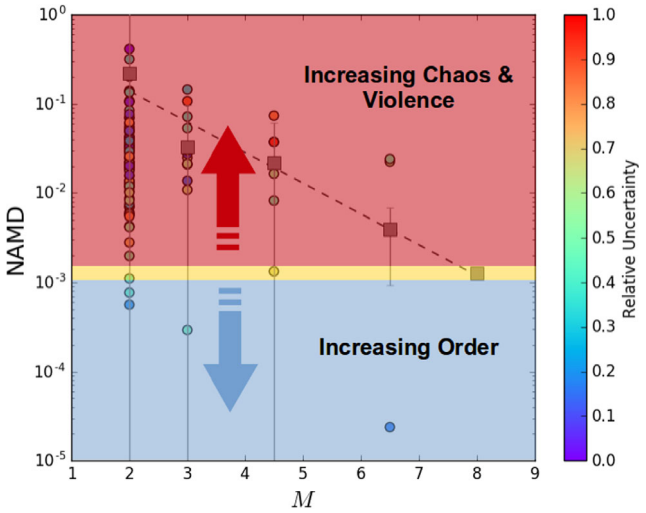


**Fig. 11** Illustrative example of "dynamical temperature" scale built using Trappist-1 and the Solar System as reference systems. The underlying plot shows the dynamical excitation, quantified by the NAMD, of the 99 best-characterized planetary systems (filled circles) grouped according to the multiplicity of the planetary systems (i.e. their number of planets) with the systems with $M$=4 and $M$=5 and with $M$=6 and $M$=7 respectively grouped together to increase statistics. Each planetary system is color-coded according to the relative uncertainty of its NAMD value. Also shown are the mean NAMD values of each multiplicity population (filled squares), computed as weighted-averages over the uncertainties of the individual systems. The overlaid coloured areas showcase an illustrative division between increasing likelyness of dynamical violence (red) and orderly evolution (blue), separated by an uncertainty region (yellow) centered on the Solar System. Figure adapted from [264]

## 9 Concluding remarks

As introduced in Section 1 and further discussed in Sections 6, 7, and 8, the planet formation process plays a fundamental role in shaping the final composition of planets and, consequently, of their atmospheres. Ariel's observations will therefore provide an unprecedented wealth of data to advance our understanding of planet formation in our Galaxy. However, as the discussion in Sections 2-5 highlights, a number of *environmental factors* linked to the star and its own formation process *affect the final outcome*: the galactic environment in which the star formation process takes places, the stellar composition and the thermal and physical structure and evolution of the protoplanetary disc.

As the implications of these environmental factors are still poorly constrained or understood, they can act as a *source of uncertainty* or noise in the interpretation of the atmospheric data Ariel will provide and the reconstruction of the formation and evolution history of the observed planets. As a consequence, care should be taken, particularly during the initial phases of the nominal mission, to *keep these factors into account in the selection of Ariel's targets* (and their stellar hosts) to *minimize the free parameters* in this already complex problem.

The same considerations expressed above, however, also mean that the *potential impact of Ariel's observations for understanding and quantifying the role played by these environmental factors is huge*, particularly when considering an extended mission and the even larger and more diverse observational sample it will bring. As illustrated in particular in Section 6, the wide spectral coverage and the resulting large number of molecules that can be traced by Ariel means that the mission is uniquely suited to explore in unprecedented details and from different angles the *link between the star formation and the planet formation processes*.

**Acknowledgments** D.T., S.F., S.M., E.S., and A.N. acknowledge the support of the Italian Space Agency (ASI) through the ASI-INAF contract 2018-22-HH.0. D.T., C.C., D.F., and L.P. acknowledge the support of the PRIN-INAF 2016 "The Cradle of Life - GENESIS-SKA (General Conditions in Early Planetary Systems for the rise of life with SKA". D.T., S.F., S.M. D.F, J.M., F.O., P.W. acknowledge the support of the Italian National Institute of Astrophysics (INAF) through the INAF *Main Stream* project "Ariel and the astrochemical link between circumstellar discs and planets" (CUP: C54I19000700005). S.M. acknowledges support from the European Research Council via the Horizon 2020 Framework Programme ERC Synergy "ECOGAL" Project GA-855130. M.K. acknowledges funding by the University of Tartu ASTRA project 2014-2020.4.01.16-0029 KOMEET "Benefits for Estonian Society from Space Research and Application", financed by the EU European Regional Development Fund. J.M.D.K. gratefully acknowledges funding from the Deutsche Forschungsgemeinschaft (DFG, German Research Foundation) through an Emmy Noether Research Group (grant number KR4801/1-1) and the DFG Sachbeihilfe (grant number KR4801/2-1), as well as from the European Research Council (ERC) under the European Union's Horizon 2020 research and innovation programme via the ERC Starting Grant MUSTANG (grant agreement number 714907). The research of O.P. is funded by the Royal Society, through Royal Society Dorothy Hodgkin Fellowship DH140243. M.P. thanks the support to NuGrid from STFC (through the University of Hull's Consolidated Grant ST/R000840/1), and access to VIPER, the University of Hull High Performance Computing Facility. M.P. acknowledges the support from the "Lendulet-2014" Program of the Hungarian Academy of Sciences (Hungary), from the ERC Consolidator Grant (Hungary) funding scheme (Project RADIOSTAR, G.A. n. 724560), by the National Science Foundation (NSF, USA) under grant No. PHY-1430152 (JINA Center for the Evolution of the Elements). M.P. also thanks the UK network BRIDGCE and the ChETEC COST Action (CA16117), supported by COST (European Cooperation in Science and Technology). M.I. thanks the support by JSPS KAKENHI 18H05439. C.D. acknowledges financial support from the State Agency for Research of the Spanish MCIU through the "Center of Excellence Severo Ochoa" award to the Instituto de Astrofísica de Andalucía (SEV-2017-0709), and the Group project Ref. PID2019-110689RB-I00/AEI/10.13039/501100011033.

**Funding** Open access funding provided by Istituto Nazionale di Astrofisica within the CRUI-CARE Agreement.



## References

1. Tinetti, G., Drossart, P., Eccleston, P., Hartogh, P., Heske, A., Leconte, J., Micela, G., Ollivier, M., Pilbratt, G., Puig, L., Turrini, D., Vandenbussche, B., Wolkenberg, P., Beaulieu, J.-P., Buchave, L.A.,

Ferus, M., Griffin, M., Guedel, M., Justtanont, K., Lagage, P.-O., Machado, P., Malaguti, G., Min, M., Nørgaard-Nielsen, H.U., Rataj, M., Ray, T., Ribas, I., Swain, M., Szabo, R., Werner, S., Barstow, J., Burleigh, M., Cho, J., du Foresto, VC., Coustenis, A., Decin, L., Encrenaz, T., Galand, M., Gillon, M., Helled, R., Morales, J.C., Muñoz, A.G., Moneti, A., Pagano, I., Pascale, E., Piccioni, G., Pinfield, D., Sarkar, S., Selsis, F., Tennyson, J., Triaud, A., Venot, O., Waldmann, I., Waltham, D., Wright, G., Amiaux, J., Auguères, J.-L., Berthé, M., Bezawada, N., Bishop, G., Bowles, N., Coffey, D., Colomé, J., Crook, M., Crouzet, P.-E., Da Peppo, V., Sanz, I.E., Focardi, M., Frericks, M., Hunt, T., Kohley, R., Middleton, K., Morgante, G., Ottensamer, R., Pace, E., Pearson, C., Stamper, R., Symonds, K., Rengel, M., Renotte, E., Ade, P., Affer, L., Alard, C., Allard, N., Altieri, F., André, Y., Arena, C., Argyriou, I., Aylward, A., Baccani, C., Bakos, G., Banaszkiewicz, M., Barlow, M., Batista, V., Bellucci, G., Benatti, S., Bernardi, P., B.ézard, B., Blecka, M., Bolmont, E., Bonfond, B., Bonito, R., Bonomo, A.S., Brucato, J.R., Brun, AS., Bryson, I., Bujwan, W., Casewell, S., Charnay, B., Pestellini, C.C., Chen, G., Ciaravella, A., Claudi, R., Clédassou, R., Damasso, M., Damiano, M., Danielski, C., Deroo, P., Di Giorgio, A.M., Dominik, C., Doublier, V., Doyle, S., Doyon, R., Drummond, B., Duong, B., Eales, S., Edwards, B., Farina, M., Flaccomio, E., Fletcher, L., Forget, F., Fossey, S., Fränz, M., Fujii, Y., García-Piquer, A., Gear, W., Geoffray, H., Gérard, J.C., Gesa, L., Gomez, H., Graczyk, R., Griffith, C., Grodent, D., Guarcello, MG., Gustin, J., Hamano, K., Hargrave, P., Hello, Y., Heng, K., Herrero, E., Hornstrup, A., Hubert, B., Ida, S., Ikoma, M., Iro, N., Irwin, P., Jarchow, C., Jaubert, J., Jones, H., Julien, Q., Kameda, S., Kerschbaum, F., Kervella, P., Koskinen, T., Krijger, M., Krupp, N., Lafarga, M., Landini, F., Lellouch, E., Leto, G., Luntzer, A., Rank-Lüftinger, T., Maggio, A., Maldonado, J., Maillard, J.-P., Mall, U., Marquette, J.-B., Mathis, S., Maxted, P., Matsuo, T., Medvedev, A., Miguel, Y., Minier, V., Morello, G., Mura, A., Narita, N., Nascimbeni, V., Nguyen Tong, N., Noce, V., Oliva, F., Palle, E., Palmer, P., Pancrazzi, M., Papageorgiou, A., Parmentier, V., Perger, M., Petralia, A., Pezzuto, S., Pierrehumbert, R., Pillitteri, I., Piotto, G., Pisano, G., Prisinzano, L., Radioti, A., Réess, J.-M., Rezac, L., Rocchetto, M., Rosich, A., Sanna, N., Santerne, A., Savini, G., Scandariato, G., Sicardy, B., Sierra, C., Sindoni, G., Skup, K., Snellen, I., Sobiecki, M., Soret, L., Sozzetti, A., Stiepen, A., Strugarek, A., Taylor, J., Taylor, W., Terenzi, L., Tessenyi, M., Tsiaras, A., Tucker, C., Valencia, D., Vasisht, G., Vazan, A., Vilardell, F., Vinatier, S., Viti, S., Waters, R., Wawer, P., Wawrzaszek, A., Whitworth, A., Yung, Y.L., Yurchenko, S.N., Osorio, M.R.Z., Zellem, R., Zingales, T., Zwart, F.: A chemical survey of exoplanets with ARIEL. Exp. Astron. **46**(1), 135–209 (2018). https://doi.org/10.1007/s10686-018-9598-x

2. Zingales, T., Tinetti, G., Pillitteri, I., Leconte, J., Micela, G., Sarkar, S.: The ARIEL mission reference sample. Exp. Astron. **46**(1), 67–100 (2018). https://doi.org/10.1007/s10686-018-9572-7, 1706.08444
3. Turrini, D., Miguel, Y., Zingales, T., Piccialli, A., Helled, R., Vazan, A., Oliva, F., Sindoni, G., Panić, O., Leconte, J., Min, M., Pirani, S., Selsis, F., Coudé du Foresto, V., Mura, A., Wolkenberg, P.: The contribution of the ARIEL space mission to the study of planetary formation. Exp. Astron. **46**(1), 45–65 (2018). https://doi.org/10.1007/s10686-017-9570-1, 1804.06179
4. Edwards, B., Mugnai, L., Tinetti, G., Pascale, E., Sarkar, S.: An Updated Study of Potential Targets for Ariel. AJ **157**(6), 242 (2019). https://doi.org/10.3847/1538-3881/ab1cb9, 1905.04959
5. Lada, C.J.: Star formation: from OB associations to protostars. In: Peimbert, M., Jugaku, J. (eds.) Star Forming Regions, vol. 115, p. 1. IAU Symposium (1987)
6. Tychoniec, L., Tobin, J.J., Karska, A., Chand ler, C., Dunham, M.M., Harris, R.J., Kratter, K.M., Li, Z.-Y., Looney, L.W., Melis, C., Pérez, L.M., Sadavoy, S.I., Segura-Cox, D., van Dishoeck, E.F.: The VLA Nascent Disk and Multiplicity Survey of Perseus Protostars (VANDAM). IV. Free-Free Emission from Protostars: Links to Infrared Properties, Outflow Tracers, and Protostellar Disk Masses. ApJ **238**(2), 19 (2018). https://doi.org/10.3847/1538-4365/aaceae, 1806.02434
7. Bohlin, R.C., Savage, BD., Drake, JF.: A survey of interstellar H I from Lalpha absorption measurements. II. ApJ **224**, 132–142 (1978). https://doi.org/10.1086/156357
8. D'Alessio, P., Calvet, N., Hartmann, L.: Accretion Disks around Young Objects. III. Grain Growth. ApJ **553**(1), 321–334 (2001). https://doi.org/10.1086/320655, astro-ph/0101443
9. Armitage, P.J.: Astrophysics of planet formation. Cambridge University Press (2009)
10. Avenhaus, H., Quanz, S.P., Garufi, A., Perez, S., Casassus, S., Pinte, C., Bertrang, G.H.M., Caceres, C., Benisty, M., Dominik, C.: Disks around T Tauri Stars with SPHERE (DARTTS-S). I. SPHERE/IRDIS Polarimetric Imaging of Eight Prominent T Tauri Disks. ApJ **863**(1), 44 (2018). https://doi.org/10.3847/1538-4357/aab846, 1803.10882

11. Villenave, M., Ménard, F., Dent, W.R.F., Duchêne, G., Stapelfeldt, K.R., Benisty, M., Boehler, Y., van der Plas, G., Pinte, C., Telkamp, Z., Wolff, S., Flores, C., Lesur, G., Louvet, F., Riols, A., Dougados, C., Williams, H., Padgett, D.: Observations of edge-on protoplanetary disks with ALMA. I. Results from continuum data. A&A **642**, A164 (2020). https://doi.org/10.1051/0004-6361/202038087, 2008.06518
12. Dominik, C., Habing, H.: Old and Young Vega-like Stars. In: Astronomische Gesellschaft Meeting Abstracts, vol. 17. Astronomische Gesellschaft Meeting Abstracts (2000)
13. Matthews, B., Kennedy, G., Sibthorpe, B., Booth, M., Wyatt, M., Broekhoven-Fiene, H., Macintosh, B., Marois, C.: Resolved Imaging of the HR 8799 Debris Disk with Herschel. ApJ **780**(1), 97 (2014). https://doi.org/10.1088/0004-637X/780/1/97, 1311.2977
14. Miley, J.M., Panić, O., Wyatt, M., Kennedy, G.M.: Unlocking the secrets of the midplane gas and dust distribution in the young hybrid disc HD 141569. A&A **615**, L10 (2018). https://doi.org/10.1051/0004-6361/201833381, 1805.02476
15. Péricaud, J., di Folco, E., Dutrey, A., Augereau, J.C., Piétu, V., Guilloteau, S.: HD141569A: Disk Dissipation Caught in Action. In: Kastner, J.H., Stelzer, B., Metchev, S.A. (eds.) Young Stars & Planets Near the Sun, vol. 314, pp. 201–202. IAU Symposium (2016)
16. Turrini, D., Marzari, F., Polychroni, D., Testi, L.: Dust-to-gas Ratio Resurgence in Circumstellar Disks Due to the Formation of Giant Planets: The Case of HD 163296. ApJ **877**(1), 50 (2019). https://doi.org/10.3847/1538-4357/ab18f5, 1802.04361
17. Helled, R., Bodenheimer, P., Podolak, M., Boley, A., Meru, F., Nayakshin, S., Fortney, JJ., Mayer, L., Alibert, Y., Boss, A.P.: Giant Planet Formation, Evolution, and Internal Structure. In: Beuther, H., Klessen, R.S., Dullemond, C.P., Henning, T. (eds.) Protostars and Planets VI, p. 643 ( 2014)
18. D'Angelo, G., Lissauer, JJ.: Formation of Giant Planets. In: Deeg, H.J., Belmonte, J.A. (eds.) Handbook of Exoplanets, p. 140 (2018)
19. Thi, W.F., van Dishoeck, E.F., Blake, G.A., van Zadelhoff, G.J., Horn, J., Becklin, E.E., Mannings, V., Sargent, A.I., van den Ancker, ME., Natta, A., Kessler, J.: $H_2$ and CO Emission from Disks around T Tauri and Herbig Ae Pre-Main-Sequence Stars and from Debris Disks around Young Stars: Warm and Cold Circumstellar Gas. ApJ **561**(2), 1074–1094 (2001). https://doi.org/10.1086/323361, astro-ph/0107006
20. Trapman, L., Miotello, A., Kama, M., van Dishoeck, E.F., Bruderer, S.: Far-infrared HD emission as a measure of protoplanetary disk mass. A&A **605**, A69 (2017). https://doi.org/10.1051/0004-6361/201630308, 1705.07671
21. Prodanović, T., Steigman, G., Fields, B.D.: The deuterium abundance in the local interstellar medium. MNRAS **406**(2), 1108–1115 (2010). https://doi.org/10.1111/j.1365-2966.2010.16734.x, 0910.4961
22. Bergin, E.A., Cleeves, L.I., Crockett, N.R., Favre, C., Neill, J.L.: Chemistry in Star Forming Regions - Herschel Looking Towards ALMA. In: Kawabe, R., Kuno, N., Yamamoto, S. (eds.) New Trends in Radio Astronomy in the ALMA Era: The 30th Anniversary of Nobeyama Radio Observatory, Astronomical Society of the Pacific Conference Series, vol. 476, p. 185. Astronomical Society of the Pacific, San Francisco (2013)
23. McClure, M.K., Bergin, E.A., Cleeves, L.I., van Dishoeck, E.F., Blake, G.A., Evans, I.I., Green, J.D., Henning, T., Öberg, K.I., Pontoppidan, K.M., Salyk, C.: Mass Measurements in Protoplanetary Disks from Hydrogen Deuteride. ApJ **831**(2), 167 (2016). https://doi.org/10.3847/0004-637X/831/2/167, 1608.07817
24. Kama, M., Trapman, L., Fedele, D., Bruderer, S., Hogerheijde, M.R., Miotello, A., van Dishoeck, EF., Clarke, C., Bergin, E.A.: Mass constraints for 15 protoplanetary discs from HD 1-0. A&A **634**, A88 (2020). https://doi.org/10.1051/0004-6361/201937124, 1912.11883
25. Fedele, D., van Dishoeck, E.F., Kama, M., Bruderer, S., Hogerheijde, M.R.: Probing the 2D temperature structure of protoplanetary disks with Herschel observations of high-J CO lines. A&A **591**, A95 (2016). https://doi.org/10.1051/0004-6361/201526948, 1604.02055
26. Dartois, E., Dutrey, A., Guilloteau, S.: Structure of the DM Tau Outer Disk: Probing the vertical kinetic temperature gradient. A&A **399**, 773–787 (2003). https://doi.org/10.1051/0004-6361:20021638
27. Panić, O., Hogerheijde, M.R., Wilner, D., Qi, C.: Gas and dust mass in the disc around the Herbig Ae star HD 169142. A&A **491**(1), 219–227 (2008). https://doi.org/10.1051/0004-6361:20079261

28. Dutrey, A., Guilloteau, S., Duvert, G., Prato, L., Simon, M., Schuster, K., Menard, F.: Dust and gas distribution around T Tauri stars in Taurus-Auriga. I. Interferometric 2.7mm continuum and Î3ĈO J=1-0 observations. A&A **309**, 493–504 (1996)
29. Ansdell, M., Williams, J.P., van der Marel, N., Carpenter, J.M., Guidi, G., Hogerheijde, M., Mathews, G.S., Manara, C.F., Miotello, A., Natta, A., Oliveira, I., Tazzari, M., Testi, L., van Dishoeck, E.F., van Terwisga, S.E.: ALMA Survey of Lupus Protoplanetary Disks. I. Dust and Gas Masses. ApJ **828**(1), 46 (2016). https://doi.org/10.3847/0004-637X/828/1/46, 1604.05719
30. Miotello, A., van Dishoeck, E.F., Kama, M., Bruderer, S.: Determining protoplanetary disk gas masses from CO isotopologues line observations. A&A **594**, A85 (2016). https://doi.org/10.1051/0004-6361/201628159, 1605.07780
31. Zhang, K., Bergin, E.A., Blake, G.A., Cleeves, L.I., Schwarz, K.R.: Mass inventory of the giant-planet formation zone in a solar nebula analogue. Nat. Astron. **1**, 0130 (2017). https://doi.org/10.1038/s41550-017-0130, 1705.04746
32. Booth, A.S., Walsh, C., Ilee, J.D., Notsu, S., Qi, C., Nomura, H., Akiyama, E.: The First Detection of $^{13}C^{17}O$ in a Protoplanetary Disk: A Robust Tracer of Disk Gas Mass. ApJ **882**(2), L31 (2019). https://doi.org/10.3847/2041-8213/ab3645, 1908.05045
33. Booth, A.S., Ilee, J.D.: $^{13}C^{17}O$ suggests gravitational instability in the HL Tau disc. MNRAS **493**(1), L108–L113 (2020). https://doi.org/10.1093/mnrasl/slaa014, 2001.07550
34. Bruderer, S., van Dishoeck, E.F., Doty, S.D., Herczeg, G.J.: The warm gas atmosphere of the HD 100546 disk seen by Herschel. Evidence of a gas-rich, carbon-poor atmosphere? A&A **541**, A91 (2012). https://doi.org/10.1051/0004-6361/201118218, 1201.4860
35. Favre, C., Cleeves, L.I., Bergin, E.A., Qi, C., Blake, G.A.: A Significantly Low CO Abundance toward the TW Hya Protoplanetary Disk: A Path to Active Carbon Chemistry? ApJ **776**(2), L38 (2013). https://doi.org/10.1088/2041-8205/776/2/L38, 1309.5370
36. Du, F., Bergin, EA., Hogerheijde, MR.: Volatile depletion in the TW Hydrae disk atmosphere. ApJ **807**(2), L32 (2015). https://doi.org/10.1088/2041-8205/807/2/L32, 1506.03510
37. Kama, M., Bruderer, S., van Dishoeck, E.F., Hogerheijde, M., Folsom, C.P., Miotello, A., Fedele, D., Belloche, A., Güsten, R., Wyrowski, F.: Volatile-carbon locking and release in protoplanetary disks. A study of TW Hya and HD 100546. A&A **592**, A83 (2016). https://doi.org/10.1051/0004-6361/201526991, 1605.05093
38. Woitke, P., Min, M., Pinte, C., Thi, W.F., Kamp, I., Rab, C., Anthonioz, F., Antonellini, S., Baldovin-Saavedra, C., Carmona, A., Dominik, C., Dionatos, O., Greaves, J., Güdel, M., Ilee, J.D., Liebhart, A., Ménard, F., Rigon, L., Waters, L.B.F.M., Aresu, G., Meijerink, R., Spaans, M.: Consistent dust and gas models for protoplanetary disks. I. Disk shape, dust settling, opacities, and PAHs. A&A **586**, A103 (2016). https://doi.org/10.1051/0004-6361/201526538, 1511.03431
39. Du, F., Bergin, EA., Hogerheijde, M., van Dishoeck, E.F., Blake, G., Bruderer, S., Cleeves, I., Dominik, C., Fedele, D., Lis, DC., Melnick, G., Neufeld, D., Pearson, J., Yıldız, U.: Survey of Cold Water Lines in Protoplanetary Disks: Indications of Systematic Volatile Depletion. ApJ **842**(2), 98 (2017). https://doi.org/10.3847/1538-4357/aa70ee, 1705.00799
40. Zhu, Z., Zhang, S., Jiang, Y.-F., Kataoka, A., Birnstiel, T., Dullemond, C.P., Andrews, S.M., Huang, J., Pérez, L.M., Carpenter, J.M., Bai, X.-N., Wilner, D.J., Ricci, L.: One Solution to the Mass Budget Problem for Planet Formation: Optically Thick Disks with Dust Scattering. ApJ **877**(2), L18 (2019). https://doi.org/10.3847/2041-8213/ab1f8c, 1904.02127
41. Krijt, S., Schwarz, K.R., Bergin, E.A., Ciesla, F.J.: Transport of CO in Protoplanetary Disks: Consequences of Pebble Formation, Settling, and Radial Drift. ApJ **864**(1), 78 (2018). https://doi.org/10.3847/1538-4357/aad69b, 1808.01840
42. Schwarz, K.R., Bergin, E.A., Cleeves, L.I., Zhang, K., Öberg, K.I., Blake, G.A., Anderson, D.: Unlocking CO Depletion in Protoplanetary Disks. I. The Warm Molecular Layer. ApJ **856**(1), 85 (2018). https://doi.org/10.3847/1538-4357/aaae08, 1802.02590
43. Isella, A., Hull, C.L.H., Moullet, A., Galván-Madrid, R., Johnstone, D., Ricci, L., Tobin, J., Testi, L., Beltran, M., Lazio, J., Siemion, A., Liu, H.B., Du, F., Öberg, K.I., Bergin, T., Caselli, P., Bourke, T., Carilli, C., Perez, L., Butler, B., de Pater, I., Qi, C., Hofstadter, M., Moreno, R., Alexander, D., Williams, J., Goldsmith, P., Wyatt, M., Loinard, L., Di Francesco, J., Wilner, D., Schilke, P., Ginsburg, A., Sánchez-Monge, A., Zhang, Q., Beuther, H.: Next Generation Very Large Array Memo No. 6, Science Working Group 1: The Cradle of Life. arXiv:1510.06444 (2015)
44. Carr, J.S., Najita, J.R.: Organic Molecules and Water in the Planet Formation Region of Young Circumstellar Disks. Science **319**(5869), 1504 (2008). https://doi.org/10.1126/science.1153807

45. Mandell, A.M., Mumma, M.J., Blake, GA., Bonev, BP., Villanueva, GL., Salyk, C.: Discovery .of OH in Circumstellar Disks around Young Intermediate-Mass Stars. ApJ **681**(1), L25 (2008). https://doi.org/10.1086/590180, 0805.3502
46. Pontoppidan, K.M., Salyk, C., Blake, G.A., Meijerink, R., Carr, J.S., Najita, J.: A Spitzer Survey of Mid-infrared Molecular Emission from Protoplanetary Disks. I. Detection Rates. ApJ **720**(1), 887–903 (2010). https://doi.org/10.1088/0004-637X/720/1/887, 1006.4189
47. Salyk, C., Pontoppidan, KM., Blake, GA., Najita, JR., Carr, JS.: A Spitzer Survey of Mid-infrared Molecular Emission from Protoplanetary Disks. II. Correlations and Local Thermal Equilibrium Models. ApJ **731**(2), 130 (2011). https://doi.org/10.1088/0004-637X/731/2/130, 1104.0948
48. Fedele, D., Pascucci, I., Brittain, S., Kamp, I., Woitke, P., Williams, J.P., Dent, W.R.F., Thi, W.F.: Water Depletion in the Disk Atmosphere of Herbig AeBe Stars. ApJ **732**(2), 106 (2011). https://doi.org/10.1088/0004-637X/732/2/106, 1103.6039
49. Mandell, A.M., Bast, J., van Dishoeck, E.F., Blake, G.A., Salyk, C., Mumma, M.J., Villanueva, G.: First Detection of Near-infrared Line Emission from Organics in Young Circumstellar Disks. ApJ **747**(2), 92 (2012). https://doi.org/10.1088/0004-637X/747/2/92, 1201.0766
50. Fedele, D., Bruderer, S., van Dishoeck, E.F., Herczeg, G.J., Evans, N.J., Bouwman, J., Henning, T., Green, J.: Warm $H_2O$ and OH in the disk around the Herbig star HD 163296. A&A **544**, L9 (2012). https://doi.org/10.1051/0004-6361/201219615, 1207.3969
51. Fedele, D., Bruderer, S., van Dishoeck, EF., Carr, J., Herczeg, G.J., Salyk, C., Evans, N.J., Bouwman, J., Meeus, G., Henning, T., Green, J., Najita, J.R., Güdel, M.: DIGIT survey of far-infrared lines from protoplanetary disks. I. [O i], [C ii], OH, $H_2O$, and $CH^+$. A&A **559**, A77 (2013). https://doi.org/10.1051/0004-6361/201321118, 1308.1578
52. Pontoppidan, K.M., Blake, G.A., van Dishoeck, E.F., Smette, A., Ireland, MJ., Brown, J.: Spectroastrometric Imaging of Molecular Gas within Protoplanetary Disk Gaps. ApJ **684**(2), 1323–1329 (2008). https://doi.org/10.1086/590400, 0805.3314
53. Brittain, S.D., Najita, J.R., Carr, J.S.: Tracing the Inner Edge of the Disk Around H.D 100546 with Rovibrational CO Emission Lines. ApJ **702**(1), 85–99 (2009). https://doi.org/10.1088/0004-637X/702/1/85, 0907.0047
54. van der Plas, G., van den Ancker, M.E., Acke, B., Carmona, A., Dominik, C., Fedele, D., Waters, L.B.F.M.: Evidence for CO depletion in the inner regions of gas-rich protoplanetary disks. A&A **500**(3), 1137–1141 (2009). https://doi.org/10.1051/0004-6361/200811148, 0810.3417
55. Brown, JM., Pontoppidan, KM., van Dishoeck, EF., Herczeg, GJ., Blake, GA., Smette, A.: VLT-CRIRES Survey of Rovibrational CO Emission from Protoplanetary Disks. ApJ **770**(2), 94 (2013). https://doi.org/10.1088/0004-637X/770/2/94, 1304.4961
56. Pascucci, I., Apai, D., Luhman, K., Henning, T., Bouwman, J., Meyer, M.R., Lahuis, F., Natta, A.: The Different Evolution of Gas and Dust in Disks around Sun-Like and Cool Stars. ApJ **696**(1), 143–159 (2009). https://doi.org/10.1088/0004-637X/696/1/143, 0810.2552
57. Gibb, E.L., Horne, D.: Detection of $CH_4$ in the GV Tau N Protoplanetary Disk. ApJ **776**(2), L28 (2013). https://doi.org/10.1088/2041-8205/776/2/L28
58. Woitke, P., Thi, W.F., Kamp, I., Hogerheijde, M.R.: Hot and cool water in Herbig Ae protoplanetary disks. A challenge for Herschel. A&A **501**(1), L5–L8 (2009). https://doi.org/10.1051/0004-6361/200912249, 0906.0448
59. Walsh, C., Nomura, H., van Dishoeck, E.: The molecular composition of the planet-forming regions of protoplanetary disks across the luminosity regime. A&A **582**, A88 (2015). https://doi.org/10.1051/0004-6361/201526751, 1507.08544
60. Agúndez, M., Roueff, E., Le Petit, F., Le Bourlot, J.: The chemistry of disks around T Tauri and Herbig Ae/Be stars. A&A **616**, A19 (2018). https://doi.org/10.1051/0004-6361/201732518, 1803.09450
61. Hogerheijde, M.R., Bergin, E.A., Brinch, C., Cleeves, L.I., Fogel, J.K.J., Blake, G.A., Dominik, C., Lis, D.C., Melnick, G., Neufeld, D., Panić, O., Pearson, J.C., Kristensen, L., Yıldız, U.A., van Dishoeck, E.F.: Detection of the Water Reservoir in a Forming Planetary System. Science **334**(6054), 338 (2011). https://doi.org/10.1126/science.1208931, 1110.4600
62. van Dishoeck, E.F., Kristensen, L.E., the WISH Team.: Water in star-forming regions (WISH): Physics and chemistry from clouds to disks as probed by Herschel spectroscopy. arXiv:2102.02225 (2021)

63. Walsh, C., Loomis, R.A., Öberg, K.I., Kama, M., van 't Hoff, M.L.R., Millar, T.J., Aikawa, Y., Herbst, E., Widicus Weaver, S.L., Nomura, H.: First Detection of Gas-phase Methanol in a Protoplanetary Disk. ApJ **823**(1), L10 (2016). https://doi.org/10.3847/2041-8205/823/1/L10, 1606.06492
64. Öberg, K.I., Guzmán, V.V., Furuya, K., Qi, C., Aikawa, Y., Andrews, S.M., Loomis, R., Wilner, D.J.: The comet-like composition of a protoplanetary disk as revealed by complex cyanides. Nature **520**(7546), 198–201 (2015). https://doi.org/10.1038/nature14276, 1505.06347
65. Favre, C., Fedele, D., Semenov, D., Parfenov, S., Codella, C., Ceccarelli, C., Bergin, E.A., Chapillon, E., Testi, L., Hersant, F., Lefloch, B., Fontani, F., Blake, G.A., Cleeves, L.I., Qi, C., Schwarz, KR., Taquet, V.: First Detection of the Simplest Organic Acid in a Protoplanetary Disk. ApJ **862**(1), L2 (2018). https://doi.org/10.3847/2041-8213/aad046, 1807.05768
66. van 't Hoff, M.L.R., Tobin, J.J., Trapman, L., Harsono, D., Sheehan, P.D., Fischer, W.J., Megeath, S.T., van Dishoeck, E.F.: Methanol and its Relation to the Water Snowline in the Disk around the Young Outbursting Star V883 Ori. ApJ **864**(1), L23 (2018). https://doi.org/10.3847/2041-8213/aadb8a, 1808.08258
67. Lee, J.-E., Lee, S., Baek, G., Aikawa, Y., Cieza, L., Yoon, S.-Y., Herczeg, G., Johnstone, D., Casassus, S.: The ice composition in the disk around V883 Ori revealed by its stellar outburst. Nat. Astron. **3**, 314–319 (2019). https://doi.org/10.1038/s41550-018-0680-0, 1809.00353
68. Andrews, S.M., Huang, J., Pérez, L.M., Isella, A., Dullemond, C.P., Kurtovic, N.T., Guzmán, V.V., Carpenter, J.M., Wilner, D.J., Zhang, S., Zhu, Z., Birnstiel, T., Bai, X.-N., Benisty, M., Hughes, A.M., Öberg, K.I., Ricci, L.: The Disk Substructures at High Angular Resolution Project (DSHARP). I. Motivation, Sample, Calibration, and Overview. ApJ **869**(2), L41 (2018). https://doi.org/10.3847/2041-8213/aaf741, 1812.04040
69. Jermyn, AS., Kama, M.: Stellar photospheric abundances as a probe of discs and planets. MNRAS **476**(4), 4418–4434 (2018). https://doi.org/10.1093/MNRAS/sty429, 1804.06414
70. Kama, M., Folsom, C.P., Pinilla, P.: Fingerprints of giant planets in the photospheres of Herbig stars. A&A **582**, L10 (2015). https://doi.org/10.1051/0004-6361/201527094, 1509.02741
71. Kama, M., Shorttle, O., Jermyn, A.S., Folsom, C.P., Furuya, K., Bergin, E.A., Walsh, C., Keller, L.: Abundant Refractory Sulfur in Protoplanetary Disks. ApJ **885**(2), 114 (2019). https://doi.org/10.3847/1538-4357/ab45f8, 1908.05169
72. Palme, H., Lodders, K., Jones, A.: Solar System Abundances of the Elements. In: Davis, A.M. (ed.) Planets, Asteriods, Comets and The Solar System, Volume 2 of Treatise on Geochemistry (Second Edition)., vol. 2, pp. 15–36. Elsevier (2014)
73. Lodders, K.: Solar Elemental Abundances. arXiv:1912.00844 (2019)
74. Altwegg, K., Balsiger, H., Fuselier, S.A.: Cometary Chemistry and the Origin of Icy Solar System Bodies: The View After Rosetta. ARA&A **57**, 113–155 (2019). https://doi.org/10.1146/annurev-astro-091918-104409, 1908.04046
75. Rubin, M., Engrand, C., Snodgrass, C., Weissman, P., Altwegg, K., Busemann, H., Morbidelli, A., Mumma, M.: On the Origin and Evolution of the Material in 67P/Churyumov-Gerasimenko. Space Sci. Rev. **216**(5), 102 (2020). https://doi.org/10.1007/s11214-020-00718-2
76. Ardila, DR., Herczeg, GJ., Gregory, SG., Ingleby, L., France, K., Brown, A., Edwards, S., Johns-Krull, C., Linsky, J.L., Yang, H., Valenti, J.A., Abgrall, H., Alexander, R.D., Bergin, E., Bethell, T., Brown, J.M., Calvet, N., Espaillat, C., Hillenbrand, L.A., Hussain, G., Roueff, E., Schindhelm, E.R., Walter, F.M.: Hot Gas Lines in T Tauri Stars. ApJ **207**(1), 1 (2013). https://doi.org/10.1088/0067-0049/207/1/1, 1304.3746
77. McClure, M.K.: Carbon depletion observed inside T Tauri inner rims. Formation of icy, kilometer size planetesimals by 1 Myr. A&A **632**, A32 (2019). https://doi.org/10.1051/0004-6361/201834361, 1910.06029
78. Booth, R.A., Clarke, C.J., Madhusudhan, N., Ilee, J.D.: Chemical enrichment of giant planets and discs due to pebble drift. MNRAS **469**(4), 3994–4011 (2017). https://doi.org/10.1093/MNRAS/stx1103, 1705.03305
79. Dutrey, A., Wakelam, V., Boehler, Y., Guilloteau, S., Hersant, F., Semenov, D., Chapillon, E., Henning, T., Piétu, V., Launhardt, R., Gueth, F., Schreyer, K.: Chemistry in disks. V. Sulfur-bearing molecules in the protoplanetary disks surrounding LkCa15, MWC480, DM Tauri, and GO Tauri. A&A **535**, A104 (2011). https://doi.org/10.1051/0004-6361/201116931, 1109.5870
80. Semenov, D., Favre, C., Fedele, D., Guilloteau, S., Teague, R., Henning, T., Dutrey, A., Chapillon, E., Hersant, F., Piétu, V.: Chemistry in disks. XI. Sulfur-bearing species as tracers of protoplanetary disk physics and chemistry: the DM Tau case. A&A **617**, A28 (2018). https://doi.org/10.1051/0004-6361/201832980, 1806.07707

81. Kama, M., Bruderer, S., Carney, M., Hogerheijde, M., van Dishoeck, E.F., Fedele, D., Baryshev, A., Boland, W., Güsten, R., Aikutalp, A., Choi, Y., Endo, A., Frieswijk, W., Karska, A., Klaassen, P., Koumpia, E., Kristensen, L., Leurini, S., Nagy, Z., Perez Beaupuits, J.P., Risacher, C., van der Marel, N., van Kempen, T.A., van Weeren, R.J., Wyrowski, F., Yıldız, U.A.: Observations and modelling of CO and [C I] in protoplanetary disks. First detections of [C I] and constraints on the carbon abundance. A&A **588**, A108 (2016). https://doi.org/10.1051/0004-6361/201526791, 1601.01449
82. Cleeves, L.I., Öberg, K.I., Wilner, D.J., Huang, J., Loomis, R.A., Andrews, SM., Guzman, VV.: Constraining Gas-phase Carbon, Oxygen, and Nitrogen in the IM Lup Protoplanetary Disk. ApJ **865**(2), 155 (2018). https://doi.org/10.3847/1538-4357/aade96, 1808.10682
83. Krumholz, M.R., McKee, C.F.: A General Theory of Turbulence-regulated Star Formation, from Spirals to Ultraluminous Infrared Galaxies. ApJ **630**(1), 250–268 (2005). https://doi.org/10.1086/431734, astro-ph/0505177
84. Kennicutt, R.C., Evans, N.J.: Star Formation in the Milky Way and Nearby Galaxies. ARA&A **50**, 531–608 (2012). https://doi.org/10.1146/annurev-astro-081811-125610, 1204.3552
85. Elmegreen, B.G., Falgarone, E.: A Fractal Origin for the Mass Spectrum of Interstellar Clouds. ApJ **471**, 816 (1996). https://doi.org/10.1086/178009
86. Kruijssen, J.M.D.: On the fraction of star formation occurring in bound stellar clusters. MNRAS **426**(4), 3008–3040 (2012). https://doi.org/10.1111/j.1365-2966.2012.21923.x, 1208.2963
87. Hopkins, P.F.: Why do stars form in clusters? An analytic model for stellar correlation functions. MNRAS **428**(3), 1950–1957 (2013). https://doi.org/10.1093/MNRAS/sts147, 1202.2122
88. Adams, FC.: The Birth Environment of the Solar System. ARA&A **48**, 47–85 (2010). https://doi.org/10.1146/annurev-astro-081309-130830, 1001.5444
89. Kruijssen, J.M.D., Longmore, SN.: The implications of clustered star formation for (proto)planetary systems and habitability. In: Elmegreen, B.G., Tóth, L.V., Güdel, M. (eds.) IAU Symposium, vol. 345, pp. 61–65. IAU Symposium (2020)
90. Scally, A., Clarke, C.: Destruction of protoplanetary discs in the Orion Nebula Cluster. MNRAS **325**(2), 449–456 (2001). https://doi.org/10.1046/j.1365-8711.2001.04274.x, astro-ph/0012098
91. Winter, AJ., Clarke, CJ., Rosotti, G., Ih, J., Facchini, S., Haworth, TJ.: Protoplanetary disc truncation mechanisms in stellar clusters: comparing external photoevaporation and tidal encounters. MNRAS **478**(2), 2700–2722 (2018). https://doi.org/10.1093/MNRAS/sty984, 1804.00013
92. Marzari, F., Picogna, G.: Circumstellar disks do erase the effects of stellar flybys on planetary systems. A&A **550**, A64 (2013). https://doi.org/10.1051/0004-6361/201220436, 1212.1561
93. Davies, MB., Adams, F.C., Armitage, P., Chambers, J., Ford, E., Morbidelli, A., Raymond, S.N., Veras, D.: The Long-Term Dynamical Evolution of Planetary Systems. In: Beuther, H., Klessen, R.S., Dullemond, C.P., Henning, T. (eds.) Protostars and Planets VI, p. 787 (2014)
94. Rosotti, GP., Dale, JE., de Juan Ovelar, M., Hubber, DA., Kruijssen, JMD., Ercolano, B., Walch, S.: Protoplanetary disc evolution affected by star-disc interactions in young stellar clusters. MNRAS **441**(3), 2094–2110 (2014). https://doi.org/10.1093/MNRAS/stu679, 1404.1931
95. Bhandare, A., Breslau, A., Pfalzner, S.: Effects of inclined star-disk encounter on protoplanetary disk size. A&A **594**, A53 (2016). https://doi.org/10.1051/0004-6361/201628086, 1608.03239
96. de Juan Ovelar, M., Kruijssen, J.M.D., Bressert, E., Testi, L., Bastian, N., Cánovas, H.: Can habitable planets form in clustered environments? A&A **546**, L1 (2012). https://doi.org/10.1051/0004-6361/201219627, 1209.2136
97. Ansdell, M., Williams, J.P., Manara, C.F., Miotello, A., Facchini, S., van der Marel, N., Testi, L., van Dishoeck, E.F.: An ALMA Survey of Protoplanetary Disks in the $\sigma$ Orionis Cluster. AJ **153**(5), 240 (2017). https://doi.org/10.3847/1538-3881/aa69c0, 1703.08546
98. Guarcello, M.G., Drake, J.J., Wright, N.J., Albacete-Colombo, J.F., Clarke, C., Ercolano, B., Flaccomio, E., Kashyap, V., Micela, G., Naylor, T., Schneider, N., Sciortino, S., Vink, J.S.: Photoevaporation and close encounters: how the environment around Cygnus OB2 affects the evolution of protoplanetary disks. arXiv:1605.01773 (2016)
99. Winter, A.J., Booth, R.A., Clarke, C.J.: Evidence of a past disc-disc encounter: HV and DO Tau. MNRAS **479**(4), 5522–5531 (2018). https://doi.org/10.1093/MNRAS/sty1866, 1807.04295
100. Winter, A.J., Kruijssen, J.M.D., Chevance, M., Keller, B.W., Longmore, S.N.: Prevalent externally driven protoplanetary disc dispersal as a function of the galactic environment. MNRAS **491**(1), 903–922 (2020). https://doi.org/10.1093/MNRAS/stz2747, 1907.04602
101. Ciesla, F.J., Sandford, S.A.: Organic Synthesis via Irradiation and Warming of Ice Grains in the Solar Nebula. Science **336**(6080), 452 (2012). https://doi.org/10.1126/science.1217291

102. Muñoz Caro, G.M., Meierhenrich, UJ., Schutte, WA., Barbier, B., Arcones Segovia, A., Rosenbauer, H., Thiemann, WHP., Brack, A., Greenberg, JM.: Amino acids from ultraviolet irradiation of interstellar ice analogues. Nature **416**(6879), 403–406 (2002). https://doi.org/10.1038/416403a
103. Throop, H.B.: UV photolysis, organic molecules in young disks, and the origin of meteoritic amino acids. Icarus **212**(2), 885–895 (2011). https://doi.org/10.1016/j.Icarus.2011.01.002, 1112.3107
104. Ciaravella, A., Jiménez-Escobar, A., Cecchi-Pestellini, C., Huang, CH., Sie, NE., Muñoz Caro, G.M., Chen, Y.J.: Synthesis of Complex Organic Molecules in Soft X-Ray Irradiated Ices. ApJ **879**(1), 21 (2019). https://doi.org/10.3847/1538-4357/ab211c, 1905.07958
105. Shuping, R.Y., Bally, J., Morris, M., Throop, H.: Evidence for Grain Growth in the Protostellar Disks of Orion. ApJ **587**(2), L109–L112 (2003). https://doi.org/10.1086/375334
106. Throop, H.B., Bally, J.: Can Photoevaporation Trigger Planetesimal Formation? ApJ **623**(2), L149–L152 (2005). https://doi.org/10.1086/430272, astro-ph/0411647
107. Balog, Z., Rieke, GH., Su, K.YL., Muzerolle, J., Young, ET.: Spitzer MIPS 24 $\mu$m Detection of Photoevaporating Protoplanetary Disks. ApJ **650**(1), L83–L86 (2006). https://doi.org/10.1086/508707, astro-ph/0608630
108. Gieles, M., Portegies Zwart, SF.: The distinction between star clusters and associations. MNRAS **410**(1), L6–L7 (2011). https://doi.org/10.1111/j.1745-3933.2010.00967.x, 1010.1720
109. Lada, C.J., Lada, E.A.: Embedded Clusters in Molecular Clouds. ARA&A **41**, 57–115 (2003). https://doi.org/10.1146/annurev.astro.41.011802.094844, astro-ph/0301540
110. Longmore, S.N., Kruijssen, J.M.D., Bastian, N., Bally, J., Rathborne, J., Testi, L., Stolte, A., Dale, J., Bressert, E., Alves, J.: The Formation and Early Evolution of Young Massive Clusters. In: Beuther, H., Klessen, R.S., Dullemond, C.P., Henning, T. (eds.) Protostars and Planets VI, p. 291 (2014)
111. Pfeffer, J., Kruijssen, J.M.D., Crain, R.A., Bastian, N.: The E-MOSAICS project: simulating the formation and co-evolution of galaxies and their star cluster populations. MNRAS **475**(4), 4309–4346 (2018). https://doi.org/10.1093/MNRAS/stx3124, 1712.00019
112. Winter, A.J., Kruijssen, J.M.D., Longmore, S.N., Chevance, M.: Stellar clustering shapes the architecture of planetary systems. Nature **586**(7830), 528–532 (2020). https://doi.org/10.1038/s41586-020-2800-0, 2010.10531
113. Kruijssen, J.M.D., Longmore, S.N., Chevance, M.: Bridging the Planet Radius Valley: Stellar Clustering as a Key Driver for Turning Sub-Neptunes into Super-Earths. The Astrophysical Journal Letters 905, id.L18. https://doi.org/10.3847/2041-8213/abccc3 (2020)
114. Longmore, SN., Chevance, M., Kruijssen, JMD.: The Impact of Stellar Clustering on the Observed Architectures of Planetary Systems. The Astrophysical Journal Letters 911, id.L16. https://doi.org/10.3847/2041-8213/abeb22 (2021)
115. Chevance, M., Kruijssen, J.M.D., Longmore, SN.: When the Peas Jump out of the Pod: How Stellar Clustering Affects the Observed Correlation of Planet Properties in Multi-Planet Systems. The Astrophysical Journal Letters 910, id. L19. https://doi.org/10.3847/2041-8213/abee20 (2021)
116. Fujimoto, Y., Krumholz, M.R., Tachibana, S.: Short-lived radioisotopes in meteorites from Galactic-scale correlated star formation. MNRAS **480**(3), 4025–4039 (2018). https://doi.org/10.1093/mnras/sty2132, 1802.08695
117. Adamo, A., Kruijssen, J.M.D., Bastian, N., Silva-Villa, E., Ryon, J.: Probing the role of the galactic environment in the formation of stellar clusters, using M83 as a test bench. MNRAS **452**(1), 246–260 (2015). https://doi.org/10.1093/MNRAS/stv1203, 1505.07475
118. Haworth, T.J., Clarke, C.J., Rahman, W., Winter, A.J., Facchini, S.: The FRIED grid of mass-loss rates for externally irradiated protoplanetary discs. MNRAS **481**(1), 452–466 (2018). https://doi.org/10.1093/MNRAS/sty2323, 1808.07484
119. Ruiz-Lara, T., Gallart, C., Bernard, E.J., Cassisi, S.: The recurrent impact of the Sagittarius dwarf on the star formation history of the Milky Way. Nat. Astron. **4**, 965–973 (2020). https://doi.org/10.1038/s41550-020-1097-0, 2003.12577
120. Wolszczan, A., Frail, D.A.: A planetary system around the millisecond pulsar PSR1257 + 12. Nature **355**(6356), 145–147 (1992). https://doi.org/10.1038/355145a0
121. Gonzalez, G.: The stellar metallicity-giant planet connection. MNRAS **285**(2), 403–412 (1997). https://doi.org/10.1093/MNRAS/285.2.403
122. Santos, N.C., Israelian, G., Mayor, M.: The metal-rich nature of stars with planets. A&A **373**, 1019–1031 (2001). https://doi.org/10.1051/0004-6361:20010648, astro-ph/0105216
123. Fischer, DA., Valenti, J.: The Planet-Metallicity Correlation. ApJ **622**(2), 1102–1117 (2005). https://doi.org/10.1086/428383

124. Sousa, S.G., Santos, N.C., Mayor, M., Udry, S., Casagrande, L., Israelian, G., Pepe, F., Queloz, D., Monteiro, MJPFG.: Spectroscopic parameters for 451 stars in the HARPS GTO planet search program. Stellar [Fe/H] and the frequency of exo-Neptunes. A&A **487**(1), 373–381 (2008). https://doi.org/10.1051/0004-6361:200809698, 0805.4826
125. Johnson, J.A., Aller, K.M., Howard, A.W., Crepp, J.R.: Giant Planet Occurrence in the Stellar Mass-Metallicity Plane. PASP **122**(894), 905 (2010). https://doi.org/10.1086/655775, 1005.3084
126. Udry, S., Mayor, M., Benz, W., Bertaux, J.L., Bouchy, F., Lovis, C., Mordasini, C., Pepe, F., Queloz, D., Sivan, J.P.: The HARPS search for southern extra-solar planets. V. A 14 Earth-masses planet orbiting HD 4308. A&A **447**(1), 361–367 (2006). https://doi.org/10.1051/0004-6361:20054084, astro-ph/0510354
127. Ghezzi, L., Cunha, K., Smith, V.V., de la Reza, R.: Lithium Abundances in a Sample of Planet-hosting Dwarfs. ApJ **724**(1), 154–164 (2010). https://doi.org/10.1088/0004-637X/724/1/154, 1009.2130
128. Mayor, M., Marmier, M., Lovis, C., Udry, S., Ségransan, D., Pepe, F., Benz, W., Bertaux, J., Bouchy, F., Dumusque, X., Lo Curto, G., Mordasini, C., Queloz, D., Santos, NC.: The HARPS search for southern extra-solar planets XXXIV. Occurrence, mass distribution and orbital properties of super-Earths and Neptune-mass planets. arXiv:1109.2497 (2011)
129. Pollack, J.B., Hubickyj, O., Bodenheimer, P., Lissauer, J.J., Podolak, M., Greenzweig, Y.: Formation of the Giant Planets by Concurrent Accretion of Solids and Gas. Icarus **124**(1), 62–85 (1996). https://doi.org/10.1006/icar.1996.0190
130. Rice, W.K.M., Armitage, P.J.: On the Formation Timescale and Core Masses of Gas Giant Planets. ApJ **598**(1), L55–L58 (2003). https://doi.org/10.1086/380390, astro-ph/0310191
131. Alibert, Y., Mordasini, C., Benz, W.: Migration and giant planet formation. A&A **417**, L25–L28 (2004). https://doi.org/10.1051/0004-6361:20040053, astro-ph/0403574
132. Jenkins, J.S., Jones, H.R.A., Tuomi, M., Díaz, M., Cordero, JP., Aguayo, A., Pantoja, B., Arriagada, P., Mahu, R., Brahm, R., Rojo, P., Soto, MG., Ivanyuk, O., Becerra Yoma, N., Day-Jones, AC., Ruiz, MT., Pavlenko, Y.V., Barnes, J.R., Murgas, F., Pinfield, D.J., Jones, M.I., López-Morales, M., Shectman, S., Butler, R.P., Minniti, D.: New planetary systems from the Calan-Hertfordshire Extrasolar Planet Search. MNRAS **466**, 443–473 (2017). https://doi.org/10.1093/MNRAS/stw2811, 1603.09391
133. Pasquini, L., Döllinger, MP., Weiss, A., Girardi, L., Chavero, C., Hatzes, AP., da Silva, L., Setiawan, J.: Evolved stars suggest an external origin of the enhanced metallicity in planet-hosting stars. A&A **473**, 979–982 (2007). https://doi.org/10.1051/0004-6361:20077814, 0707.0788
134. Maldonado, J., Villaver, E., Eiroa, C.: The metallicity signature of evolved stars with planets. A&A **554**, A84 (2013). https://doi.org/10.1051/0004-6361/201321082, 1303.3418
135. Mortier, A., Santos, NC., Sousa, SG., Adibekyan, VZ., Delgado Mena, E., Tsantaki, M., Israelian, G., Mayor, M.: New and updated stellar parameters for 71 evolved planet hosts. On the metallicity-giant planet connection. A&A **557**, A70 (2013). https://doi.org/10.1051/0004-6361/201321641, 1307.7870
136. Jofré, E., Petrucci, R., Saffe, C., Saker, L., de la Villarmois, E.A., Chavero, C., Gómez, M., Mauas, P.J.D.: Stellar parameters and chemical abundances of 223 evolved stars with and without planets. A&A **574**, A50 (2015). https://doi.org/10.1051/0004-6361/201424474, 1410.6422
137. Reffert, S., Bergmann, C., Quirrenbach, A., Trifonov, T., Künstler, A.: Precise radial velocities of giant stars. VII. Occurrence rate of giant extrasolar planets as a function of mass and metallicity. A&A **574**, A116 (2015). https://doi.org/10.1051/0004-6361/201322360, 1412.4634
138. Alibert, Y., Mordasini, C., Benz, W.: Extrasolar planet population synthesis. III. Formation of planets around stars of different masses. A&A **526**, A63 (2011). https://doi.org/10.1051/0004-6361/201014760, 1101.0513
139. Muzerolle, J., Hillenbrand, L., Calvet, N., Briceño, C., Hartmann, L.: Accretion in Young Stellar/Substellar Objects. ApJ **592**(1), 266–281 (2003). https://doi.org/10.1086/375704, astro-ph/0304078
140. Natta, A., Testi, L., Muzerolle, J., Randich, S., Comerón, F., Persi, P.: Accretion in brown dwarfs: An infrared view. A&A **424**, 603–612 (2004). https://doi.org/10.1051/0004-6361:20040356, astro-ph/0406106
141. Mendigutía, I., Calvet, N., Montesinos, B., Mora, A., Muzerolle, J., Eiroa, C., Oudmaijer, RD., Merín, B.: Accretion rates and accretion tracers of Herbig Ae/Be stars. A&A **535**, A99 (2011). https://doi.org/10.1051/0004-6361/201117444, 1109.3288

142. Mendigutía, I., Mora, A., Montesinos, B., Eiroa, C., Meeus, G., Merín, B., Oudmaijer, RD.: Accretion-related properties of Herbig Ae/Be stars. Comparison with T Tauris. A&A **543**, A59 (2012). https://doi.org/10.1051/0004-6361/201219110, 1205.4734
143. Mordasini, C., Alibert, Y., Benz, W., Klahr, H., Henning, T.: Extrasolar planet population synthesis . IV. Correlations with disk metallicity, mass, and lifetime. A&A **541**, A97 (2012). https://doi.org/10.1051/0004-6361/201117350, 1201.1036
144. Buchhave, L.A., Bizzarro, M., Latham, D.W., Sasselov, D., Cochran, W.D., Endl, M., Isaacson, H., Juncher, D., Marcy, G.W.: Three regimes of extrasolar planet radius inferred from host star metallicities. Nature **509**(7502), 593–595 (2014). https://doi.org/10.1038/nature13254, 1405.7695
145. Schlaufman, K.C.: A Continuum of Planet Formation between 1 and 4 Earth Radii. ApJ **799**(2), L26 (2015). https://doi.org/10.1088/2041-8205/799/2/L26, 1501.05953
146. Adibekyan, V.Z., Figueira, P., Santos, N.C., Mortier, A., Mordasini, C., Delgado Mena, E., Sousa, S.G., Correia, A.C.M., Israelian, G., Oshagh, M.: Orbital and physical properties of planets and their hosts: new insights on planet formation and evolution. A&A **560**, A51 (2013). https://doi.org/10.1051/0004-6361/201322551, 1311.2417
147. Wilson, R.F., Teske, J., Majewski, S.R., Cunha, K., Smith, V., Souto, D., Bender, C., Mahadevan, S., Troup, N., Allende Prieto, C., Stassun, K.G., Skrutskie, M.F., Almeida, A., García-Hernández, D.A., Zamora, O., Brinkmann, J.: Elemental Abundances of Kepler Objects of Interest in APOGEE. I. Two Distinct Orbital Period Regimes Inferred from Host Star Iron Abundances. AJ **155**(2), 68 (2018). https://doi.org/10.3847/1538-3881/aa9f27, 1712.01198
148. Maldonado, J., Villaver, E., Eiroa, C.: Chemical fingerprints of hot Jupiter planet formation. A&A **612**, A93 (2018). https://doi.org/10.1051/0004-6361/201732001, 1712.01035
149. Bashi, D., Helled, R., Zucker, S., Mordasini, C.: Two empirical regimes of the planetary mass-radius relation. A&A **604**, A83 (2017). https://doi.org/10.1051/0004-6361/201629922, 1701.07654
150. Santos, N.C., Adibekyan, V., Figueira, P., Andreasen, D.T., Barros, S.C.C., Delgado-Mena, E., Demangeon, O., Faria, J.P., Oshagh, M., Sousa, S.G., Viana, P.T.P., Ferreira, A.C.S.: Observational evidence for two distinct giant planet populations. A&A **603**, A30 (2017). https://doi.org/10.1051/0004-6361/201730761, 1705.06090
151. Ma, B., Ge, J.: Statistical properties of brown dwarf companions: implications for different formation mechanisms. MNRAS **439**, 2781–2789 (2014). https://doi.org/10.1093/MNRAS/stu134, 1303.6442
152. Maldonado, J., Villaver, E.: Searching for chemical signatures of brown dwarf formation. A&A **602**, A38 (2017). https://doi.org/10.1051/0004-6361/201630120, 1702.02904
153. Schlaufman, KC.: Evidence of an Upper Bound on the Masses of Planets and Its Implications for Giant Planet Formation. ApJ **853**, 37 (2018). https://doi.org/10.3847/1538-4357/aa961c, 1801.06185
154. Maldonado, J., Villaver, E., Eiroa, C., Micela, G.: Connecting substellar and stellar formation: the role of the host star's metallicity. A&A **624**, A94 (2019). https://doi.org/10.1051/0004-6361/201833827, 1903.01141
155. Haywood, M.: A peculiarity of metal-poor stars with planets? A&A **482**(2), 673–676 (2008). https://doi.org/10.1051/0004-6361:20079141, 0804.2954
156. Adibekyan, V.Z., Santos, N.C., Sousa, SG., Israelian, G., Delgado Mena, E., González Hernández, J.I., Mayor, M., Lovis, C., Udry, S.: Overabundance of $\alpha$-elements in exoplanet-hosting stars. A&A **543**, A89 (2012). https://doi.org/10.1051/0004-6361/201219564, 1205.6670
157. Reddy, B.E., Tomkin, J., Lambert, D.L., Allende Prieto, C.: The chemical compositions of Galactic disc F and G dwarfs. MNRAS **340**(1), 304–340 (2003). https://doi.org/10.1046/j.1365-8711.2003.06305.x, astro-ph/0211551
158. Reddy, B.E., Lambert, D.L., Allende Prieto, C.: Elemental abundance survey of the Galactic thick disc. MNRAS **367**(4), 1329–1366 (2006). https://doi.org/10.1111/j.1365-2966.2006.10148.x, astro-ph/0512505
159. Robinson, S.E., Laughlin, G., Bodenheimer, P., Fischer, D.: Silicon and Nickel Enrichment in Planet Host Stars: Observations and Implications for the Core Accretion Theory of Planet Formation. ApJ **643**, 484–500 (2006). https://doi.org/10.1086/502795, arXiv:0601656
160. Gonzalez, G.: Stars with planets and the thick disc. MNRAS **399**, L103–L107 (2009). https://doi.org/10.1111/j.1745-3933.2009.00734.x
161. Lodders, K.: Solar System Abundances and Condensation Temperatures of the Elements. ApJ **591**, 1220–1247 (2003). https://doi.org/10.1086/375492

162. Bodaghee, A., Santos, N.C., Israelian, G., Mayor, M.: Chemical abundances of planet-host stars. Results for alpha and Fe-group elements. A&A **404**, 715–727 (2003). https://doi.org/10.1051/0004-6361:20030543, astro-ph/0304360
163. Gilli, G., Israelian, G., Ecuvillon, A., Santos, N.C., Mayor, M.: Abundances of refractory elements in the atmospheres of stars with extrasolar planets. A&A **449**(2), 723–736 (2006). https://doi.org/10.1051/0004-6361:20053850, astro-ph/0512219
164. Ecuvillon, A., Israelian, G., Santos, N.C., Mayor, M., Villar, V., Bihain, G.: C, S, Zn and Cu abundances in planet-harbouring stars. A&A **426**, 619–630 (2004). https://doi.org/10.1051/0004-6361:20041136, astro-ph/0406584
165. Ecuvillon, A., Israelian, G., Santos, N.C., Mayor, M., Gilli, G.: Abundance ratios of volatile vs. refractory elements in planet-harbouring stars: hints of pollution? A&A **449**(2), 809–816 (2006). https://doi.org/10.1051/0004-6361:20054534, astro-ph/0512221
166. Gonzalez, G.: The Chemical Compositions of Stars with Planets: A Review. PASP **118**(849), 1494–1505 (2006). https://doi.org/10.1086/509792, astro-ph/0609829
167. da Silva, R., Milone, A.C., Reddy, B.E.: Homogeneous photospheric parameters and C abundances in G and K nearby stars with and without planets. A&A **526**, A71 (2011). https://doi.org/10.1051/0004-6361/201015907, 1011.5768
168. Perryman, M. The exoplanet handbook, 2nd edn. Cambridge University Press, Cambridge (2018)
169. Israelian, G., Santos, N.C., Mayor, M., Rebolo, R.: Lithium in stars with exoplanets. A&A **414**, 601–611 (2004). https://doi.org/10.1051/0004-6361:20034398, astro-ph/0310378
170. Gonzalez, G.: Parent stars of extrasolar planets - IX. Lithium abundances. MNRAS **386**(2), 928–934 (2008). https://doi.org/10.1111/j.1365-2966.2008.13067.x, 0802.0434
171. Gonzalez, G., Carlson, M.K., Tobin, RW.: Parent stars of extrasolar planets - XI. Trends with condensation temperature revisited. MNRAS **407**(1), 314–320 (2010). https://doi.org/10.1111/j.1365-2966.2010.16900.x, 1004.3313
172. Delgado Mena, E., Israelian, G., González Hernández, J.I., Sousa, S.G., Mortier, A., Santos, N.C., Adibekyan, V.Z., Fernand es, J., Rebolo, R., Udry, S., Mayor, M.: Li depletion in solar analogues with exoplanets. Extending the sample. A&A **562**, A92 (2014). https://doi.org/10.1051/0004-6361/201321493, 1311.6414
173. Delgado Mena, E., Bertrán de Lis, S., Adibekyan, V..Z., Sousa, SG., Figueira, P., Mortier, A., González Hernández, J.I., Tsantaki, M., Israelian, G., Santos, N.C.: Li abundances in F stars: planets, rotation, and Galactic evolution. A&A **576**, A69 (2015). https://doi.org/10.1051/0004-6361/201425433, 1412.4618
174. Ramírez, I., Fish, J.R., Lambert, D.L., Allende Prieto, C.: Lithium Abundances in nearby FGK Dwarf and Subgiant Stars: Internal Destruction, Galactic Chemical Evolution, and Exoplanets. ApJ **756**(1), 46 (2012). https://doi.org/10.1088/0004-637X/756/1/46, 1207.0499
175. Adamów, M., Niedzielski, A., Villaver, E., Nowak, G., Wolszczan, A.: BD+48 740—Li Overabundant Giant Star with a Planet: A Case of Recent Engulfment? ApJ **754**(1), L15 (2012). https://doi.org/10.1088/2041-8205/754/1/L15, 1206.4938
176. Adamów, M., Niedzielski, A., Villaver, E., Wolszczan, A., Nowak, G.: The Penn State - Toruń Centre for Astronomy Planet Search stars. II. Lithium abundance analysis of the red giant clump sample. A&A **569**, A55 (2014). https://doi.org/10.1051/0004-6361/201423400, 1407.4956
177. Nowak, G., Niedzielski, A., Wolszczan, A., Adamów, M., Maciejewski, G.: BD+15 2940 and HD 233604: Two Giants with Planets Close to the Engulfment Zone. ApJ **770**(1), 53 (2013). https://doi.org/10.1088/0004-637X/770/1/53, 1304.6755
178. Delgado Mena, E., Israelian, G., González Hernández, J.I., Santos, NC., Rebolo, R.: Be Abundances in Cool Main-sequence Stars with Exoplanets. ApJ **746**(1), 47 (2012). https://doi.org/10.1088/0004-637X/746/1/47, 1111.3495
179. Meléndez, J., Asplund, M., Gustafsson, B., Yong, D.: The Peculiar Solar Composition and Its Possible Relation to Planet Formation. ApJ **704**(1), L66–L70 (2009). https://doi.org/10.1088/0004-637X/704/1/L66, 0909.2299
180. Ramírez, I., Meléndez, J., Asplund, M.: Accurate abundance patterns of solar twins and analogs. Does the anomalous solar chemical composition come from planet formation? A&A **508**(1), L17–L20 (2009). https://doi.org/10.1051/0004-6361/200913038
181. Ramírez, I., Asplund, M., Baumann, P., Meléndez, J., Bensby, T.: A possible signature of terrestrial planet formation in the chemical composition of solar analogs. A&A **521**, A33 (2010). https://doi.org/10.1051/0004-6361/201014456, 1008.3161

182. Ramírez, I., Bajkova, A.T., Bobylev, V.V., Roederer, I.U., Lambert, D.L., Endl, M., Cochran, WD., MacQueen, P.J., Wittenmyer, R.A.: Elemental Abundances of Solar Sibling Candidates. ApJ **787**(2), 154 (2014). https://doi.org/10.1088/0004-637X/787/2/154, 1405.1723
183. Gonzalez, G.: Parent stars of extrasolar planets - XII. Additional evidence for trends with v sin i, condensation temperature and chromospheric activity. MNRAS **416**(1), L80–L83 (2011). https://doi.org/10.1111/j.1745-3933.2011.01102.x, 1106.5002
184. González Hernández, J.I., Israelian, G., Santos, N.C., Sousa, S., Delgado-Mena, E., Neves, V., Udry, S.: Searching for the Signatures of Terrestrial Planets in Solar Analogs. ApJ **720**(2), 1592–1602 (2010). https://doi.org/10.1088/0004-637X/720/2/1592, 1007.0580
185. González Hernández, J.I., Delgado-Mena, E., Sousa, S.G., Israelian, G., Santos, N.C., Adibekyan, V.Z., Udry, S.: Searching for the signatures of terrestrial planets in F-, G-type main-sequence stars. A&A **552**, A6 (2013). https://doi.org/10.1051/0004-6361/201220165, 1301.2109
186. Schuler, S.C., Flateau, D., Cunha, K., King, J.R., Ghezzi, L., Smith, V.V.: Abundances of Stars with Planets: Trends with Condensation Temperature. ApJ **732**(1), 55 (2011). https://doi.org/10.1088/0004-637X/732/1/55, 1103.0757
187. Maldonado, J., Eiroa, C., Villaver, E., Montesinos, B., Mora, A.: Searching for signatures of planet formation in stars with circumstellar debris discs. A&A **579**, A20 (2015). https://doi.org/10.1051/0004-6361/201525764, 1502.07100
188. Adibekyan, V.Z., González Hernández, J.I., Delgado Mena, E., Sousa, S.G., Santos, N.C., Israelian, G., Figueira, P., Bertran de Lis, S.: On the origin of stars with and without planets. $T_c$ trends and clues to Galactic evolution. A&A **564**, L15 (2014). https://doi.org/10.1051/0004-6361/201423435, 1404.4514
189. Maldonado, J., Villaver, E.: Evolved stars and the origin of abundance trends in planet hosts. A&A **588**, A98 (2016). https://doi.org/10.1051/0004-6361/201527883, 1602.00835
190. Dumusque, X., Pepe, F., Lovis, C., Ségransan, D., Sahlmann, J., Benz, W., Bouchy, F., Mayor, M., Queloz, D., Santos, N., Udry, S.: An Earth-mass planet orbiting $\alpha$ Centauri B. Nature **491**(7423), 207–211 (2012). https://doi.org/10.1038/nature11572
191. Isaacson, H., Fischer, D.: Chromospheric Activity and Jitter Measurements for 2630 Stars on the California Planet Search. ApJ **725**(1), 875–885 (2010). https://doi.org/10.1088/0004-637X/725/1/875, 1009.2301
192. Arriagada, P.: Chromospheric Activity of Southern Stars from the Magellan Planet Search Program. ApJ **734**(1), 70 (2011). https://doi.org/10.1088/0004-637X/734/1/70, 1104.3186
193. Canto Martins, B.L., Das Chagas, M.L., Alves, S., Leão, I.C., de Souza Neto, L.P., de Medeiros, JR..: Chromospheric activity of stars with planets. A&A **530**, A73 (2011). https://doi.org/10.1051/0004-6361/201015314, 1103.5332
194. Kashyap, V.L., Drake, J.J., Saar, S.H.: Extrasolar Giant Planets and X-Ray Activity. ApJ **687**(2), 1339–1354 (2008). https://doi.org/10.1086/591922, 0807.1308
195. Poppenhaeger, K., Robrade, J., Schmitt, JHMM.: Coronal properties of planet-bearing stars. A&A **515**, A98 (2010). https://doi.org/10.1051/0004-6361/201014245, 1003.5802
196. Scandariato, G., Maggio, A., Lanza, A.F., Pagano, I., Fares, R., Shkolnik, E.L., Bohlender, D., Cameron, A.C., Dieters, S., Donati, J.F., Martínez Fiorenzano, A.F., Jardine, M., Moutou, C.: A coordinated optical and X-ray spectroscopic campaign on HD 179949: searching for planet-induced chromospheric and coronal activity. A&A **552**, A7 (2013). https://doi.org/10.1051/0004-6361/201219875, 1301.7748
197. Shkolnik, E., Walker, G.A.H., Bohlender, D.A., Gu, P.G., Kürster, M.: Hot Jupiters and Hot Spots: The Short- and Long-Term Chromospheric Activity on Stars with Giant Planets. ApJ **622**(2), 1075–1090 (2005). https://doi.org/10.1086/428037, astro-ph/0411655
198. Walker, G.A.H., Croll, B., Matthews, J.M., Kuschnig, R., Huber, D., Weiss, W.W., Shkolnik, E., Rucinski, S.M., Guenther, D.B., Moffat, A.F.J., Sasselov, D.: MOST detects variability on $\tau$ Bootis A possibly induced by its planetary companion. A&A **482**(2), 691–697 (2008). https://doi.org/10.1051/0004-6361:20078952, 0802.2732
199. Maggio, A., Pillitteri, I., Scandariato, G., Lanza, A.F., Sciortino, S., Borsa, F., Bonomo, A.S., Claudi, R., Covino, E., Desidera, S., Gratton, R., Micela, G., Pagano, I., Piotto, G., Sozzetti, A., Cosentino, R., Maldonado, J.: Coordinated X-Ray and Optical Observations of Star-Planet Interaction in HD 17156. ApJ **811**(1), L2 (2015). https://doi.org/10.1088/2041-8205/811/1/L2, 1509.00662
200. Bond, J.C., O'Brien, D..P., Lauretta, D.S.: The Compositional Diversity of Extrasolar Terrestrial Planets. I. In Situ Simulations. ApJ **715**(2), 1050–1070 (2010). https://doi.org/10.1088/0004-637X/715/2/1050, 1004.0971

201. Delgado Mena, E., Israelian, G., González Hernández, J.I., Bond, J.C., Santos, N.C., Udry, S., Mayor, M.: Chemical Clues on the Formation of Planetary Systems: C/O Versus Mg/Si for HARPS GTO Sample. ApJ **725**(2), 2349–2358 (2010). https://doi.org/10.1088/0004-637X/725/2/2349, 1009.5224
202. Piersanti, L., Straniero, O., Cristallo, S.: A method to derive the absolute composition of the Sun, the solar system, and the stars. A&A **462**(3), 1051–1062 (2007). https://doi.org/10.1051/0004-6361:20054505, astro-ph/0611229
203. Ritter, C., Côté, B.: NuPyCEE: NuGrid Python Chemical Evolution Environment (2016)
204. Côté, B., O'Shea, BW., Ritter, C., Herwig, F., Venn, K.A.: The Impact of Modeling Assumptions in Galactic Chemical Evolution Models. ApJ **835**(2), 128 (2017). https://doi.org/10.3847/1538-4357/835/2/128, 1604.07824
205. Timmes, FX., Woosley, SE., Weaver, TA.: Galactic Chemical Evolution: Hydrogen through Zinc. ApJ **98**, 617 (1995). https://doi.org/10.1086/192172, astro-ph/9411003
206. Kobayashi, C., Karakas, A.I., Umeda, H.: The evolution of isotope ratios in the Milky Way Galaxy. MNRAS **414**(4), 3231–3250 (2011). https://doi.org/10.1111/j.1365-2966.2011.18621.x, 1102.5312
207. Mishenina, T., Pignatari, M., Côté, B., Thielemann, F.K., Soubiran, C., Basak, N., Gorbaneva, T., Korotin, SA., Kovtyukh, V.V., Wehmeyer, B., Bisterzo, S., Travaglio, C., Gibson, B.K., Jordan, C., Paul, A., Ritter, C., Herwig, F., NuGrid Collaboration.: Observing the metal-poor solar neighbourhood: a comparison of galactic chemical evolution predictions*†. MNRAS **469**(4), 4378–4399 (2017). https://doi.org/10.1093/MNRAS/stx1145, 1705.03642
208. Lugaro, M., Ott, U., Kereszturi, A.: Radioactive nuclei from cosmochronology to habitability. Prog. Part. Nucl. Phys. **102**, 1–47 (2018). https://doi.org/10.1016/j.ppnp.2018.05.002, 1808.00233
209. Côté, B., Lugaro, M., Reifarth, R., Pignatari, M., Világos, B., Yagüe, A., Gibson, BK.: Galactic Chemical Evolution of Radioactive Isotopes. ApJ **878**(2), 156 (2019). https://doi.org/10.3847/1538-4357/ab21d1, 1905.07828
210. Koll, D., Korschinek, G., Faestermann, T., Gómez-Guzmán, J.M., Kipfstuhl, S., Merchel, S., Welch, J.M.: Interstellar $^{60}$Fe in Antarctica. Phys. Rev. Lett. **123**(7), 072701 (2019). https://doi.org/10.1103/PhysRevLett.123.072701
211. Ludwig, P., Bishop, S., Egli, R., Chernenko, V., Deneva, B., Faestermann, T., Famulok, N., Fimiani, L., Gómez-Guzmán, J.M., Hain, K., Korschinek, G., Hanzlik, M., Merchel, S., Rugel, G.: Time-resolved 2-million-year-old supernova activity discovered in Earth's microfossil record. Proc. Natl. Acad. Sci. **113**(33), 9232–9237 (2016). https://doi.org/10.1073/pnas.1601040113, 1710.09573
212. Melott, A.L., Marinho, F., Paulucci, L.: Hypothesis: Muon Radiation Dose and Marine Megafaunal Extinction at the End-Pliocene Supernova. Astrobiology **19**(6), 825–830 (2019). https://doi.org/10.1089/ast.2018.1902, 1712.09367
213. Timmes, F.X., Woosley, S.E., Hartmann, D.H., Hoffman, R.D., Weaver, T.A., Matteucci, F.: 26Al and 60Fe from Supernova Explosions. ApJ **449**, 204 (1995). https://doi.org/10.1086/176046, astro-ph/9503120
214. Limongi, M., Chieffi, A.: The Nucleosynthesis of $^{26}$Al and $^{60}$Fe in Solar Metallicity Stars Extending in Mass from 11 to 120 $M_{solar}$: The Hydrostatic and Explosive Contributions. ApJ **647**(1), 483–500 (2006). https://doi.org/10.1086/505164, astro-ph/0604297
215. Jones, S.W., Möller, H., Fryer, C.L., Fontes, C.J., Trappitsch, R., Even, W.P., Couture, A., Mumpower, M.R., Safi-Harb, S.: $^{60}$Fe in core-collapse supernovae and prospects for X-ray and gamma-ray detection in supernova remnants. MNRAS **485**(3), 4287–4310 (2019). https://doi.org/10.1093/MNRAS/stz536, 1902.05980
216. Côté, B., Yagüe, A., Világos, B., Lugaro, M.: Stochastic Chemical Evolution of Radioactive Isotopes with a Monte Carlo Approach. ApJ **887**(2), 213 (2019). https://doi.org/10.3847/1538-4357/ab5a88
217. Cowan, J.J., Sneden, C., Lawler, JE., Aprahamian, A., Wiescher, M., Langanke, K., Martínez-Pinedo, G., Thielemann, F.-K.: Making the Heaviest Elements in the Universe: A Review of the Rapid Neutron Capture Process. arXiv:1901.01410 (2019)
218. Côté, B., Eichler, M., Arcones, A., Hansen, CJ., Simonetti, P., Frebel, A., Fryer, C.L., Pignatari, M., Reichert, M., Belczynski, K., Matteucci, F.: Neutron Star Mergers Might Not Be the Only Source of r-process Elements in the Milky Way. ApJ **875**(2), 106 (2019). https://doi.org/10.3847/1538-4357/ab10db, 1809.03525
219. Guilloteau, S., Di Folco, E., Dutrey, A., Simon, M., Grosso, N., Piétu, V.: A sensitive survey for $^{13}$CO, CN, $H_2CO$, and SO in the disks of T Tauri and Herbig Ae stars. A&A **549**, A92 (2013). https://doi.org/10.1051/0004-6361/201220298, 1211.4776

220. Guilloteau, S., Reboussin, L., Dutrey, A., Chapillon, E., Wakelam, V., Piétu, V., Di Folco, E., Semenov, D., Henning, T.: Chemistry in disks. X. The molecular content of protoplanetary disks in Taurus. A&A **592**, A124 (2016). https://doi.org/10.1051/0004-6361/201527088, 1604.05028
221. Öberg, K.I., Qi, C., Fogel, J.K.J., Bergin, E.A., Andrews, S.M., Espaillat, C., van Kempen, T.A., Wilner, D.J., Pascucci, I.: The Disk Imaging Survey of Chemistry with SMA. I. Taurus Protoplanetary Disk Data. ApJ **720**(1), 480–493 (2010). https://doi.org/10.1088/0004-637X/720/1/480, 1007.1476
222. Öberg, K.I., Qi, C., Fogel, J.K.J., Bergin, E.A., Andrews, S.M., Espaillat, C., Wilner, D.J., Pascucci, I., Kastner, J.H.: Disk Imaging Survey of Chemistry with SMA. II. Southern Sky Protoplanetary Disk Data and Full Sample Statistics. ApJ **734**(2), 98 (2011). https://doi.org/10.1088/0004-637X/734/2/98, 1104.1236
223. Podio, L., Kamp, I., Codella, C., Cabrit, S., Nisini, B., Dougados, C., Sandell, G., Williams, JP., Testi, L., Thi, W.F., Woitke, P., Meijerink, R., Spaans, M., Aresu, G., Ménard, F., Pinte, C.: Water Vapor in the Protoplanetary Disk of DG Tau. ApJ **766**(1), L5 (2013). https://doi.org/10.1088/2041-8205/766/1/L5, 1302.1410
224. Phuong, N.T., Chapillon, E., Majumdar, L., Dutrey, A., Guilloteau, S., Piétu, V., Wakelam, V., Diep, P.N., Tang, Y.W., Beck, T., Bary, J.: First detection of $H_2S$ in a protoplanetary disk. The dense GG Tauri A ring. A&A **616**, L5 (2018). https://doi.org/10.1051/0004-6361/201833766, 1808.00652
225. Teague, R., Henning, T., Guilloteau, S., Bergin, EA., Semenov, D., Dutrey, A., Flock, M., Gorti, U., Birnstiel, T.: Temperature, Mass, and Turbulence: A Spatially Resolved Multiband Non-LTE Analysis of CS in TW Hya. ApJ **864**(2), 133 (2018). https://doi.org/10.3847/1538-4357/aad80e, 1808.01768
226. Le Gal, R., Öberg, K.I., Loomis, R.A., Pegues, J., Bergner, J.B.: Sulfur Chemistry in Protoplanetary Disks: CS and $H_2CS$. ApJ **876**(1), 72 (2019). https://doi.org/10.3847/1538-4357/ab1416, 1903.11105
227. Codella, C., Podio, L., Garufi, A., Perrero, J., Ugliengo, P., Fedele, D., Favre, C., Bianchi, E., Ceccarelli, C., Mercimek, S., Bacciotti, F., Rygl, K.L.J., Testi, L.: ALMA chemical survey of disk-outflow sources in Taurus (ALMA-DOT). IV. Thioformaldehyde ($H_2CS$) in protoplanetary disks: spatial distributions and binding energies. arXiv:2011.02305 (2020)
228. Garufi, A., Podio, L., Codella, C., Rygl, K., Bacciotti, F., Facchini, S., Fedele, D., Miotello, A., Teague, R., Testi, L.: ALMA chemical survey of disk-outflow sources in Taurus (ALMA-DOT): I. CO, CS, CN, and H2CO around DG Tau B. arXiv:2002.10195 (2020)
229. Garufi, A., Podio, L., Codella, C., Fedele, D., Bianchi, E., Favre, C., Bacciotti, F., Ceccarelli, C., Mercimek, S., Rygl, K., Teague, R., Testi, L.: ALMA chemical survey of disk-outflow sources in Taurus (ALMA-DOT) V: Sample, overview, and demography of disk molecular emission. arXiv:2012.07667 (2020)
230. Loomis, R.A., Öberg, K.I., Andrews, S.M., Bergin, E., Bergner, J., Blake, G.A., Cleeves, L.I., Czekala, I., Huang, J., Le Gal, R., Ménard, F., Pegues, J., Qi, C., Walsh, C., Williams, J.P., Wilner, D.J.: An Unbiased ALMA Spectral Survey of the LkCa 15 and MWC 480 Protoplanetary Disks. ApJ **893**(2), 101 (2020). https://doi.org/10.3847/1538-4357/ab7cc8
231. van't Hoff, M.L.R., Harsono, D., Tobin, JJ., Bosman, AD., van Dishoeck, EF., Jørgensen, JK., Miotello, A., Murillo, N.M., Walsh, C.: Temperature Structures of Embedded Disks: Young Disks in Taurus Are Warm. ApJ **901**(2), 166 (2020). https://doi.org/10.3847/1538-4357/abb1a2
232. Aikawa, Y., Herbst, E.: Molecular evolution in protoplanetary disks. Two-dimensional distributions and column densities of gaseous molecules. A&A **351**, 233–246 (1999)
233. Willacy, K., Woods, P.M.: Deuterium Chemistry in Protoplanetary Disks. II. The Inner 30 AU. ApJ **703**(1), 479–499 (2009). https://doi.org/10.1088/0004-637X/703/1/479, 0908.1114
234. Walsh, C., Millar, T.J., Nomura, H., Herbst, E., Widicus Weaver, S., Aikawa, Y., Laas, J.C., Vasyunin, A.I.: Complex organic molecules in protoplanetary disks. A&A **563**, A33 (2014). https://doi.org/10.1051/0004-6361/201322446, 1403.0390
235. Loomis, R.A., Cleeves, L.I., Öberg, K.I., Guzman, V.V., Andrews, S.M.: The Distribution and Chemistry of $H_2CO$ in the DM Tau Protoplanetary Disk. ApJ **809**(2), L25 (2015). https://doi.org/10.1088/2041-8205/809/2/L25, 1508.07004
236. Fulle, M., Blum, J., Green, SF., Gundlach, B., Herique, A., Moreno, F., Mottola, S., Rotundi, A., Snodgrass, C.: The refractory-to-ice mass ratio in comets. MNRAS **482**(3), 3326–3340 (2019). https://doi.org/10.1093/MNRAS/sty2926

237. Qi, C., Öberg, K.I., Wilner, D.J., Rosenfeld, K.A.: First Detection of c-$C_3H_2$ in a Circumstellar Disk. ApJ **765**(1), L14 (2013). https://doi.org/10.1088/2041-8205/765/1/L14, 1302.0251
238. Öberg, K.I., Guzmán, V.V., Merchantz, C.J., Qi, C., Andrews, S.M., Cleeves, L.I., Huang, J., Loomis, R.A., Wilner, DJ., Brinch, C., Hogerheijde, M.: $H_2CO$ Distribution and Formation in the TW HYA Disk. ApJ **839**(1), 43 (2017). https://doi.org/10.3847/1538-4357/aa689a, 1704.05133
239. Carney, M.T., Hogerheijde, M.R., Loomis, R.A., Salinas, V.N., Öberg, K.I., Qi, C., Wilner, D.J.: Increased $H_2CO$ production in the outer disk around HD 163296. A&A **605**, A21 (2017). https://doi.org/10.1051/0004-6361/201629342, 1705.10188
240. Carney, M.T., Hogerheijde, M.R., Guzmán, V.V., Walsh, C., Öberg, K.I., Fayolle, E.C., Cleeves, L.I., Carpenter, J.M., Qi, C.: Upper limits on $CH_3OH$ in the HD 163296 protoplanetary disk. Evidence for a low gas-phase $CH_3OH$-to-$H_2CO$ ratio. A&A **623**, A124 (2019). https://doi.org/10.1051/0004-6361/201834353, 1901.02689
241. Podio, L., Bacciotti, F., Fedele, D., Favre, C., Codella, C., Rygl, K.L.J., Kamp, I., Guidi, G., Bianchi, E., Ceccarelli, C., Coffey, D., Garufi, A., Testi, L.: Organic molecules in the protoplanetary disk of DG Tauri revealed by ALMA. A&A **623**, L6 (2019). https://doi.org/10.1051/0004-6361/201834475, 1902.02720
242. Pegues, J., Öberg, K.I., Bergner, J.B., Loomis, R.A., Qi, C., Le Gal, R., Cleeves, L.I., Guzmán, VV., Huang, J., Jørgensen, J.K., Andrews, S.M., Blake, G.A., Carpenter, J.M., Schwarz, KR., Williams, JP., Wilner, DJ.: An ALMA Survey of $H_2CO$ in Protoplanetary Disks. ApJ **890**(2), 142 (2020). https://doi.org/10.3847/1538-4357/ab64d9, 2002.12525
243. Podio, L., Garufi, A., Codella, C., Fedele, D., Bianchi, E., Bacciotti, F., Ceccarelli, C., Favre, C., Mercimek, S., Rygl, K., Testi, L.: ALMA chemical survey of disk-outflow sources in Taurus (ALMA-DOT). II. Vertical stratification of CO, CS, CN, $H_2CO$, and $CH_3OH$ in a Class I disk. A&A **642**, L7 (2020). https://doi.org/10.1051/0004-6361/202038952, 2008.12648
244. Podio, L., Garufi, A., Codella, C., Fedele, D., Rygl, K., Favre, C., Bacciotti, F., Bianchi, E., Ceccarelli, C., Mercimek, S., Teague, R., Testi, L.: ALMA chemical survey of disk-outflow sources in Taurus (ALMA-DOT). III. The interplay between gas and dust in the protoplanetary disk of DG Tau. A&A **644**, A119 (2020). https://doi.org/10.1051/0004-6361/202038600, 2011.01081
245. Terwisscha van Scheltinga, J., Hogerheijde, M.R., Cleeves, L.I., Loomis, R.A., Walsh, C., Öberg, K.I., Bergin, E.A., Bergner, J.B., Blake, G.A., Calahan, J.K., Cazzoletti, P., van Dishoeck, E.F., Guzmán, VV., Huang, J., Kama, M., Qi, C., Teague, R., Wilner, DJ.: The TW Hya Rosetta Stone Project. II. Spatially Resolved Emission of Formaldehyde Hints at Low-temperature Gas-phase Formation. ApJ **906**(2), 111 (2021). https://doi.org/10.3847/1538-4357/abc9ba, 2011.07073
246. Bergner, J.B., Guzmán, V.G., Öberg, K.I., Loomis, RA., Pegues, J.: A Survey of $CH_3CN$ and $HC_3N$ in Protoplanetary Disks. ApJ **857**(1), 69 (2018). https://doi.org/10.3847/1538-4357/aab664, 1803.04986
247. Lee, C.-F., Codella, C., Li, Z.-Y., Liu, S.-Y.: First Abundance Measurement of Organic Molecules in the Atmosphere of HH 212 Protostellar Disk. ApJ **876**(1), 63 (2019). https://doi.org/10.3847/1538-4357/ab15db, 1904.10572
248. Codella, C., Bianchi, E., Tabone, B., Lee, C.F., Cabrit, S., Ceccarelli, C., Podio, L., Bacciotti, F., Bachiller, R., Chapillon, E., Gueth, F., Gusdorf, A., Lefloch, B., Leurini, S., Pineau des Forêts, G., Rygl, K.L.J., Tafalla, M.: Water and interstellar complex organics associated with the HH 212 protostellar disc. On disc atmospheres, disc winds, and accretion shocks. A&A **617**, A10 (2018). https://doi.org/10.1051/0004-6361/201832765, 1806.07967
249. Codella, C., Ceccarelli, C., Lee, C.-F., Bianchi, E., Balucani, N., Podio, L., Cabrit, S., Gueth, F., Gusdorf, A., Lefloch, B., Tabone, B.: The HH 212 Interstellar Laboratory: Astrochemistry as a Tool To Reveal Protostellar Disks on Solar System Scales around a Rising Sun. ACS Earth Space Chem. **3**(10), 2110–2121 (2019). https://doi.org/10.1021/acsearthspacechem.9b00136, 1910.04442
250. Lee, C.-F., Li, Z.-Y., Ho, P.TP., Hirano, N., Zhang, Q., Shang, H.: Formation and Atmosphere of Complex Organic Molecules of the HH 212 Protostellar Disk. ApJ **843**(1), 27 (2017). https://doi.org/10.3847/1538-4357/aa7757, 1706.06041
251. Sakai, N., Sakai, T., Hirota, T., Watanabe, Y., Ceccarelli, C., Kahane, C., Bottinelli, S., Caux, E., Demyk, K., Vastel, C., Coutens, A., Taquet, V., Ohashi, N., Takakuwa, S., Yen, H.-W., Aikawa, Y., Yamamoto, S.: Change in the chemical composition of infalling gas forming a disk around a protostar. Nature **507**(7490), 78–80 (2014). https://doi.org/10.1038/nature13000
252. Bianchi, E., Codella, C., Ceccarelli, C., Vazart, F., Bachiller, R., Balucani, N., Bouvier, M., De Simone, M., Enrique-Romero, J., Kahane, C., Lefloch, B., López-Sepulcre, A., Ospina-Zamudio, J., Podio, L., Taquet, V.: The census of interstellar complex organic molecules in the Class I hot

corino of SVS13-A. MNRAS **483**(2), 1850–1861 (2019). https://doi.org/10.1093/MNRAS/sty2915, 1810.11411
253. Drozdovskaya, M.N., van Dishoeck, E.F., Rubin, M., Jørgensen, J.K., Altwegg, K.: Ingredients for solar-like systems: protostar IRAS 16293-2422 B versus comet 67P/Churyumov-Gerasimenko. MNRAS **490**(1), 50–79 (2019). https://doi.org/10.1093/MNRAS/stz2430, 1908.11290
254. Shibata, S., Helled, R., Ikoma, M.: The origin of the high metallicity of close-in giant exoplanets. Combined effects of resonant and aerodynamic shepherding. A&A **633**, A33 (2020). https://doi.org/10.1051/0004-6361/201936700, 1911.02292
255. Miller, N., Fortney, J.J.: The Heavy-element Masses of Extrasolar Giant Planets, Revealed. ApJ **736**(2), L29 (2011). https://doi.org/10.1088/2041-8205/736/2/L29, 1105.0024
256. Thorngren, D.P., Fortney, JJ., Murray-Clay, R.A., Lopez, E.D.: The Mass-Metallicity Relation for Giant Planets. ApJ **831**(1), 64 (2016). https://doi.org/10.3847/0004-637X/831/1/64, 1511.07854
257. Wakeford, H.R., Sing, D.K., Kataria, T., Deming, D., Nikolov, N., Lopez, ED., Tremblin, P., Amundsen, DS., Lewis, NK., Mandell, AM., Fortney, JJ., Knutson, H., Benneke, B., Evans, TM.: HAT-P-26b: A Neptune-mass exoplanet with a well-constrained heavy element abundance. Science **356**(6338), 628–631 (2017). https://doi.org/10.1126/science.aah4668, 1705.04354
258. Sing, D.K.: Observational techniques with transiting exoplanetary atmospheres. In: Bozza, V., Mancini, L., Sozzetti, A. (eds.) Astrophysics of Exoplanetary Atmospheres: 2nd Advanced School on Exoplanetary Science, pp. 3–48. Springer International Publishing, Cham (2018). https://doi.org/10.1007/978-3-319-89701-1_1
259. Shibata, S., Ikoma, M.: Capture of solids by growing proto-gas giants: effects of gap formation and supply limited growth. MNRAS **487**(4), 4510–4524 (2019). https://doi.org/10.1093/MNRAS/stz1629, 1906.05530
260. Turrini, D., Nelson, R.P., Barbieri, M.: The role of planetary formation and evolution in shaping the composition of exoplanetary atmospheres. Exp. Astron. **40**(2-3), 501–522 (2015). https://doi.org/10.1007/s10686-014-9401-6, 1401.5119
261. Turrini, D., Schisano, E., Fonte, S., Molinari, S., Politi, R., Fedele, D., Panic, O., Kama, M., Changeat, Q., Tinetti, G.: Tracing the formation history of giant planets in protoplanetary disks with Carbon, Oxygen, Nitrogen and Sulphur. ApJ **909**(1), id.40 (2021). https://doi.org/10.3847/1538-4357/abd6e5, 2012.14315
262. Zinzi, A., Turrini, D.: Anti-correlation between multiplicity and orbital properties in exoplanetary systems as a possible record of their dynamical histories. A&A **605**, L4 (2017). https://doi.org/10.1051/0004-6361/201731595, 1709.00003
263. Laskar, J., Petit, A.C.: AMD-stability and the classification of planetary systems. A&A **605**, A72 (2017). https://doi.org/10.1051/0004-6361/201630022, 1703.07125
264. Turrini, D., Zinzi, A., Belinchon, JA.: Normalized angular momentum deficit: a tool for comparing the violence of the dynamical histories of planetary systems. A&A **636**, A53 (2020). https://doi.org/10.1051/0004-6361/201936301, 2003.05366
265. He, M.Y., Ford, E.B., Ragozzine, D., Carrera, D.: Architectures of Exoplanetary Systems. III. Eccentricity and Mutual Inclination Distributions of AMD-stable Planetary Systems. AJ **160**(6), 276 (2020). https://doi.org/10.3847/1538-3881/abba18, 2007.14473
266. Rasio, F.A., Ford, E.B.: Dynamical instabilities and the formation of extrasolar planetary systems. Science **274**, 954–956 (1996). https://doi.org/10.1126/science.274.5289.954
267. Weidenschilling, SJ., Marzari, F.: Gravitational scattering as a possible origin for giant planets at small stellar distances. Nature **384**(6610), 619–621 (1996). https://doi.org/10.1038/384619a0
268. Brouwers, M.G., Vazan, A., Ormel, C.W.: How cores grow by pebble accretion. I. Direct core growth. A&A **611**, A65 (2018). https://doi.org/10.1051/0004-6361/201731824, 1708.05392
269. Valletta, C., Helled, R.: The distribution of heavy-elements in giant protoplanetary atmospheres: the importance of planetesimal-envelope interactions. arXiv:1811.10904 (2018)
270. Bodenheimer, P., Stevenson, DJ., Lissauer, JJ., D'Angelo, G.: New Formation Models for the Kepler-36 System. ApJ **868**(2), 138 (2018). https://doi.org/10.3847/1538-4357/aae928, 1810.07160
271. Vazan, A., Helled, R., Kovetz, A., Podolak, M.: Convection and Mixing in Giant Planet Evolution. ApJ **803**, 32 (2015). https://doi.org/10.1088/0004-637X/803/1/32, 1502.03270
272. Mordasini, C., Mollière, P., Dittkrist, K.M., Jin, S., Alibert, Y.: Global models of planet formation and evolution. Int. J. Astrobiol. **14**(2), 201–232 (2015). https://doi.org/10.1017/S1473550414000263, 1406.5604

273. Podolak, M., Haghighipour, N., Bodenheimer, P., Helled, R., Podolak, E.: Detailed Calculations of the Efficiency of Planetesimal Accretion in the Core-accretion Model. ApJ **899**(1), 45 (2020). https://doi.org/10.3847/1538-4357/ab9ec1, 1911.12998
274. Vazan, A., Helled, R., Podolak, M., Kovetz, A.: The Evolution and Internal Structure of Jupiter and Saturn with Compositional Gradients. ApJ **829**, 118 (2016). https://doi.org/10.3847/0004-637X/829/2/118, 1606.01558
275. Vazan, A., Helled, R., Guillot, T.: Jupiter's evolution with primordial composition gradients. A&A **610**, L14 (2018). https://doi.org/10.1051/0004-6361/201732522, 1801.08149
276. Vazan, A., Helled, R.: Explaining the low luminosity of Uranus: a self-consistent thermal and structural evolution. A&A **633**, A50 (2020). https://doi.org/10.1051/0004-6361/201936588, 1908.10682
277. Eistrup, C., Walsh, C., van Dishoeck, E.F.: Setting the volatile composition of (exo)planet-building material. Does chemical evolution in disk midplanes matter? A&A **595**, A83 (2016). https://doi.org/10.1051/0004-6361/201628509, 1607.06710
278. Eistrup, C., Walsh, C., van Dishoeck, E.F.: Molecular abundances and C/O ratios in chemically evolving planet-forming disk midplanes. A&A **613**, A14 (2018). https://doi.org/10.1051/0004-6361/201731302, 1709.07863
279. Panić, O., Min, M.: Effects of disc mid-plane evolution on CO snowline location. MNRAS **467**(1), 1175–1185 (2017). https://doi.org/10.1093/mnras/stx114, 1703.09708
280. Piso, A.-M.A., Pegues, J., Öberg, KI.: The Role of Ice Compositions for Snowlines and the C/N/O Ratios in Active Disks. ApJ **833**(2), 203 (2016). https://doi.org/10.3847/1538-4357/833/2/203, 1611.00741
281. Booth, R.A., Ilee, J.D.: Planet-forming material in a protoplanetary disc: the interplay between chemical evolution and pebble drift. MNRAS **487**(3), 3998–4011 (2019). https://doi.org/10.1093/mnras/stz1488, 1905.12639
282. Bosman, A.D., Cridland, A.J., Miguel, Y.: Jupiter formed as a pebble pile around the $N_2$ ice line. A&A **632**, L11 (2019). https://doi.org/10.1051/0004-6361/201936827, 1911.11154
283. Oberg, K.I., Bergin, E.A.: Astrochemistry and compositions of planetary systems. Phys. Rep. arXiv:2010.03529 (2020)
284. Manara, C.F., Morbidelli, A., Guillot, T.: Why do protoplanetary disks appear not massive enough to form the known exoplanet population? A&A **618**, L3 (2018). https://doi.org/10.1051/0004-6361/201834076, 1809.07374
285. Scott, E.RD.: Chondrites and the Protoplanetary Disk. Annu. Rev. Earth Planet. Sci. **35**(1), 577–620 (2007). https://doi.org/10.1146/annurev.earth.35.031306.140100
286. Schiller, M., Bizzarro, M., Fernandes, V.A.: Isotopic evolution of the protoplanetary disk and the building blocks of Earth and the Moon. Nature **555**(7697), 507–510 (2018). https://doi.org/10.1038/nature25990
287. Madhusudhan, N., Agúndez, M., Moses, J.I., Hu, Y.: Exoplanetary Atmospheres—Chemistry, Formation Conditions, and Habitability. Space Sci. Rev. **205**(1-4), 285–348 (2016). https://doi.org/10.1007/s11214-016-0254-3, 1604.06092
288. Madhusudhan, N.: Exoplanetary Atmospheres: Key Insights, Challenges, and Prospects. ARA&A **57**, 617–663 (2019). https://doi.org/10.1146/annurev-astro-081817-051846, 1904.03190
289. Mordasini, C., van Boekel, R., Mollière, P., Henning, T., Benneke, B.: The Imprint of Exoplanet Formation History on Observable Present-day Spectra of Hot Jupiters. ApJ **832**(1), 41 (2016). https://doi.org/10.3847/0004-637X/832/1/41, 1609.03019
290. Cridland, A.J., van Dishoeck, E.F., Alessi, M., Pudritz, R.E.: Connecting planet formation and astrochemistry. A main sequence for C/O in hot exoplanetary atmospheres. A&A **632**, A63 (2019). https://doi.org/10.1051/0004-6361/201936105, 1910.13171
291. Lodders, K.: Solar System Abundances of the Elements. Astrophys. Space Sci. Proc. **16**, 379 (2010). https://doi.org/10.1007/978-3-642-10352-0_8, 1010.2746
292. Lodders, K.: Exoplanet Chemistry. , pp. 157. https://doi.org/10.1002/9783527629763.ch8 (2010)
293. Johnson, T.V., Mousis, O., Lunine, JI., Madhusudhan, N.: Planetesimal Compositions in Exoplanet Systems. ApJ **757**(2), 192 (2012). https://doi.org/10.1088/0004-637X/757/2/192, 1208.3289
294. Thiabaud, A., Marboeuf, U., Alibert, Y., Cabral, N., Leya, I., Mezger, K.: From stellar nebula to planets: The refractory components. A&A **562**, A27 (2014). https://doi.org/10.1051/0004-6361/201322208, 1312.3085
295. Marboeuf, U., Thiabaud, A., Alibert, Y., Cabral, N., Benz, W.: From stellar nebula to planetesimals. A&A **570**, A35 (2014). https://doi.org/10.1051/0004-6361/201322207, 1407.7271

296. Marboeuf, U., Thiabaud, A., Alibert, Y., Cabral, N., Benz, W.: From planetesimals to planets: volatile molecules. A&A **570**, A36 (2014). https://doi.org/10.1051/0004-6361/201423431, 1407.7282
297. Bergin, E.A., Blake, G.A., Ciesla, F., Hirschmann, MM., Li, J.: Tracing the ingredients for a habitable earth from interstellar space through planet formation. Proc. Natl. Acad. Sci. **112**(29), 8965–8970 (2015). https://doi.org/10.1073/pnas.1500954112, 1507.04756
298. Bardyn, A., Baklouti, D., Cottin, H., Fray, N., Briois, C., Paquette, J., Stenzel, O., Engrand, C., Fischer, H., Hornung, K., Isnard, R., Langevin, Y., Lehto, H., Le Roy, L., Ligier, N., Merouane, S., Modica, P., Orthous-Daunay, F.-R., Rynö, J., Schulz, R., Silén, J., Thirkell, L., Varmuza, K., Zaprudin, B., Kissel, J., Hilchenbach, M.: Carbon-rich dust in comet 67P/Churyumov-Gerasimenko measured by COSIMA/Rosetta. MNRAS **469**, S712–S722 (2017). https://doi.org/10.1093/mnras/stx2640
299. Isnard, R., Bardyn, A., Fray, N., Briois, C., Cottin, H., Paquette, J., Stenzel, O., Alexander, C., Baklouti, D., Engrand, C., Orthous-Daunay, F.R., Siljeström, S., Varmuza, K., Hilchenbach, M.: H/C elemental ratio of the refractory organic matter in cometary particles of 67P/Churyumov-Gerasimenko. A&A **630**, A27 (2019). https://doi.org/10.1051/0004-6361/201834797
300. Doyle, A.E., Young, E.D., Klein, B., Zuckerman, B., Schlichting, H.E.: Oxygen fugacities of extrasolar rocks: Evidence for an Earth-like geochemistry of exoplanets. Science **366**(6463), 356–359 (2019). https://doi.org/10.1126/science.aax3901, 1910.12989
301. ALMA Partnership., Brogan, C.L., Pérez, L.M., Hunter, T.R., Dent, W.R.F., Hales, A.S., Hills, R.E., Corder, S., Fomalont, E.B., Vlahakis, C., Asaki, Y., Barkats, D., Hirota, A., Hodge, J.A., Impellizzeri, C.M.V., Kneissl, R., Liuzzo, E., Lucas, R., Marcelino, N., Matsushita, S., Nakanishi, K., Phillips, N., Richards, A.M.S., Toledo, I., Aladro, R., Broguiere, D., Cortes, JR., Cortes, PC., Espada, D., Galarza, F., Garcia-Appadoo, D., Guzman-Ramirez, L., Humphreys, E.M., Jung, T., Kameno, S., Laing, RA., Leon, S., Marconi, G., Mignano, A., Nikolic, B., Nyman, LA., Radiszcz, M., Remijan, A., Rodón, J.A., Sawada, T., Takahashi, S., Tilanus, R.P.J., Vila Vilaro, B., Watson, L.C., Wiklind, T., Akiyama, E., Chapillon, E., de Gregorio-Monsalvo, I., Di Francesco, J., Gueth, F., Kawamura, A., Lee, C.F., Nguyen Luong, Q., Mangum, J., Pietu, V., Sanhueza, P., Saigo, K., Takakuwa, S., Ubach, C., van Kempen, T., Wootten, A., Castro-Carrizo, A., Francke, H., Gallardo, J., Garcia, J., Gonzalez, S., Hill, T., Kaminski, T., Kurono, Y., Liu, H.Y., Lopez, C., Morales, F., Plarre, K., Schieven, G., Testi, L., Videla, L., Villard, E., Andreani, P., Hibbard, J.E., Tatematsu, K.: The 2014 ALMA Long Baseline Campaign: First Results from High Angular Resolution Observations toward the HL Tau Region. ApJ **808**(1), L3 (2015). https://doi.org/10.1088/2041-8205/808/1/L3, 1503.02649
302. Isella, A., Guidi, G., Testi, L., Liu, S., Li, H., Li, S., Weaver, E., Boehler, Y., Carperter, J.M., De Gregorio-Monsalvo, I., Manara, C.F., Natta, A., Pérez, L.M., Ricci, L., Sargent, A., Tazzari, M., Turner, N.: Ringed Structures of the HD 163296 Protoplanetary Disk Revealed by ALMA. Phys. Rev. Lett. **117**(25), 251101 (2016). https://doi.org/10.1103/PhysRevLett.117.251101
303. Fedele, D., Carney, M., Hogerheijde, M.R., Walsh, C., Miotello, A., Klaassen, P., Bruderer, S., Henning, T., van Dishoeck, E.F.: ALMA unveils rings and gaps in the protoplanetary system ¡ASTROBJ¿HD 169142¡/ASTROBJ¿: signatures of two giant protoplanets. A&A **600**, A72 (2017). https://doi.org/10.1051/0004-6361/201629860, 1702.02844
304. Fedele, D., Tazzari, M., Booth, R., Testi, L., Clarke, C.J., Pascucci, I., Kospal, A., Semenov, D., Bruderer, S., Henning, T., Teague, R.: ALMA continuum observations of the protoplanetary disk AS 209. Evidence of multiple gaps opened by a single planet. A&A **610**, A24 (2018). https://doi.org/10.1051/0004-6361/201731978, 1711.05185
305. Long, F., Pinilla, P., Herczeg, G.J., Harsono, D., Dipierro, G., Pascucci, I., Hendler, N., Tazzari, M., Ragusa, E., Salyk, C., Edwards, S., Lodato, G., van de Plas, G., Johnstone, D., Liu, Y., Boehler, Y., Cabrit, S., Manara, C.F., Menard, F., Mulders, GD., Nisini, B., Fischer, W.J., Rigliaco, E., Banzatti, A., Avenhaus, H., Gully-Santiago, M.: Gaps and Rings in an ALMA Survey of Disks in the Taurus Star-forming Region. ApJ **869**(1), 17 (2018). https://doi.org/10.3847/1538-4357/aae8e1, 1810.06044
306. Barstow, J.K., Changeat, Q., Garland, R., Line, M.R., Rocchetto, M., Waldmann, IP.: A comparison of exoplanet spectroscopic retrieval tools. MNRAS **493**(4), 4884–4909 (2020). https://doi.org/10.1093/mnras/staa548, 2002.01063
307. Pollack, J.B., Hollenbach, D., Beckwith, S., Simonelli, D.P., Roush, T., Fong, W.: Composition and Radiative Properties of Grains in Molecular Clouds and Accretion Disks. ApJ **421**, 615 (1994). https://doi.org/10.1086/173677
308. Öberg, K.I., Wordsworth, R.: Jupiter's Composition Suggests its Core Assembled Exterior to the $N_2$ Snowline. A.J **158**(5), 194 (2019). https://doi.org/10.3847/1538-3881/ab46a8, 1909.11246

309. Asplund, M., Grevesse, N., Sauval, A.J., Scott, P.: The Chemical Composition of the Sun. ARA&A **47**(1), 481–522 (2009). https://doi.org/10.1146/annurev.astro.46.060407.145222, 0909.0948
310. Batalha, N.M.: Exploring exoplanet populations with NASA's Kepler Mission. PNAS **111**(35), 12647–12654 (2014). https://doi.org/10.1073/pnas.1304196111, 1409.1904
311. Miguel, Y., Cridland, A., Ormel, C.W., Fortney, J.J., Ida, S.: Diverse outcomes of planet formation and composition around low-mass stars and brown dwarfs. MNRAS, 2610. https://doi.org/10.1093/MNRAS/stz3007, 1909.12320 (2019)
312. Tanaka, H., Takeuchi, T., Ward, W.R.: Three-Dimensional Interaction between a Planet and an Isothermal Gaseous Disk. I. Corotation and Lindblad Torques and Planet Migration. ApJ **565**(2), 1257–1274 (2002). https://doi.org/10.1086/324713
313. Kimura, T., Ikoma, M.: Formation of aqua planets with water of nebular origin: effects of water enrichment on the structure and mass of captured atmospheres of terrestrial planets. MNRAS **496**(3), 3755–3766 (2020). https://doi.org/10.1093/mnras/staa1778, 2006.09068
314. Nikolaou, A., Katyal, N., Tosi, N., Godolt, M., Grenfell, J.L., Rauer, H.: What Factors Affect the Duration and Outgassing of the Terrestrial Magma Ocean? ApJ **875**(1), 11 (2019). https://doi.org/10.3847/1538-4357/ab08ed, 1903.07436
315. Miguel, Y., Kaltenegger, L., Fegley, B., Schaefer, L.: Compositions of Hot Super-earth Atmospheres: Exploring Kepler Candidates. ApJ **742**(2), L19 (2011). https://doi.org/10.1088/2041-8205/742/2/L19, 1110.2426
316. Ikoma, M., Genda, H.: Constraints on the Mass of a Habitable Planet with Water of Nebular Origin. ApJ **648**(1), 696–706 (2006). https://doi.org/10.1086/505780, astro-ph/0606117
317. Ikoma, M., Elkins-Tanton, L., Hamano, K., Suckale, J.: Water Partitioning in Planetary Embryos and Protoplanets with Magma Oceans. SSRv **214**(4), 76 (2018). https://doi.org/10.1007/s11214-018-0508-3, 1804.09294
318. Limbach, M.A., Turner, E.L.: Exoplanet orbital eccentricity: Multiplicity relation and the Solar System. Proc. Natl. Acad. Sci. **112**(1), 20–24 (2015). https://doi.org/10.1073/pnas.1406545111, 1404.2552
319. Bach-Møller, N., Jørgensen, UG.: Orbital eccentricity-multiplicity correlation for planetary systems and comparison to the Solar system. MNRAS **500**(1), 1313–1322 (2021). https://doi.org/10.1093/mnras/staa3321, 2010.10371
320. Carleo, I., Desidera, S., Nardiello, D., Malavolta, L., Lanza, AF., Livingston, J., Locci, D., Marzari, F., Messina, S., Turrini, D., Baratella, M., Borsa, F., D'Orazi, V., Nascimbeni, V., Pinamonti, M., Rainer, M., Alei, E., Bignamini, A., Gratton, R., Micela, G., Montalto, M., Sozzetti, A., Squicciarini, V., Affer, L., Benatti, S., Biazzo, K., Bonomo, A.S., Claudi, R., Cosentino, R., Covino, E., Damasso, M., Esposito, M., Fiorenzano, A., Frustagli, G., Giacobbe, P., Harutyunyan, A., Leto, G., Magazzù, A., Maggio, A., Mainella, G., Maldonado, J., Mallonn, M., Mancini, L., Molinari, E., Molinaro, M., Pagano, I., Pedani, M., Piotto, G., Poretti, E., Redfield, S., Scandariato, G.: The GAPS Programme at TNG. XXVIII. A pair of hot-Neptunes orbiting the young star TOI-942. A&A **645**, A71 (2021). https://doi.org/10.1051/0004-6361/202039042, 2011.13795
321. Tamayo, D., Rein, H., Petrovich, C., Murray, N.: Convergent Migration Renders TRAPPIST-1 Long-lived. ApJ **840**(2), L19 (2017). https://doi.org/10.3847/2041-8213/aa70ea, 1704.02957
322. Papaloizou, J.C.B., Szuszkiewicz, E., Terquem, C.: The TRAPPIST-1 system: orbital evolution, tidal dissipation, formation and habitability. MNRAS **476**(4), 5032–5056 (2018). https://doi.org/10.1093/mnras/stx2980, 1711.07932
323. Nesvorný, D.: Dynamical Evolution of the Early Solar System. ARA&A **56**, 137–174 (2018). https://doi.org/10.1146/annurev-astro-081817-052028, 1807.06647

## Affiliations

**Diego Turrini[1,2] · Claudio Codella[3] · Camilla Danielski[4] · Davide Fedele[2,3] · Sergio Fonte[1] · Antonio Garufi[3] · Mario Giuseppe Guarcello[5] · Ravit Helled[6] · Masahiro Ikoma[7] · Mihkel Kama[8,9] · Tadahiro Kimura[7] · J. M. Diederik Kruijssen[10] · Jesus Maldonado[5] · Yamila Miguel[11,12] · Sergio Molinari[1] · Athanasia Nikolaou[13,14] · Fabrizio Oliva[1] · Olja Panić[15] · Marco Pignatari[16,17,18] · Linda Podio[3] · Hans Rickman[19] · Eugenio Schisano[1] · Sho Shibata[7] · Allona Vazan[20] · Paulina Wolkenberg[1]**

1 Institute of Space Astrophysics and Planetology INAF-IAPS, Via Fosso del Cavaliere 100, I-00133, Rome, Italy

2 INAF - Osservatorio Astrofisico di Torino, Via Osservatorio 20, I-10025, Pino Torinese, Italy

3 INAF - Osservatorio Astrofisico di Arcetri, Largo E. Fermi 5, I-50127 Firenze, Italy

4 Instituto de Astrofísica de Andalucía (IAA-CSIC), Glorieta de la Astronomía s/n, 18008 Granada, Spain

5 INAF - Osservatorio Astronomico di Palermo, Piazza del Parlamento 1, I-90134, Palermo, Italy

6 Institute for Computational Science, Center for Theoretical Astrophysics and Cosmology, University of Zurich, CH-8057 Zurich, Switzerland

7 Department of Earth and Planetary Science, The University of Tokyo, 7-3-1 Hongo, Bunkyo-ku, Tokyo 113-0033, Japan

8 Department of Physics and Astronomy, University College London, London, WC1E 6BT, UK

9 Tartu Observatory, University of Tartu, Observatooriumi 1, 61602, Tõravere, Estonia

10 Astronomisches Rechen-Institut, Zentrum für Astronomie der Universität Heidelberg, Mönchhofstraße 12-14, 69120 Heidelberg, Germany

11 Leiden Observatory, Leiden University, Niels Bohrweg 2, 2333CA Leiden, The Netherlands

12 SRON - Netherlands Institute for Space Research, Sorbonnelaan 2, NL-3584 CA Utrecht, The Netherlands

13 Sapienza University of Rome, Piazzale Aldo Moro 2, Rome, 00185, Italy

14 European Space Agency, ESRIN, ESA Φ-lab, Largo Galileo Galilei 1, 00044 Frascati, Italy

15 School of Physics and Astronomy, E. C. Stoner Building, University of Leeds, Leeds, LS2 9JT, UK

16 E.A. Milne Centre for Astrophysics, Department of Physics, Mathematics, University of Hull, Hull, HU6 7RX, UK

17 Konkoly Observatory, Research Centre for Astronomy and Earth Sciences, Hungarian Academy of Sciences, Konkoly Thege Miklos ut 15-17, H-1121 Budapest, Hungary

18 Joint Institute for Nuclear Astrophysics - Center for the Evolution of the Elements & NuGrid Collaboration, www.nugridstars.org, Notre Dame, USA

19 Centrum Badań Kosmicznykh Polskiej Akademii Nauk (CBK PAN), Bartycka 18A, 00-716 Warszawa, Poland

20 Department of Natural Sciences and Astrophysics Research Center of the Open university (ARCO), The Open University of Israel, 4353701 Raanana, Israel